



NATIONAL AND KAPODISTRIAN UNIVERSITY OF ATHENS
SCHOOL OF NATURAL SCIENCES
DEPARTMENT OF CHEMISTRY

MASTER OF SCIENCE «ANALYTICAL CHEMISTRY & QUALITY ASSURANCE»

MASTER THESIS

**“Determination of Metoprolol and its potential
biotransformation products in zebrafish (*Danio rerio*)
embryos from exposure experiments under three different pH
values, using LC-ESI-QTOF-MS”**

VASILIKI TZEPKINLI

CHEMIST

ATHENS
OCTOBER 2021

MASTER THESIS

Determination of Metoprolol and its potential biotransformation products in zebrafish (*Danio Rerio*) embryos from exposure experiments under three different pH values by LC-ESI-QTOF-MS

VASILIKI TZEPKINLI

Registration Number: 192215

SUPERVISOR PROFESSOR:

Thomaidis Nikolaos, Professor, NKUA

THREE-MEMBER EXAMINATION COMMITTEE

Gkikas Evaggelos, Professor, NKUA

Oikonomou Anastasios, Professor, NKUA

Thomaidis Nikolaos, Professor, NKUA

DEFENDING DATE: 21/10/2021

ΕΡΕΥΝΗΤΙΚΗ ΕΡΓΑΣΙΑ ΔΙΠΛΩΜΑΤΟΣ ΕΙΔΙΚΕΥΣΗΣ

Προσδιορισμός της Μετοπρολόης και των πιθανών προϊόντων βιομετατροπής της σε έμβρυα Zebrafish (*Danio rerio*) από πειράματα έκθεσης σε τρεις διαφορετικές τιμές pH, με LC-ESI-QTOF-MS.

ΒΑΣΙΛΙΚΗ ΤΖΕΠΚΙΝΛΗ

A.M.: 192215

ΕΠΙΒΛΕΠΩΝ ΚΑΘΗΓΗΤΗΣ:

Θωμαΐδης Νικόλαος, Καθηγητής ΕΚΠΑ

ΤΡΙΜΕΛΗΣ ΕΞΕΤΑΣΤΙΚΗ ΕΠΙΤΡΟΠΗ

Γκίκας Ευάγγελος, Καθηγητής, ΕΚΠΑ

Οικονόμου Αναστάσιος, Καθηγητής, ΕΚΠΑ

Θωμαΐδης Νικόλαος, Καθηγητής, ΕΚΠΑ

ΗΜΕΡΟΜΗΝΙΑ ΕΞΕΤΑΣΗΣ: 21/10/2021

ABSTRACT

Over the last decades, the presence of emerging contaminants in the aquatic environment has become an issue of concern among scientists. Pharmaceutical compounds are one of the main categories of emerging contaminants and their consumption has significantly increased in the last decades. Pharmaceutical compounds end up in the aquatic environment, due to their inefficient removal from the conventional WWTPs. Once they release into the aquatic ecosystem, pharmaceuticals may bioaccumulate in aquatic organisms causing negative effects. Additionally, the majority of the pharmaceuticals are ionizable organic compounds (IOCs); therefore, their chemical speciation (ionic or neutral form) is defined by the surrounding pH value. The uptake of the IOCs, and as a result their toxicity, is strongly affected by their speciation, and hence by the different pH values. The non-ionized form of an IOC, which is less polar, can transport faster across membranes than the corresponding ionized one, and thus it may be more toxic for the organisms. Among IOCs is the Metoprolol (MET), a cardioselective β -blocker which widely used for the treatment of cardiovascular diseases. More specifically, MET is a secondary amine with $pK_a = 9.68$. Therefore, the percentage of the neutral form is increased with pH increasing, and as a result, the uptake and the toxicity of MET are expected to be higher at alkaline pH values. However, so far, the pH-dependent toxicity of Metoprolol has not been extensively investigated. Zebrafish (*Danio rerio*) has emerged as a powerful alternative model organism, which is widely used in ecotoxicological research studies for evaluating the potential effects of xenobiotics on aquatic organisms. Zebrafish embryos (ZFE) exhibit numerous beneficial traits, such as their capacity to biotransform xenobiotics via Phase I and Phase II reactions.

Considering all the above, one of the main objectives of the current master thesis was the study of the influence of environmentally relevant pH values on the uptake, potential toxicity, and bioaccumulation of Metoprolol in ZFE. Another important purpose was the investigation of the biotransformation capacity of ZFE exposed to MET and the identification of the tentative biotransformation products (bio-TPs). The final goal was to elucidate the main metabolic pathways of MET in ZFE.

For this purpose, the fish embryo test (FET) with ZFE was conducted at three pH values 6, 8, and 9. The ZFE were exposed to Metoprolol for 96 hours in a range of different concentrations for each pH value to determine the LC50 of MET at each pH value. Afterward, the ZFE (96 hpf) were exposed to MET at a concentration equivalent at their

LC50 value per each pH value. The water samples from the start (0 h) and the end (96 h) of the toxicokinetic experiment, as well as the ZFE samples, were analyzed utilizing liquid chromatography coupled to quadrupole-time-of-flight mass spectrometry (LC-QTOF-MS) by combinatorial use of reversed-phase liquid chromatography (RPLC) and hydrophilic interaction liquid chromatography (HILIC), in positive and negative ionization mode. For the identification of the parent, compound MET target screening approach was followed, while the identification of the (bio-TPs) was carried out with suspect screening.

Determining the LC50 values of MET at the three pH values, it was found that MET is more toxic at pH 9 since the LC50 value at pH 9 was 300 times lower than the LC50 at pH 6. These results were associated with a higher percentage of the neutral species of MET at higher pH values. Respectively, the bioconcentration factor (BCF) of MET at pH 9 was 155 times higher than the BCF at pH 6. On the other hand, the internal concentrations (C_{int}) of MET were at a similar range at all pH values. The results of our study confirm the pH-dependent toxicity and bioaccumulation of MET and the pH-independence of internal concentrations. For this reason, it was concluded that C_{int} is a more accurate measurement of the toxicity of a test compound. Moreover, the importance of investigating the pH factor in the environmental toxicity tests of the IOCs is pointed out. Otherwise, the toxicity of the IOCs may be under-or over-estimated.

Regarding the biotransformation of MET in ZFE, a total of ten (10) bio-TPs were detected and all of them were tentatively identified. The primary metabolic pathway of MET was the hydroxylation (phase I reaction). The complementary use of two different chromatographic techniques, RPLC and HILIC, achieved the orthogonal identification for the most bio-TPs. To the best of our knowledge, this is the first time that biotransformation of MET in ZFE is investigated. The fact that the compound Metoprolol is highly biotransformed in the ZFE highlights the importance to study thoroughly the biotransformation in toxicokinetic studies.

SUBJECT AREA: Analytical Chemistry

KEYWORDS: Metoprolol, pH, toxicity, uptake, bioaccumulation, biotransformation, ZFE, LC-ESI-QTOF-MS

ΠΕΡΙΛΗΨΗ

Τις τελευταίες δεκαετίες, η παρουσία των αναδυόμενων ρύπων στο υδάτινο περιβάλλον αποτελεί θέμα ανησυχίας μεταξύ των επιστημόνων. Οι φαρμακευτικές ενώσεις είναι μία από τις κύριες κατηγορίες αναδυόμενων ρύπων και η κατανάλωση τους έχει αυξηθεί ραγδαία τις τελευταίες δεκαετίες. Οι φαρμακευτικές ενώσεις συχνά καταλήγουν στα υδάτινα οικοσυστήματα εξαιτίας της αναποτελεσματικής απομάκρυνσής τους από τα κέντρα επεξεργασίας λυμάτων. Η απελευθέρωση των φαρμακευτικών ενώσεων στο υδάτινο περιβάλλον μπορεί να έχει ως αποτέλεσμα τη βιοσυσσώρευση και την πρόκληση αρνητικών επιπτώσεων στους υδρόβιους οργανισμούς και ίσως τελικά στην υγεία των ανθρώπων. Η πλειοψηφία των φαρμακευτικών ενώσεων είναι ιονίζουσες οργανικές ενώσεις, και συνεπώς, η χημική τους μορφή (ουδέτερη ή ιονισμένη) καθορίζεται από την τιμή pH του περιβάλλοντος. Η πρόσληψη των ιονίζουσων οργανικών ενώσεων, και άρα και η τοξικότητά τους, επηρεάζεται σημαντικά από τη μορφή με την οποία βρίσκονται και συνεπώς από τις διαφορετικές τιμές pH. Η ουδέτερη μορφή μιας ιονίζουσας ένωσης λόγω της χαμηλής της πολικότητας μπορεί να διαπεράσει ευκολότερα μέσω των μεμβρανών και άρα η τοξικότητα της ενδέχεται να είναι μεγαλύτερη. Μεταξύ των ιονίζουσων ενώσεων είναι και η Μετοπρολόη, ένας εκλεκτικός β-αναστολέας που χρησιμοποιείται ευρέως για τη θεραπεία καρδιοαγγειακών παθήσεων. Πιο συγκεκριμένα, πρόκειται για μια δευτερογάγης αμίνη με $pKa = 9.68$. Αυτό σημαίνει ότι το ποσοστό της ουδέτερης μορφής της αυξάνεται με την αύξηση του pH, και συνεπώς αναμένεται η πρόσληψη και η τοξικότητα της μετοπρολόης να είναι αυξημένες σε αλκαλικές τιμές pH. Παρόλα αυτά, μέχρι στιγμής, δεν έχει μελετηθεί εκτενώς η επίδραση του pH στην τοξικότητα της μετοπρολόης. Το zebrafish αποτελεί ένα ισχυρό εναλλακτικό μοντέλο-οργανισμός με ευρεία χρήση της οικοτοξικολογικές μελέτες για την αξιολόγηση των πιθανών επιπτώσεων των ξενοβιοτικών της υδρόβιους οργανισμούς. Το zebrafish εμφανίζει πολλά πλεονεκτήματα, μεταξύ των οποίων είναι η ικανότητα βιομετατροπής των ξενοβιοτικών μέσω αντιδράσεων της φάσης I και φάσης II.

Λαμβάνοντας υπόψιν όλα τα παραπάνω, της από της κυριότερους στόχους της παρούσας εργασίας ήταν η μελέτη της της επίδρασης του pH στην πρόσληψη, στην τοξικότητα και τη βιοσυσσώρευση της μετοπρολόης σε έμβρυα zebrafish. Της ακόμα σημαντικός στόχος ήταν η μελέτη της ικανότητας βιομετατροπής της μετοπρολόης των εμβρύων zebrafish και η ανίχνευση των πιθανών προϊόντων βιομετατροπής. Ο τελικός στόχος ήταν η πρόταση της πιθανού μεταβολικού μονοπατιού της μετοπρολόης.

Για το σκοπό αυτό, πραγματοποιήθηκε τεστ τοξικότητας με έμβρυα zebrafish σε τρεις τιμές pH 6, 8 και 9. Τα έμβρυα zebrafish εκτέθηκαν στη μετοπρολόλη σε ένα εύρος συγκεντρώσεων, με σκοπό να προσδιοριστούν οι τιμές LC50 της μετοπρολόλης σε κάθε τιμή pH. Στη συνέχεια πραγματοποιήθηκε τοξικοκινητικό πείραμα όπου τα έμβρυα zebrafish εκτέθηκαν στη μετοπρολόλη σε συγκέντρωση που αντιστοιχούσε στην τιμή LC50 για κάθε τιμή pH. Τα δείγματα νερού από την αρχή (0 h) και από το τέλος (96h) του τοξικοκινητικού πειράματος, καθώς και τα δείγματα zebrafish αναλύθηκαν με LC-Q-TOF-MS κάνοντας χρήση δύο χρωματογραφικών τεχνικών (RPLC και HILIC) και δύο πολικοτήτων (θετική και αρνητική). Για την ταυτοποίηση της μετοπρολόλης, εφαρμόστηκε στοχευμένη σάρωση, ενώ για την ταυτοποίηση των προϊόντων βιομετατροπής, εφαρμόστηκε σάρωση ύποπτων ενώσεων.

Προσδιορίζοντας τις τιμές LC50 της μετοπρολόλης στις τρεις τιμές pH, βρέθηκε ότι η μετοπρολόλη είναι πιο τοξική στο pH 9, καθώς η τιμή LC50 στο pH 9 ήταν περίπου 300 φορές χαμηλότερη από το στο pH 6. Τα αποτελέσματα αυτά συσχετίστηκαν με το αυξημένο ποσοστό ουδέτερης μορφής της μετοπρολόλης σε υψηλότερες τιμές pH. Αντίστοιχα, ο παράγοντας βιομετατροπής της μετοπρολόλης στο pH 9 ήταν 155 φορές μεγαλύτερος από τον παράγοντα βιομετατροπής στο pH 6. Από την άλλη πλευρά, οι εσωτερικές συγκεντρώσεις ήταν στο ίδιο εύρος τιμών σε όλες τις τιμές pH. Τα αποτελέσματα της μελέτης μας επιβεβαιώνουν την εξάρτηση της τοξικότητας και της βιοσυσσώρευσης της μετοπρολόλης από το pH, και της μη εξάρτησης της εσωτερικής συγκέντρωσης από το pH. Για το λόγο αυτό, οι εσωτερικές συγκεντρώσεις ακριβέστερο μέτρο της τοξικότητας μιας ένωσης. Επιπλέον, τονίζεται η σημασία της μελέτης του pH στις δοκιμές τοξικότητας των ιονίζουσαν οργανικών ενώσεων καθώς σε αντίθετη περίπτωση, η τοξικότητά τους μπορεί να υπό/υπέρ-εκτιμηθεί.

Όσων αφορά τη βιομετατροπή στα έμβρυα zebrafish, ανιχνεύθηκαν συνολικά δέκα (10) προϊόντα βιομετατροπής. Το κύριο μονοπάτι βιομετατροπής της μετοπρολόλης ήταν η υδροξυλίωση. Η συνδυαστική χρήση δύο χρωματογραφικών τεχνικών (RPLC και HILIC) συνέβαλε στην ορθογώνια ταυτοποίηση των περισσότερων προϊόντων βιομετατροπής. Βασιζόμενοι στα υπάρχοντα δεδομένα, αυτή είναι η πρώτη φορά που μελετάται η βιομετατροπή της μετοπρολόλης στα έμβρυα zebrafish. Το γεγονός ότι η μετοπρολόλη βιομετατρέπεται σε μεγάλο βαθμό στα έμβρυα zebrafish υπογραμμίζει την ανάγκη να συμπεριλαμβάνεται η μελέτη της βιομετατροπής στις μελέτες τοξικότητας.

ΘΕΜΑΤΙΚΗ ΠΕΡΙΟΧΗ: Αναλυτική Χημεία

ΛΕΞΕΙΣ-ΚΛΕΙΔΙΑ: Μετοπρολόη, pH, τοξικότητα, πρόσληψη, βιοσυσσώρευση, βιομετατροπή, ZFE, LC-ESI-QTOF-MS

CONTENTS

Chapter 1.....	23
Introduction.....	23
1.1. Emerging Contaminants	23
1.2. Pharmaceutical Compounds.....	24
1.3. Toxicokinetic process and internal concentration	26
1.4. Biotransformation procedure.....	28
1.5. pH-dependent toxicity	29
1.6. Metoprolol.....	30
1.6.1. Metoprolol as a pharmaceutical compound	30
1.6.2. Metoprolol in the aquatic environment	32
1.7. Zebrafish as a model organism.....	33
Chapter 2.....	37
Literature Review.....	37
2.1. Metoprolol aquatic toxicity	37
2.2. Metoprolol pH-dependent toxicity	37
2.3. Biotransformation of Metoprolol	38
2.4. Methods of determination of Metoprolol and other pharmaceutical compounds.....	39
2.4.1. Sample preparation	39
2.4.2. Analytical techniques	40
2.5. Identification approaches.....	41
2.5.1. Target screening	42
2.5.2. Suspect screening	42
2.5.3. Non-target screening	42

2.6. Identification confidence levels	43
2.7. Literature review table	44
Chapter 3.....	53
Scope and Objectives	53
Chapter 4.....	55
Materials and Methods	55
4.1. Chemicals	55
4.2. Zebrafish Embryos Exposure Experiments	55
4.2.1. Fish Embryo Test (FET)	55
4.2.2. Toxicokinetic Experiment.....	56
4.3. Samples	56
4.3.1. Water exposure samples	56
4.3.2. Zebrafish embryos samples.....	57
4.4. Sample Preparation.....	58
4.4.1. Water Samples	58
4.4.2. Zebrafish Embryos (ZFE) Samples.....	59
4.5. LC-HRMS Analysis.....	60
4.6. Identification Procedure	62
4.6.1. Target Screening	62
4.6.2. Suspect Screening	63
4.6.3. Identification Criteria.....	63
4.6.4. Identification Confidence levels	65
4.7. Quantification procedure of Metoprolol	65
4.7.1. Calibration curve of Metoprolol	65
4.7.2. LOD and LOQ	67
4.7.2. Quantification of Metoprolol in the samples	67

4.7.3. Bioconcentration Factors (BCFs)	68
Chapter 5.....	69
Results and Discussion	69
5.1. Results from the Metoprolol exposure experiments	69
5.1.1. Acute toxicity (LC50 values) results from FET with ZFE	69
5.1.2. Determination of the concentration of Metoprolol in water samples from the exposure experiment	71
5.1.3. Determination of the internal concentrations of Metoprolol in the zebrafish embryos samples from the exposure experiments	73
5.1.4. Determination of Bioconcentration Factors (BCFs) of Metoprolol in the zebrafish embryos samples	74
5.2. Metoprolol biotransformation results.....	75
5.2.1. Identification of M284	78
5.2.2. Identification of M254	85
5.2.3. Identification of M268	89
5.2.4. Identification of M226	91
5.2.5. Identification of M241	95
5.2.6. Identification of M254	96
5.2.7. Identification of M270	98
5.2.8. Identification of M282	100
5.2.9. Identification of M460	101
5.2.10. Identification of M444	103
5.3. Proposed biotransformation pathway of Metoprolol	105
Chapter 6.....	107
Conclusions	107
Chapter 7.....	109
Future Perspectives.....	109

ACRONYMS –ABBREVIATIONS	111
Appendix	113
References	115

INDEX OF FIGURES

Figure 1: Different pathways of pharmaceuticals are released into the environment.	25
Figure 2: Relationship between toxicokinetics and toxicodynamics with external and internal concentration [19].	27
Figure 3. Chemical structures and molecular weights of selected β -blockers [39]....	31
Figure 4. Metabolic pathway of Metoprolol in humans [37].....	32
Figure 5. Maximum reported concentrations (logarithmic scale of concentrations expressed in ng L-1) of antihypertensive pharmaceuticals found in surface waters [42].	
33	
Figure 6. Life stages of the zebrafish embryo a. 5 hpf, b. 24 hpf, c. 48 hpf and d. 72 hpf [16].	35
Figure 7. Screening workflow for the identification of TPs [65]	41
Figure 8. Identification confidence levels in HRMS [67].....	44
Figure 9. The Eppendorf tubes containing the shipped ZFE.	57
Figure 10. Sample preparation of water samples from exposure experiments to Metoprolol	59
Figure 11. Sample preparation of the ZFE samples from exposure experiments to Metoprolol	60
Figure 12. Identification and confirmation criteria for the identification of the bio-TPs.	
65	
Figure 13. The LC50 values from the exposure experiment of Metoprolol at each pH value.....	69
Figure 14. The % percentage of neutral species of Metoprolol at each pH value.....	70
Figure 15. Diagram of logD versus the pLC50 of Metoprolol at each pH values.	71
Figure 16. The measured concentrations of Metoprolol in the water samples at pH 6 from the start and the end of the exposure experiment.	72
Figure 17. The measured concentrations of Metoprolol in the water samples at pH 8 from the start and the end of the exposure experiment.	72
Figure 18. The measured concentrations of Metoprolol in the water samples at pH 9 from the start and the end of the exposure experiment.	72
Figure 19. The measured internal concentrations of Metoprolol in the ZFE samples.	
74	
Figure 20. Boxplots with BCF data of ZFE samples per pH value from Metoprolol exposure experiments.	75
Figure 21. Hydroxylation of Metoprolol.....	78
Figure 22. Structure of hydroxy metoprolol	79

Figure 23. EIC of M284 in RPLC and HILIC in positive ionization mode.....	79
Figure 24. MS spectra of M284 in RPLC (above) and HILIC(below) in positive ionization mode.	80
Figure 25. Common fragment ions in the MS/MS spectra of M284 (above) and Metoprolol (below)	81
Figure 26. MS/MS spectra of M284 in RPLC (above) and HILIC (below) in positive ionization mode.....	82
Figure 27. Structure and detected fragment ions of a-hydroxy metoprolol obtained by MetFrag.....	83
Figure 28. Structure and detected fragment ions of bio-TP formed through benzylic hydroxylation of Metoprolol obtained by MetFrag...	83
Figure 29. Structure and detected fragment ions of bio-TP formed through hydroxylation of the isopropyl group of Metoprolol obtained by MetFrag.....	84
Figure 30. Structure of a-hydroxy metoprolol	84
Figure 31. Structure of hydroxybenzyl metoprolol.....	84
Figure 32. Structure of O-demethyl metoprolol	85
Figure 33. EIC of M254 in RPLC (above) and HILIC (below) in positive ionization mode.	86
Figure 34: MS spectra of M254 in RPLC and HILIC in positive ionization mode.	86
Figure 35. MS/MS spectra of M254 in RPLC and HILIC in positive ionization mode.	88
Figure 36. Structure of Metoprolol acid.	89
Figure 37. EIC of M268 in RPLC (above) and HILIC (below) in positive ionization mode.	89
Figure 38. MS spectra of M268 in RPLC (above) and HILIC (below) in positive ionization mode.....	90
Figure 39. MS/MS spectra of M268 in RPLC (above) and HILIC (below) in positive ionization mode.....	91
Figure 40. Structure of N-deisopropyl metoprolol	92
Figure 41. EIC of M226 in RPLC (above) and HILIC (below) in positive ionization mode	92
Figure 42. MS spectra of M226 in RPLC (above) and HILIC (below) in positive ionization mode.....	93
Figure 43. MS/MS spectra of M226 in RPLC (above) and HILIC (below) in positive ionization mode.....	94
Figure 44. EIC of M241 in RPLC in positive (above) and negative (below) ionization modes.....	95

Figure 45. MS spectra of M241 in RPLC in positive (above) and negative (below) ionization modes	96
Figure 46. Structure of deaminated metoprolol	96
Figure 47. EIC of M254 in RPLC (above) and HILIC (below) in positive ionization mode	
97	
Figure 48. MS spectra of M254 in RPLC (above) and HILIC (below) in positive ionization mode	97
Figure 49. Structure of M254	98
Figure 50. Structure of hydroxy-demethyl metoprolol	99
Figure 51. EIC of M270 in RPLC in positive ionization mode	99
Figure 52. MS spectrum of M270 in RPLC in positive ionization mode.....	99
Figure 53. EIC of M282 in RPLC (above) and HILIC (below) in positive ionization mode	
100	
Figure 54. MS spectrum of M282 in RPLC in positive ionization mode.....	100
Figure 55. Structure of glucuronide of hydroxy metoprolol	101
Figure 56. EIC of M460 in RPLC (above) and HILIC (below) in positive ionization mode	
102	
Figure 57. MS spectra of M460 in RPLC (above) and HILIC (below) in positive ionization mode.....	102
Figure 58. MS/MS spectra of M460 in RPLC (above) and HILIC (below) in positive ionization mode.....	103
Figure 59. Structure of glucuronide of metoprolol	104
Figure 60. EIC of M444 in RPLC (above) and HILIC (below) in positive ionization mode.	
104	
Figure 61. MS spectrum of M444 in RPLC in positive ionization mode.....	104
Figure 62. Proposed Biotransformation pathway of Metoprolol in ZFE	106
Figure 63. Calibration curve of Metoprolol	113

INDEX OF TABLES

Table 1. A literature overview about the toxicity and biotransformation of pharmaceutical compounds (mainly b-blockers) in aquatic organisms	46
Table 2. Metoprolol water exposure samples.....	57
Table 3. ZFE samples accompanied with the information including the number of the embryos, their status, the exact weight of the sample and the labeling of the Eppendorfs.....	58
Table 4. The measured concentrations of Metoprolol in the exposure water samples from the toxicokinetic experiment.....	71
Table 5. The measured internal concentrations of Metoprolol in the ZFE samples ..	73
Table 6. The average BCF values of Metoprolol \pm SD at the different pH values	74
Table 7. A summary of the detected and identified bio-TPs of Metoprolol in the ZFE.	77
Table 8. LOD and LOQ derived from the calibration curve of Metoprolol.....	113

PREFACE

The current master thesis was performed at the Laboratory of Analytical Chemistry (Department of Chemistry, University of Athens, Greece) under the supervision of the Professor, Nikolaos Thomaidis.

So, first of all, I would like to thank my supervisor, Prof. Nikolaos Thomaidis, for giving me the opportunity to become a member of his research group, as well as for his valuable guidance and support during my master. Also, I would like to thank the other two members of the examination committee, Professor Evangelos Gkikas and Professor Anastasios Oikonomou for their insightful comments and remarks regarding my master thesis.

In addition, I am so grateful for the collaboration with PhD candidates Elena Panagopoulou and Dimitris Damalas that supervised my master thesis. So, I would like to warmly thank them for their valuable assistance, the time they devoted, and for the cooperation we had during the master. But most of all, I would like to thank them for conveying their love for science and their work. Also, I would like to thank the postgraduate students Nasia Drempela and Christina Gatou for their contribution in the experimental process.

A special thanks to all of the members of the laboratory and, in particular to post-doctoral researcher Maristina Nika, PhD candidate Giorgos Gkotsis for their advice and cooperation. Finally, I would like to thank my colleagues Anastasia Orfanioti and Antonia Athanasopoulou for sharing ideas and providing the most joyful working environment.

Last but not least, I would like to thank my family and my friends for the support and the encouragement throughout these two years and for every decision in my life in general.

AKNOWLEDGEMENTS

This master thesis has been financed through the program “Acidity-not always fun: pH effects on toxicity and bioaccumulation of ionic substances”

Chapter 1

Introduction

1.1. Emerging Contaminants

Emerging contaminants (ECs) or emerging pollutants (EPs) are defined as synthetic or naturally occurring chemicals, that are not currently included in (inter)national monitoring programs. However, they have the potential to enter into the environment and cause adverse effects to the ecosystem, or/and human health [1,2]. In some cases, ECs have been released in the environment for a long time, but their existence was not known until new detection methods were developed, or their ecotoxicological effects were not realized. In other cases, the synthesis of new chemicals, as well as potential changes in the use and disposal of existing chemicals, could create new sources of emerging pollutants [1,3].

According to Norman, more than 700 emerging contaminants, classified in 20 different categories, are identified in the European aquatic environment [4]. The most prominent categories are human and veterinary pharmaceuticals, personal care products, pesticides, disinfection by-products, surfactants, plasticizers, and industrial additives [1,2,5,6]. The European Union Water Framework Directive (EC, 2013) listed 45 emerging pollutants as priority compounds with environmental quality standards (EQS) to be respected in aquatic environments due to their high occurrence and their expected risk for aquatic life and (or) human health [6].

Emerging pollutants can reach the environment by being transported and distributed via different routes. The principal discharge sources of emerging contaminants in the environment are the urban and industrial wastewater treatment plants (WWTPs). This is because most of the current WWTPs are not designed to treat effectively these types of compounds [2,5]. In addition, crop and animal production and atmospheric deposition are important pathways from which the emerging pollutants enter the environment [1,2].

ECs are present in the aquatic environment in very low concentration levels of ng L^{-1} to low $\mu\text{g L}^{-1}$ range [5]. However, currently, no laws or regulations

illustrating the upper limits of concentrations of emerging contaminants in the aquatic environment exist [6].

1.2. Pharmaceutical Compounds

Human and veterinary pharmaceuticals are considered as one of the most important categories of emerging contaminants. Pharmaceuticals, such as non-steroidal anti-inflammatory drugs (NSAIDs), psychiatric drugs, cardiovascular drugs, sex and steroid hormones, human and veterinary antibiotics are designed to prevent, cure and treat disease and improve health [6–8]. Their usage and consumption are increasing consistently mainly due to the discoveries of new drugs and the expanding population [9].

After intake, human pharmaceutical compounds undergo metabolic processes in the organism. Significant fractions of the parent compound are excreted in unmetabolized form or as (active or inactive) metabolites into WWTPs. The conventional applied wastewater treatment is not efficient enough to remove pollutants, such as pharmaceutical ingredients, and as a result, they are released into the aquatic environment. Also, sewage treatment plant effluents may be reused for irrigation, and biosolids produced are reused in agriculture as a soil amendment or disposed to landfill. Thus, WWTPs are considered to be the primary pathway of pharmaceuticals to the environment. Disposal of drug leftovers to sewage and trash is another source of entry [5,6,9]. Veterinary drugs used for the treatment and prevention of diseases in farming are introduced into the environment when liquid manure is sprayed on agricultural fields as fertilizers. These veterinary drugs and their metabolites contaminate the soil and the groundwater [2,8,10]. The sources of which pharmaceuticals end up in the aquatic environment are presented in figure 1 below.

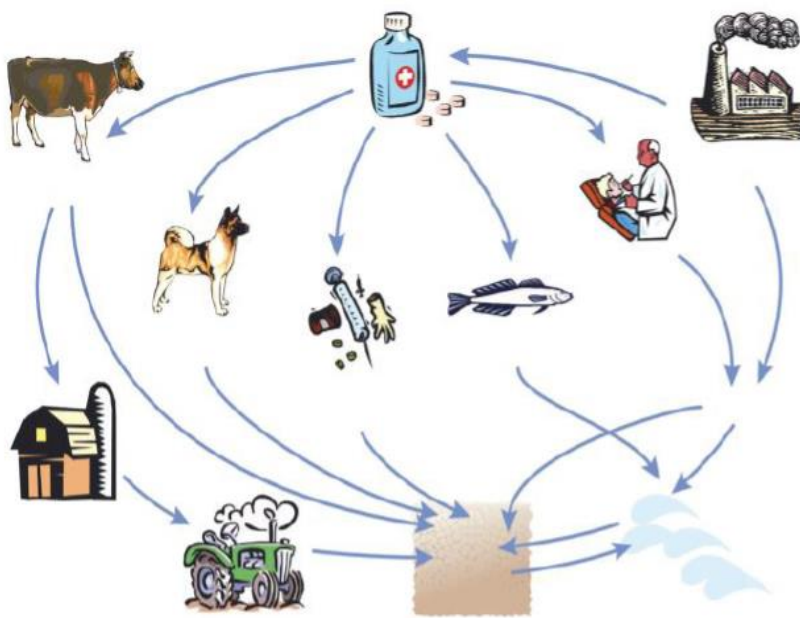


Figure 1: Different pathways of pharmaceuticals are released into the environment [11].

More than 160 different pharmaceuticals have so far been detected in aquatic ecosystems in very low concentrations of ng L^{-1} to $\mu\text{g L}^{-1}$ range [6]. Despite their relatively low concentration in the freshwater environment, once they entered the aquatic ecosystems, pharmaceutical compounds and their biologically active metabolites may bioaccumulate and cause adverse effects on aquatic organisms [9,10,12]. This is because, pharmaceutical compounds were designed to maximize their biological activity at low doses to target metabolic, enzymatic, or cell-signaling mechanisms and when they are introduced in the environment, they may affect the same pathways in aquatic organisms [7,8,10]. Until now, the knowledge about the ecotoxicological impacts of pharmaceuticals on aquatic life forms is inadequate. Pharmaceuticals are assessed for their acute toxicity using established laboratory organisms such as algae, zooplankton, and other invertebrates and fish. It has been concluded that acute toxicity to aquatic organisms is unlikely to occur at measured environmental concentrations, as acute effect concentrations are 10^3 - 10^7 times higher than residues found in the aquatic environment [2,7,8]. However, pharmaceuticals do not occur as isolated compounds, but as a complex mixture with their metabolites, other drugs, and/or chemical pollutants. Ecotoxicological data showed that mixtures have

different effects than single compounds. In some cases, the simultaneous presence of several pharmaceuticals follows the concept of addition resulting in great toxicity to non-target organisms than the predicted one for individual active substances [7,10,13]. Data of chronic effects are less investigated. However, long-term exposures are more appropriate to evaluate the potential ecotoxicological effects of the pharmaceutical compounds, because some species are exposed to these molecules for long time periods or even for their entire life cycle [2,7,10].

1.3. Toxicokinetic process and internal concentration

In routine environmental toxicity tests, it is investigated how exposure to a pollutant can cause negative effects to organisms and ecosystems. In most cases, observed effects are linked to the ambient concentration of the chemical compound to which the organisms are exposed [14]. More specifically, the concentration of the test compound in the exposure environment resulting in lethality for the 50% of the test organisms (LC50) and the concentration of the examined chemical that produces a particular effect in the 50% of the test organisms (EC50) are usually determined [15,16]. The ambient concentration of the toxicant to which the organisms are exposed is known as external effect concentration (C_{external}) [14,17]. However, only the fraction of the chemical compound that is taken up and reaches its target site is toxicologically active, and as a result, it can be harmful [14,15,17,18]. Toxicokinetic processes including uptake, distribution to target and non-target sites, metabolism, and excretion, determine the fraction of the substance that interacts with the target and may lead to toxic effects (toxicodynamics) [14,15,19,20]. The relationship between toxicokinetics and toxicodynamics is described in figure 2. Therefore, the determination of the target-site concentrations is a more accurate measurement of the toxicity of each test compound because factors related to the uptake, distribution, and biotransformation are ruled out. However, internal concentration (C_{int}) is a sufficient approximation of target-site concentration, mainly for compounds that act via nonspecific baseline toxicity [15,19,21]. So, it is concluded that the internal concentration reflects the biologically effective concentration more precisely than the external effect concentration and thus its

determination has been strongly suggested to be used in toxicity tests and for risk assessments [14].

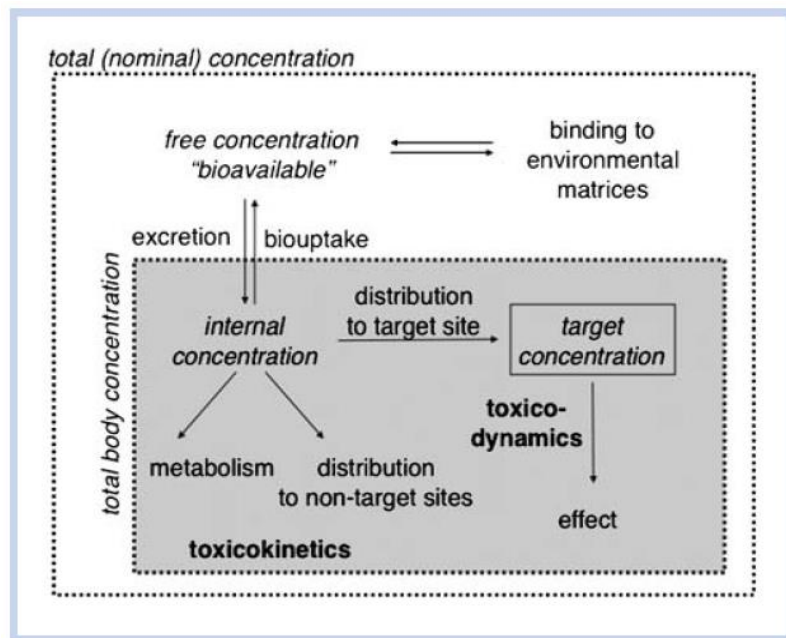


Figure 2: Relationship between toxicokinetics and toxicodynamics with external and internal concentration [19].

Various factors can affect the internal concentration of a substance in the organism, the most important of them are the physicochemical properties of the compound, the lipid content of the exposed organism, the exposure concentration of the substance as well as the exposure duration [14]. Also, the excretion and metabolism rates of the test compound are other crucial factors that influence its internal concentration. More specifically, if the excretion or the metabolism rate exceeds the uptake rate, the internal concentration of the examined substance may decrease. To account for such effects, in toxicity tests the internal concentration should be determined throughout the experiment, rather than the end only [16,18,22]. Regarding the physicochemical properties of the test compound, it is found that the uptake rate of hydrophobic (non-polar) compounds is higher than that of hydrophilic (polar) compounds [22]. As a consequence, LC50 decreases with increasing hydrophobicity expressed as the octanol/water partition (K_{ow}) [21]. However, once they arrive at their target site, polar and non-polar compounds are equally effective [15].

Biotransformation plays a crucial role in regulating the toxicity of chemical compounds in organisms. More specifically, biotransformation products (bio-TPs) may contribute significantly to the toxicity of their parent compound when they are formed with a high yield and reach high internal concentrations, they are persistent, or they are highly toxic (lipophilic compounds). In addition, the bio-TPs may have synergistic effects, as they often exhibit the same mode of toxicity action with their parent compound. As a result, the toxicity is caused by a mixture of the parent compound and the metabolite(s), even if the test organisms are exposed to a single chemical externally [19,20]. So, it is concluded that the biotransformation procedure should be taken into account in toxicity studies.

1.4. Biotransformation procedure

Metabolism or biotransformation is several enzymic reactions that are performed by hepatic and extra-hepatic enzyme systems and usually, they convert non-polar xenobiotics to more polar and less lipophilic metabolites, facilitating their elimination from the body via the urinary and biliary routes. The major site of xenobiotic metabolism for the human is the liver, while the kidney and lung comprise secondary organs for biotransformation. Biotransformation reactions are generally divided into two phases, namely phase I (functionalization reactions including oxidation, reduction, and hydrolysis) and phase II (conjugative reactions with sugars, peptides, or amino acids). During phase I, a functional group is generally introduced or uncovered in the xenobiotic molecule. Such metabolites not only are more polar than the parent compound but, furthermore, are capable of undergoing Phase II metabolism, conjugation, where endogenous substrates, e.g., glucuronic acid and sulphate, are added to them to form highly hydrophilic molecules, ensuring in this way their elimination. However, metabolism may lead to the formation of more lipophilic metabolites. Examples of such pathways are methylation and N-acetylation, producing less water-soluble and thus more bioaccumulative metabolites.

Phase I enzyme families involve flavin-containing monooxygenases, monoamine oxidases, cyclooxygenases, dihydrodiol dehydrogenases,

NAD(P)H:quinone oxidoreductases, alcohol dehydrogenases, and aldehyde dehydrogenases, but the most important are the polymorphic cytochrome P450 (CYP) enzymes, 50-60 kD heme-thiolate monooxygenases with broad substrate specificity in oxidative xenobiotic metabolism. There is a wide variety of reactions that can be catalyzed by CYP enzymes, ranging from monooxidation of compounds to the dehydration, dehydrogenation, isomerization, and reduction of substrates. Phase II enzyme families include the glutathione S-transferases (GSTs), UDP glucuronosyltransferases (UGTs), sulfotransferases (STs), and N-acetyltransferases (NATs). Epoxide hydrolases (EHs), which convert epoxides to dihydrodiols, are also classified as Phase II enzymes since they act on the products of CYP-mediated Phase I metabolism [23–27].

1.5. pH-dependent toxicity

As mentioned before, the presence of pharmaceuticals in the aquatic environment has become an issue of concern over their potential toxic effects on nontarget organisms. It has been estimated that about 80% of the active pharmaceutical ingredients are ionizable organic compounds (IOCs) and therefore they can exist in both neutral and ionic form [28–30]. The chemical speciation of the IOCs is defined both by the pK_a and by the surrounding pH value [29,31,32]. For acids, the neutral form is increasing at pH levels below the pK_a ($pH \leq pK_a$) and for bases, the neutral form is increasing at pH values above the pK_a ($pH \geq pK_a$) [32].

A chemical can cause an effect in an organism only if it is taken up from the ambient environment. The uptake of IOCs is highly affected by their speciation and hence by the different pH values. Neutral species are less polar and more hydrophobic compared with their ionic ones. The lower polarity of the neutral species enables faster permeation through membranes, whereas ionic forms show hindered uptake [17,28,29]. For the majority of the IOCs, the permeability of the ion is between 1.000 and 10.000 times slower than that of the neutral species [32]. The speciation-dependent uptake results in the pH-dependent toxicity of IOCs, with higher toxicity at pH levels where the neutral species are predominant [29,31,33]. More specifically, for acids, the uptake and toxicity are higher in pH levels below the pK_a , whereas bases are more toxic at pH values

above the pKa [29,32,34]. As a result, LC50 values of the IOCs differ at different pH levels. It is observed that an increasing neutral fraction of the IOCs is accompanied by a decreasing LC50 value [28,33]. Respectively, the bioaccumulation potential of the IOCs exhibits high pH-dependency. Bioaccumulation is commonly described using as a measurement of the whole-body bioconcentration factor (BCF) and it has been reported that BCF increases at pH values where the neutral fraction dominates, indicating a higher potential for bioaccumulation [28,29,32,35]. Therefore, it is concluded that the pH of the environment is a crucial factor for the uptake, toxicity, and bioaccumulation of the IOCs, because slight shifts in the surrounding pH values, can alter the speciation of the chemical compounds and thus their toxicity. Thus, it is suggested that pH should be taken into consideration in environmental risk assessments of such compounds [29,30].

Regarding, the external effect concentration (EC) is strongly affected by the pH of the environment. The pH dependence of the external EC originated from the speciation-dependent uptake. More specifically, an increase in the neutral fraction is associated with a decrease in the external EC. However, the pH-dependence toxicity of external EC is not translated to the dependence of internal effect concentration (IEC) from the surrounding pH values. This means that the chemical speciation of the compound is relevant only for its uptake and not for the intrinsic toxicity. Therefore, it is strongly recommended to use internal concentration for evaluating the toxicity of IOCs [29,31].

1.6. Metoprolol

1.6.1. Metoprolol as a pharmaceutical compound

Metoprolol is a cardioselective β -adrenergic receptor blocker or β -blocker, commonly used in the treatment of cardiovascular disorders, including arterial hypertension, abnormal heart rhythms, and angina pectoris [36–38]. It is also used in veterinary medicine and illegally as doping in many sports [39]. Other widely known β -blockers are propranolol, atenolol, labetalol, and sotalol. Some of the compounds that belong to the category of β -blockers are presented in figure 3.

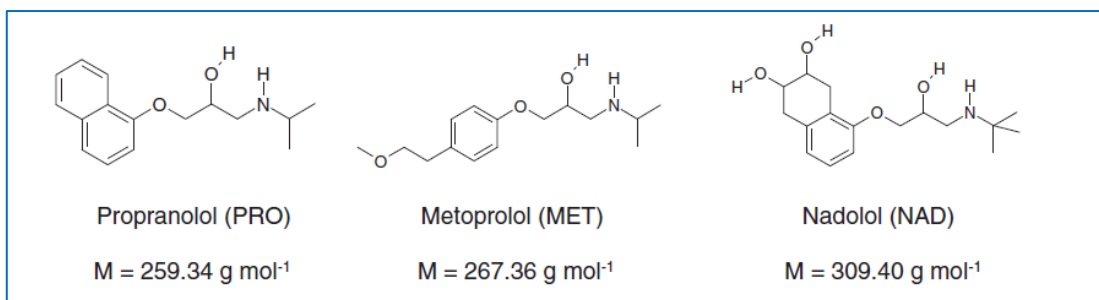


Figure 3. Chemical structures and molecular weights of selected β -blockers [39].

Metoprolol in the human body is absorbed by the intestine rapidly and almost completely; however, due to extensive first-pass metabolism, the bioavailability of Metoprolol is only approximately 50%. The half-life is in the range of 3–4 h in young adults and between 7–9 h in elderly patients [37]. The biotransformation of Metoprolol is extensive with less than 5% of an oral dose being excreted in non-metabolized form by the kidneys [37,40].

Metoprolol is primarily metabolized by hepatic cytochrome 2D6 (CYPD6), which is responsible for the metabolism of 25% of all xenobiotics [40]. Major metabolic pathways are O-demethylation to O-demethyl metoprolol and its further oxidation to metoprolol acid, N-dealkylation to N-deisopropyl metoprolol (10%), and α -hydroxylation to α -hydroxy metoprolol (10%). The α -hydroxy metoprolol and O-demethyl metoprolol are active, but they only contribute approximately 10% of the total β -blocking activity of Metoprolol [37]. A potential metabolic pathway of Metoprolol in human is described in figure 4. Approximately 85% of Metoprolol is excreted as metabolites in the urine, as well as a small amount as unmetabolized drug [26,37,38,40,41].

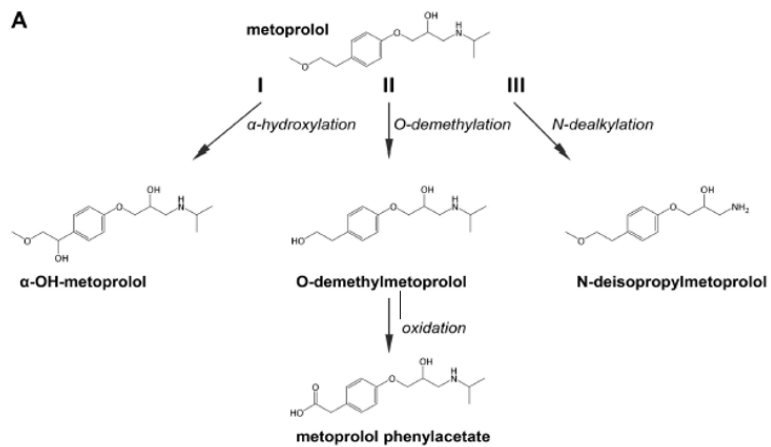


Figure 4. Metabolic pathway of Metoprolol in humans [37].

1.6.2. Metoprolol in the aquatic environment

B-blockers, such as Metoprolol, are one of the most frequent classes of pharmaceutical compounds which are detected in the environment. The main factors that cause the high presence of b-blockers in the aquatic environment are the rapidly growing pharmaceutical industry, the increasing consumption of these drugs all over the world, and their inefficient removal from the conventional WWTPs [42,43]. Among the b-blockers that are reported in the environment, the scientific community has mainly directed their attention to Atenolol and Metoprolol, because they are the antihypertensives that presented the highest maximum reported concentration in fresh surface waters [42], as it is shown in figure 5. More specifically, the maximum reported concentration of Metoprolol in surface waters is $2.2 \text{ } \mu\text{g L}^{-1}$ [42,44]. The high degree of persistence may be another reason for the frequent presence of b-blockers in the aquatic environment. It has been reported that the half-life of Metoprolol in the aquatic environment at 25°C can be more than 1 year [42].

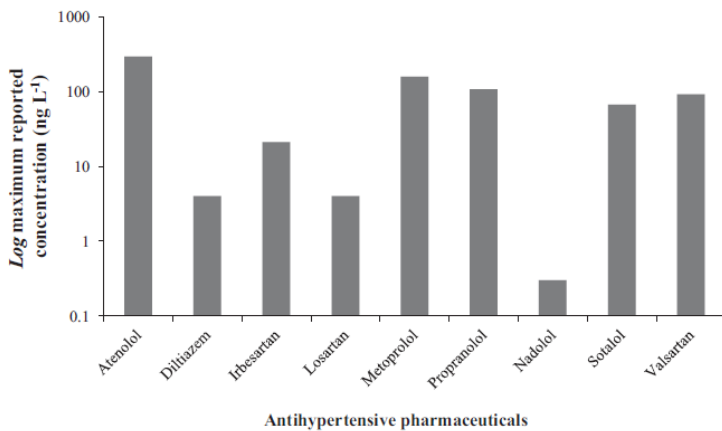


Figure 5. Maximum reported concentrations (logarithmic scale of concentrations expressed in ng L⁻¹) of antihypertensive pharmaceuticals found in surface waters [42].

Phytoplankton, zooplankton, invertebrates, and fish are species commonly employed to test the ecotoxicity of b-blockers in the environment [36]. B-blockers act by competitive inhibition of beta-adrenergic receptors, a class of receptors critical for normal functioning in the sympathetic branch of the vertebrate autonomic nervous system in vertebrates [13]. Fish, like other vertebrates, possess b-receptors in the heart, liver, and reproductive system so that prolonged exposure to drugs belonging to this therapeutic class may cause deleterious impacts including disrupting their testosterone levels and decreasing the growth, fecundity, and reproduction rates [13,36,39].

1.7. Zebrafish as a model organism

Zebrafish (*Danio rerio*) is a small, vertebrate, freshwater species [45]. Zebrafish has been established as a model organism in different fields, such as drug discovery, pharmacology, developmental biology, genetic research, embryology, and ecotoxicology [16,27,45–47]. Mammalian species, such as rats, mice and dogs were used in all the above fields. However, the testing with mammals was time-consuming and cost-effective [48]. The use of zebrafish has been explored as an alternative model to mammalian species due to its numerous advantageous traits [48,49]. The main benefits of using zebrafish as a toxicological model over other vertebrate species are regarding their size, husbandry, and fast development [46,50].

Zebrafish are very small. More specifically, zebrafish adults are approximately 1-1.5 inches long. Their minute size minimizes the test cost [46,51,52]. This is because the ability to culture a large number of zebrafish in a small volume of media requires only micrograms of each test compound for screening [48,53,54]. In addition, zebrafish has a short generation time of approximately 3-5 months, while it breeds almost all year round. Its high fecundity provides a large number of completely transparent embryos that develop outside of the mother (*ex utero*) [45,46,50,53]. It is estimated that 100-200 embryos per female can be produced in a single spawning per week [46,47,49]. The optical clarity of embryos facilitates their observation of tissue formation and organogenesis *in vivo* and manipulation of the embryos [46,49,53].

The fish embryo becomes larva at hatching or when it begins exogenous feeding. The larva undergoes metamorphosis into a juvenile and finally being termed an adult when it is sexually mature. The zebrafish hatching takes place between 48 and 72 hours post fertilization (hpf), while sex determination occurs after 21 days post fertilization (dpf) [50,53]. The life stages of the zebrafish embryo are presented in figure 6. Another significant feature of *Danio rerio* is its high genomic homology with humans (over 80%), which enables a correlation of the obtained data between the two species [52,55]. Furthermore, it has great similarities in nervous, cardiovascular, respiratory, endocrine, immune, and reproductive systems to mammal species [47]. Another important trait of zebrafish is its high pH tolerance, making it a great model organism for environmental toxicity tests [29].

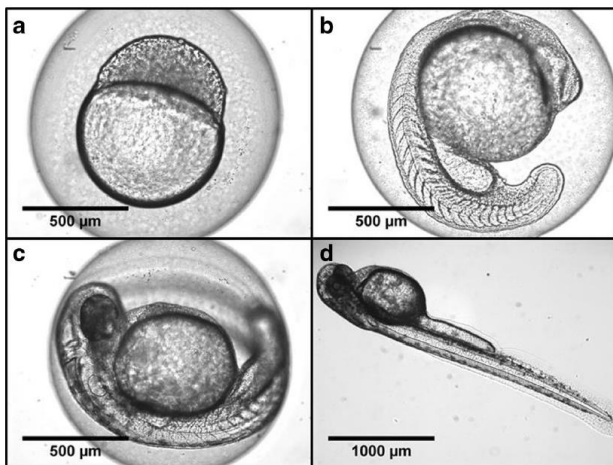


Figure 6. Life stages of the zebrafish embryo a. 5 hpf, b. 24 hpf, c. 48 hpf and d. 72 hpf [16].

Lately, there is a great interest in using the early life stage embryos as a tool for investigating the effects of contaminants in aquatic organisms as an alternative to the testing of juvenile or adult animals [29,45]. *Danio rerio* embryos are more sensitive to the tested compounds than juvenile and adult fish. The difference in sensitivity might be a result of different factors. First of all, the enzymatic system of embryos has not been developed properly yet. Also, there are important differences in absorption of the compounds into the organisms, since zebrafish embryos absorb the substance through their membranes, because their organs, such as gills, are not fully developed. Finally, there might be differences in the metabolism of chemical compounds between embryos and adult zebrafish [45]. The fish embryo test (FET) with zebrafish (*Danio rerio*) has been recommended and standardized by the Organization for Economic Co-operation and Development (OECD) as part of environmental risk assessments. In the FET with zebrafish, sublethal effects are usually observed determining LC50 values, as well reproductive, behavioral, and morphological effects [16,47].

Chapter 2

Literature Review

2.1. Metoprolol aquatic toxicity

In the ecotoxicological assessment of β -blockers, such as the Metoprolol, acute effects such as the reproduction, hatching and heart rate, and mortality of the aquatic organisms, were commonly investigated. Many studies have assessed the acute effects of β -blockers (metoprolol) on aquatic organisms, such as *Daphnia magna* and *Lemna minor*. More specifically, Cleuvers determined the EC50 value: 438 mg L⁻¹ of Metoprolol in the acute toxicity test with *D. magna*. Additionally, in this study, the BCF value and the internal effect concentration (IEC) of Metoprolol on the EC50 value were determined. The BCF value was found 0.89 and the IEC=0.57 mmol L⁻¹ [56]. On the other hand, in another study, Hugget et al. determined the LC50 value of Metoprolol 63.9 mg L⁻¹ in 48 h toxicity test with *D. magna* which is significantly lower than that of Cleuvers' study [57]. E. van den Brandhof et al. studied the effects of Metoprolol in zebrafish embryo heartbeat, hatching rate and mortality. After 72 h exposure, the No Observed Effect Concentration (NOEC) of Metoprolol was found 12.6 mg L⁻¹, while at 50.5 mg L⁻¹ effects on hatching, heartbeat and heart deformation were observed. Finally, the EC50 value was determined 31.0 mg L⁻¹ and the LC50 value \geq 101 mg L⁻¹ [58].

2.2. Metoprolol pH-dependent toxicity

Metoprolol is an IOC and therefore its chemical speciation, ionic or neutral form, is defined by the pH values of the surrounding environment. More specifically, Metoprolol is a secondary amine with pKa= 9.68. This means that at acidic and neutral pH values, its cationic form is the predominant one, while the neutral fraction is increasing towards alkaline conditions. Therefore, it is expected that the uptake and thus the toxicity of Metoprolol are increasing with increasing of pH values [29].

Bittner et al. investigated the pH-dependent effects of Metoprolol in the ZFE at three pH values, 7.0, 8.0, and 8.6, within 96 hpf. In this study, the LC50 values

of Metoprolol at each pH value were determined and it was found that the LC50 decreased from 1.91 mM at pH 7.0 to 0.054 mM at pH 8.6. This difference was related to the increased neutral fraction. Also, the internal concentrations of Metoprolol at the LC10 were determined and they were in a similar range for all pH values, concluding that the internal concentrations are pH-independent. Furthermore, the BCF values were calculated at the different pH values for assessing the influence of pH values on the bioaccumulation of Metoprolol. More specifically, the BCF value increased from 1.96 at pH 7.0 to 32.0 at pH 8.6. These findings indicated that the BCF values, and so the bioaccumulation of Metoprolol, increased with increasing the neutral fraction [29].

2.3. Biotransformation of Metoprolol

The biotransformation of toxicants aims to convert the latter to more hydrophilic compounds facilitating their excretion from the body. However, in some cases, the formed metabolites exhibit higher toxicity than the parent compound or they formed in high yield contributing to the internal concentration of the parent compound, as mentioned in Chapter 1. Since the biotransformation of xenobiotics seems to affect the toxicity, bioaccumulation, and internal concentration of the parent compound in non-target organisms, it should be investigated in ecotoxicity tests.

Until now, the biotransformation of the β -blockers in aquatic organisms has not been investigated to a great extent in the toxicity tests. More specifically, regarding the β -blocker propranolol, two studies have focused on its biotransformation in aquatic organisms. T. Miller et al. detected two biotransformation products of Propranolol in *Gammarus pulex*, the 4-hydroxy-propranolol and the 4-hydroxy-propranolol sulfate [59]. Also, A. Ribbenstedt et al. studied the biotransformation of propranolol in ZFE and they identified eight biotransformation products [60].

Regarding the substance Metoprolol, to the best of our knowledge, there is no literature about its biotransformation in aquatic organisms. However, Metoprolol is a compound of interest, because it is one of the most usually prescribed pharmaceuticals for the treatment of cardiovascular diseases. Metoprolol is heavily metabolized into the human body and 85% of Metoprolol is excreted as

metabolites. The main human metabolites of Metoprolol are α -hydroxy metoprolol, O-demethyl metoprolol, and metoprolol acid. As a result, the Metoprolol and its metabolites reach the wastewater [37]. However, due to their ineffective removal from the conventional WWTPs, they end up in the aquatic environment. Because of the presence of Metoprolol and its metabolites in the wastewater, many studies investigate their elimination through different wastewater treatments [26,43].

Among them, A. Gil et al. investigated the degradation and the transformation of Metoprolol with fungi during water treatment and they identified 14 transformation products of Metoprolol. Among them, the α -hydroxy metoprolol was classified as one of the major biotransformation products [26]. Moreover, Rubirola et al. studied the removal of Metoprolol in activated sludge and five transformation products were detected, the three of which were α -hydroxy metoprolol, O-demethyl metoprolol and metoprolol acid [61]. Also, the biotransformation of Metoprolol by the fungus *Cunninghamella blakesleeana* was studied by B. MA et al. and they found that Metoprolol was transformed to seven metabolites: O-demethyl metoprolol, metoprolol acid, N-desacyl metoprolol, deaminated metoprolol, α -hydroxy metoprolol, hydroxy-O-demethyl metoprolol, and glucoside conjugate of metoprolol [41]. All these studies highlight the importance of studying the effects of Metoprolol and its potential biotransformation products in aquatic organisms, since it is released in the aquatic environment.

2.4. Methods of determination of Metoprolol and other pharmaceutical compounds

2.4.1. Sample preparation

Before the sample preparation of ZFE, it is important to wash carefully the ZFE with double distilled water [28,29,62,63]. The aim of the washing step is to ensure that no chemical of the exposure medium would carry over. However, intensive washing could lead to loss of the analyte.

The first step of the sample preparation of the ZFE is the analyte's extraction with the proper solvent(s) through homogenization and (ultra)sonication. The

most commonly used extraction solvents are MeOH or a mixture of MeOH:H₂O [28,29,62,63]. Some studies recommend the use of two-step extraction to obtain higher extraction yield and reproducibility [64]. The extraction is followed by centrifugation. The supernatants are collected, and if necessary, they are diluted until the concentration of the analyte reaches the linear dynamic range of the instrument [22,29]. Finally, the samples are stored at low temperatures (-80°C) until their analysis [64].

2.4.2. Analytical techniques

For the identification of emerging contaminants and their transformation products (TPs) in environmental samples, liquid chromatography (LC) coupled to mass spectrometry (MS) is a technique of choice. This is because, the majority of the emerging contaminants are non-volatile; thus, they are highly compatible with LC. Regarding the TPs, they are generally more polar than their parent compound, and therefore LC is a suitable technique. The most commonly used mass analysers for the detection and identification of TPs are the triple quadrupole (QqQ), time-of-flight (ToF), orbitrap, and ion-trapping (IT). High-resolution mass spectrometry (HRMS) is preferred due to its high sensitivity in full scan acquisition mode and its high mass accuracy. Moreover, HRMS permits target, suspect, and non-target data processing, which is necessary for the TPs discovery. Another advantage of HRMS is its capacity of differentiation of isobaric compounds with the same nominal mass, but different molecular formulas due to their higher resolving power [65].

Using a complementary analytical technique is usually crucial for the successful unambiguous identification of TPs. Nuclear magnetic resonance (NMR) is one option of a complementary technique. Additionally, the combination of reversed-phase liquid chromatography (RPLC) and hydrophilic interaction liquid chromatography (HILIC) coupled to MS has emerged as an alternative powerful tool. The combinatorial use of RPLC and HILIC expands the number of detected analytes and provides more comprehensive metabolite coverage in comparison with the use of RPLC only. HILIC has numerous advantages as a complementary technique. Firstly, HILIC is fully compatible with ESI. Its increased organic solvent content enhanced the ionization efficiency and hence

the detection sensitivity. Therefore, some TPs may be detected only by HILIC. Another important benefit of HILIC is its capacity to separate structural isomers, that they have the same molecular formula, and hence they cannot be separated in terms of MS, even with HRMS instruments. Finally, HILIC may provide extra experimental results (MS/MS) for already detected TPs by RPLC enhancing the identification confidence level (orthogonal identification). For all the above reasons, HILIC is used as a complementary technique to RPLC [64,66].

2.5. Identification approaches

Liquid chromatography high-resolution mass spectrometry (LC-HRMS) is commonly used for the investigation of emerging contaminants and their transformation products (TPs) in environmental samples. After the HRMS analysis, raw data can be treated with three different approaches, target, suspect and non-target screening for the identification of the tentative TPs. The main screening workflow is described below and is elucidated in figure 7.

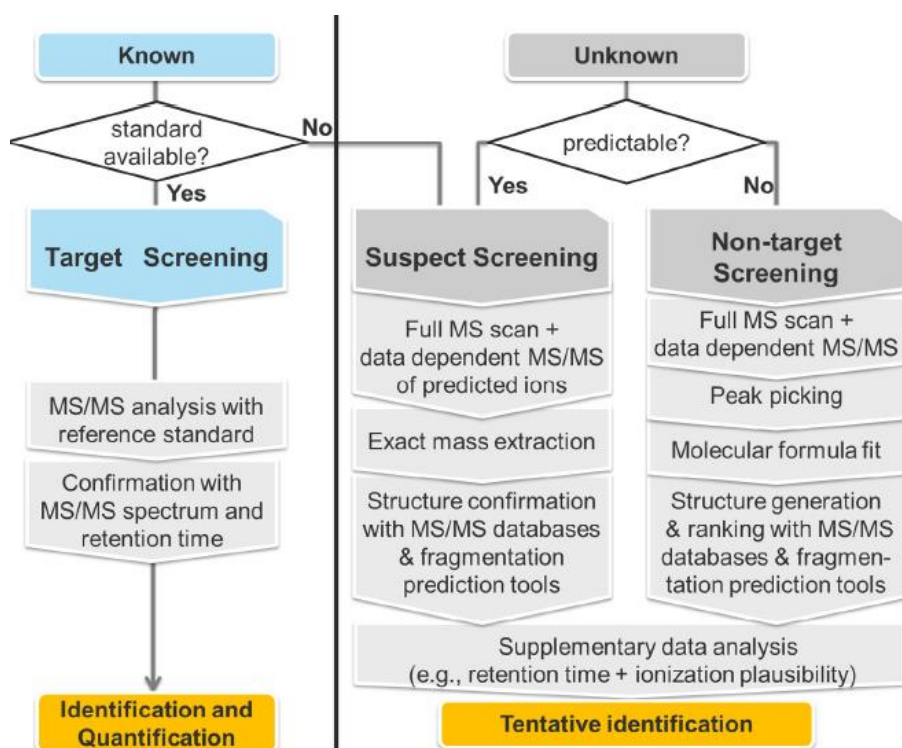


Figure 7. Screening workflow for the identification of TPs [65]

2.5.1. Target screening

Target analysis relies on the determination of already known TPs, and the identification is carried out with reference standard solutions. The reference standards should be measured under the same analytical conditions. The identification is based on mass accuracy, isotopic pattern, retention time, and if possible, MS/MS fragments.

2.5.2. Suspect screening

The suspect screening approach is carried out for the identification of TPs, for which no reference standards are available. However, their molecular formula and the structure can be predicted using *in-silico* prediction tools, such as the Metabolite Predict. So, the initial step for suspect screening is the compilation of a database containing compound-specific information for the suspected compounds. The following step is the screening of the samples with the database. Subsequently, the exact molecular mass of each tentative TP is extracted from the chromatogram and it is compared with control samples. The identification of the TPs through suspect screening relies on criteria, such as mass accuracy, retention time, isotopic pattern fitting, and ionization efficiency. The structure proposal relies on the MS/MS interpretation.

2.5.3. Non-target screening

Non-target screening implies after target and suspect screening, for the identification of compounds for which no previous knowledge is available. HRMS is required for the non-target screening to achieve high mass accuracy for confirmation of the molecular formula and reliable interpretation of the MS/MS spectra. The initial step in non-target screening approach is peak picking. In this step, the comparison of the samples with control samples is so important. The next step is the removal of noise peaks, mass recalibration, and componentization of isotopes and adducts. If the molecular formula of the tentative TP is confirmed, information for a possible structure should be collected. Databases, such as ChemSpider and PubChem, may lead to candidate structures. Structural evidence of the parent compound can restrict the number of the possible structures, relied on the assumption that many TPs

have the same fragmentation pattern with their parent compound. Additionally, criteria must be implemented for the identification of TPs, as well in suspect screening. Finally, orthogonal analytical approaches are usually crucial for the successful identification of TPs [65].

2.6. Identification confidence levels

The detection and identification of small compounds, such as emerging contaminants and their biotransformation products in environmental samples, has been improved to a great extent, due to the increased availability of high-resolution mass spectrometry (HRMS). However, confidence in these HRMS-based identifications varies between studies and substances making the communication of identification confidence to readers difficult and inaccurate. For this reason, a system of identification levels proposed by Schymanski et al., which is illustrated in figure 8, is commonly used.

Level 1. Confirmed structure. The confirmation of a structure is feasible only if a reference standard for the compound(s) of interest is available. The confirmation relies on the MS, MS/MS, and retention time matching. An orthogonal analytical approach is recommended.

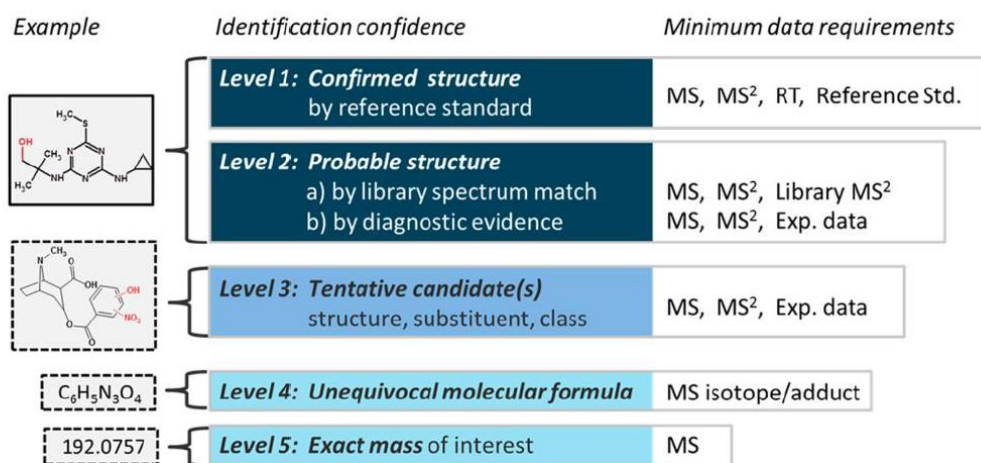
Level 2. Probable structure. The proposal of a possible structure relies on different evidence. **Level 2a: Library** spectrum data match with the experimental data unambiguously. Different acquisition parameters need to be wisely considered during spectrum comparison aiming at a valid match and the decision criteria should be presented. Additional evidence, such as retention time behavior is desirable. **Level 2b: Diagnostic** describes the case where no reference standard or literature information is available for confirmation, but according to the experimental evidence, no other structure fits. Evidence can include diagnostic MS/MS fragments and/or ionization behavior.

Level 3. Tentative structure(s) describes a grey zone, where experimental evidence exists for possible structure(s), but it is insufficient for proposing one structure only (e.g., positional isomers).

Level 4. Unequivocal molecular formula is possible when a formula can be unambiguously assigned using the experimental evidence (adduct ions, isotope

fitting et al.), but due to the inadequate evidence (absent or uninformative MS/MS), no structure can be proposed.

Level 5. Exact mass (m/z) can be determined, but lack of information about a formula or structure. The use of blank and control samples is recommended to ensure that the found masses do not arise from the sample, the sample preparation, or the measurement [67].



Note: MS² is intended to also represent any form of MS fragmentation (e.g., MS^e, MSⁿ).

Figure 8. Identification confidence levels in HRMS [67]

2.7. Literature review table

An overview of current existing literature on toxicity assessment and the biotransformation of different pharmaceuticals (mainly β -blockers) in aquatic organisms is presented in table 1. More specifically, information about the name of the examined compound(s), the analytical technique of choice for their determination and the chosen model organism, is given. For the studies that are focused on the assessment of toxicity, the LC50 or EC50 values, and the BCF values are provided in the table. Moreover, data regarding the chosen pH values are provided for investigations about the pH-dependent toxicity of β -blockers.

As it can be observed, the chosen pH range (5.0-8.6) in different studies is common, since it is environmentally relevant. Regarding the determination of the pharmaceutical compounds, LC-HRMS techniques were used. More

specifically, the most frequently used techniques were the LC-ESI-QTOF-MS and LC-ESI-Orbitrap-MS, especially in studies that focused on the identification and structural determination of the plausible biotransformation products. Because of the absence of literature about the biotransformation of the compound of interest, Metoprolol, in aquatic organisms (such as zebrafish), the table includes information about the bio-TPs of Metoprolol formed by fungi and bacteria during the wastewater treatment.

Table 1. Literature overview about the toxicity and biotransformation of pharmaceutical compounds in different organisms

a/a	Analyte(s)	Detected bio-TPs	Organism	pH-values	Sample Preparation	Technique	LC50/ IEC & BCF values	Reference
1	Metoprolol Propranolol Atenolol Labetalol	-	Zebrafish (<i>Danio rerio</i>) embryos	Metoprolol: pH: 7.0, 8.0, 8.6 Other compounds: pH: 5.5, 7.0, 8.0	Embryos samples: Decoloration & washing with MeOH:H ₂ O (20:80) & snap-freezing in liquid N ₂ . Extraction with MeOH or ACN:ammonium acetate (1:1) in a FastPrep homogenizer followed by ultrasonication	HPLC-MS/MS	LC50 (mmol L⁻¹) Metoprolol: 1.91 (pH 7.0), 0.174 (pH8), 0.054 (pH8.6) Propranolol 2.42 (pH 5.5), 0.128 (pH7), 0.023 (pH8) BCF values Metoprolol: 1.96 (pH 7.0), 12.7 (pH8), 32.0 (pH8.6) Propranolol 1.86 (pH 5.5), 23.6 (pH7), 169 (pH8)	[29]
2	Metoprolol Diclofenac Carbamazepine	-	Zebrafish (<i>Danio rerio</i>) embryos	pH: 8.0	-	UPLC-ESI-MS	Metoprolol NOEC= 12.6 mg L ⁻¹ EC50= 31.0 mg L ⁻¹ LC50= 100 mg L ⁻¹	[58]

a/a	Analyte(s)	Detected bio-TPs	Organism	pH-values	Sample Preparation	Technique	LC50/ IEC & BCF values	Reference
3	Propranolol Metoprolol Atenolol	-	<i>Daphnia magna</i>	pH 7.8	-	-	EC50 (mg L-1) Metoprolol: 438 Propranolol: 7.7 Atenolol: 313 BCF value: Metoprolol: 0.89 Propranolol: 4.47 IEC (mmol L-1) Metoprolol: 0.57 Propranolol: 0.12	[56]
4	Metoprolol Clofibric acid Valproic acid etc al.	-	Zebrafish (<i>Danio rerio</i>) embryos	pH 7.4	Embryos samples: Decolorization & washing with double distilled water. Extraction of the ZFE with MeOH and ultrasound. Adding equal parts of water for analysis with HPLC-MS/MS.	HPLC-QTrap-MS	Metoprolol BCF value 0.6 Relative internal concentration = 0.64 ± 0.25	[22]

a/a	Analyte(s)	Detected bio-TPs	Organism	pH-values	Sample Preparation	Technique	LC50/ IEC & BCF values	Reference
5	<u>Bases:</u> Metoprolol Propranolol <u>Acids:</u> Diclofenac Genistein Naproxen	-	Zebrafish (<i>Danio rerio</i>) embryos	Metoprolol: pH: 7.0, 8.0, 8.6 Other compounds: pH: 5.5, 7.0, 8.0	Embryos samples: Dechorionation and washing with MeOH:H ₂ O (20:80) & snap-freezing in liquid N ₂ . <u>Extraction</u> with MeOH or MeOH:Milli-Q (1:1 v:v) in a FastPrep homogenizer followed by ultrasonication. Centrifugation and collection of the supernatants for HPLC-MS/MS analysis.	HPLC-MS/MS	<u>LC50</u> (µM) Metoprolol: 1914 (pH7.0), 174 (pH8), 53.8 (pH8.6) Propranolol 2417 (pH 5.5), 128 (pH7), 22.8 (pH8) <u>BCF values</u> Metoprolol: 2.68 (pH7.0), 12.4 (pH8), 52.0 (pH8.6) Propranolol 2.33 (pH5.5), 33.3 (pH7), 234 (pH8)	[28]

a/a	Analyte(s)	Detected bio-TPs	Organism	pH-values	Sample Preparation	Technique	LC50/ IEC & BCF values	Reference
6	Metoprolol Propranolol Carbamazepine Diazepam etc al.	Propranolol bio-TPs: 4-hydroxy propranolol & 4-hydroxy propranolol sulphate	<i>Gammarus pulex</i>	pH 8.2	Embryos samples: <u>Extraction</u> of lyophilised and ground material with ACN and dilution with ammonium acetated buffer for SPE. Elution with ethyl acetate: acetone (1:1 v:v) with subsequent evaporation under N ₂ and reconstruction with ammonium acetate:ACN (90:10 v:v).	HPLC-ESI-QqQ-MS	BCF_{parent} (L kg ⁻¹) Metoprolol: 37 Propranolol: 72 BCF_{parent} (L kg ⁻¹) Metoprolol: 17 Propranolol: 22	[59]
7	Propranolol	8 bio-TPs: Hydroxy -propranolol, Dihydroxy propranolol Hydroxy propranolol glucuronide, Propranolol glucuronide, Hydroxy propranolol sulfate, N-deisopropyl- metoprolol, 1-Naphthol 3-(isopropylamino)-1,2-propendiol	Zebrafish (<i>Danio rerio</i>) embryos	-	Embryos samples: Removal of the exposure water and subsequent freezing the ZFE on dry ice. <u>Extraction</u> by homogenizing the ZFE in-plate using stainless stell beads with MeOH-chloroform mixture. Sonication and centrifugation before the analysis.	HPLC-MS/MS & RPLC-Orbitrap-MS (- ESI mode) & HILIC-Orbitrap-MS (+ ESI mode)	-	[60]

a/a	Analyte(s)	Detected bio-TPs	Organism	pH-values	Sample Preparation	Technique	LC50/ IEC & BCF values	Reference
8	Clofibric acid	14 bio-TPs Hydroxylation, Sulfate conjugation, Glucuronide conjugation, Taurine conjugation, Carnitine conjugation, Aminomethanesulfonic acid conjugation, Methylation	Zebrafish (<i>Danio rerio</i>) embryos	-	Embryos samples: Washing with double distilled water and shock freezing with liquid N ₂ . Extraction with MeOH and sonication. Evaporation an aliquot of the methanolic extraction to dryness and dissolving the solid with H ₂ O:MeOH (80:20 v:v).	HPLC-ESI-QTOF-MS	-	[63]
9	Benzotriazole, 4-Methyl-1-H-benzotriazole, 5-Methyl-1-H-benzotriazole	Hydroxylation, N- & O-Glucuronide conjugation, N- & O-Sulfate conjugation	Zebrafish (<i>Danio rerio</i>) larvae	-	Larvae samples: Rinsing twice with water and snap-freezing in liquid N ₂ . Homogenization with MeOH: H ₂ O (1:1 v:v) with electric homogenizer (<u>1st extraction</u>). Centrifugation and collection of the supernatant. Extraction of the pellet with CH ₂ Cl ₂ : methanol (3:1 v:v) (<u>2nd extraction</u>) and centrifugation	HPLC-ESI-QTOF-MS (+/-)	<u>LC50</u> (μ g mL ⁻¹) 4-MeBT: 59 5-MeBT: 128 BT: 170	[64]

a/a	Analyte(s)	Detected bio-TPs	Organism	pH-values	Sample Preparation	Technique	LC50/ IEC & BCF values	Reference
10	Metoprolol Metoprolol acid	14 bio-TPs of Metoprolol Hydroxylation N-deaclylation O-demethylation Oxidation	3 fungi (<i>Ganoderma lucidum</i> , <i>Trametes versicolor</i> , <i>Pleurotus ostreatus</i>)	pH 4.5	-	LC-LTQ-Orbitrap-MS/MS	-	[26]
11	Metoprolol	7 bio-TPs: O-demethyl metoprolol Metoprolol acid a-hydroxy metoprolol N-desacyl metoprolol Deaminated metoprolol Hydroxy-O-demethyl metoprolol Glucoside conjugate of O-demethyl metoprolol	fungus <i>Cunninghamella Blakesleeana</i>	-	-	LC-ESI-IT-MS (+/-)	-	[41]
12	Metoprolol	5 bio-TPs: O-demethyl-metoprolol Metoprolol acid a-hydroxy metoprolol TP226, TP282	Bacteria <i>Vibrio fischeri</i>	pH 7.7-7.8	-	UPLC-ESI-LIT (+)	-	[61]

Chapter 3

Scope and Objectives

The release of pharmaceuticals in the aquatic environment has become an issue of concern among scientists because they might cause harm to aquatic organisms and/or human health. The ecotoxicological effects of the pharmaceutical compounds in the aquatic life forms may be influenced by many different environmental factors. An utmost important factor is the surrounding pH values. This is because, the majority of the pharmaceuticals are IOCs, and therefore their chemical speciation (neutral or ionic species) is strongly dependent on the environmental pH values. The uptake and thus the toxicity of the IOCs are affected by their speciation, and hence by the different pH values. More specifically, a higher percentage of neutral species leads to enhanced uptake and bioaccumulation and thereby toxicity. However, the influence of pH values on the toxicity of the IOCs has not been investigated extensively.

Amongst IOCs, Metoprolol, with $pK_a=9.68$, is one of the most commonly used β -blockers in the treatment of cardiovascular diseases worldwide. As a result, Metoprolol is frequently detected in the aquatic environment in a concentration range from ng L^{-1} to $\mu\text{g L}^{-1}$. However, there are limited studies as far as its pH-dependent toxicity, while its biotransformation in aquatic organisms has not been studied at all.

The zebrafish embryo has emerged as a powerful model organism in environmental toxicity tests for evaluating the potential effects of xenobiotics on aquatic organisms due to its numerous beneficial traits. The main advantages of the ZFE are its rapid development, its high genomic homology with humans (over 80%), and its high capacity for xenobiotics biotransformation.

Considering all the above, the main objective of the current study was the assessment of the influence of three different environmentally relevant pH values (6, 8, and 9) on the uptake, bioaccumulation, and toxicity of Metoprolol in the ZFE. For a better interpretation of the above, another objective was to determine the LC50 values of Metoprolol, the internal concentrations (C_{int}) in ZFE, as well as the bioconcentration factors (BCFs) at the three pH values.

Another important goal was to investigate the biotransformation capacity of the ZFE exposed to Metoprolol by determining its biotransformation products. The final goal was to propose a potential biotransformation pathway of Metoprolol in the ZFE.

For this purpose, the fish embryo test (FET) with ZFE was conducted to derive the LC50 values of Metoprolol at the three pH values. Subsequently, the ZFE were exposed to Metoprolol at a concentration equivalent to their LC50 at each pH value. The water and the ZFE samples from the exposure experiment were analyzed utilizing LC-ESI-QTOF-MS. The analysis of the ZFE was carried out by both chromatographic techniques (RPLC and HILIC) in both ionization polarities (positive and negative) to detect as many biotransformation products as possible. For the identification of the parent compound Metoprolol target screening approach was followed, while the suspect screening approach was used for the identification of the biotransformation products.

Chapter 4

Materials and Methods

4.1. Chemicals

Metoprolol reference standard material was high purity ($99.0 \pm 1\%$) and was purchased as a powder from A2S, France. The isotope-labeled internal standard (I.S.), Metoprolol-D7, with purity 99.0% and was supplied from A2S, France with concentration $100 \mu\text{g mL}^{-1}$. The Metoprolol stock standard solution ($1000 \mu\text{g mL}^{-1}$) was prepared in distilled water (H_2O). The stock standard solution of Metoprolol was stored in an amber glass bottle at -20°C , while the I.S. Metoprolol-D7 was stored at 4°C .

Regarding the materials used during the sample preparation procedure, bulk beads, 1.4 mm (zirconium oxide) from Bertin Technologies, (France) and regenerated cellulose syringe RC filters (pore size $0.2 \mu\text{m}$, diameter 15mm) from Phenomenex (Torrance, CA, USA) were used.

All the solvents used for the sample preparation as well as the LC-QTOF-MS analysis were UPLC-MS grade. Methanol (MeOH) was purchased from Merck (Darmstadt, Germany) and distilled water (H_2O) was provided by a Milli-Q purification apparatus (Direct-Q UV; Millipore, Bedford, MA, USA). ACN was supplied from Merck (Darmstadt, Germany). The additives of the mobile phases, ammonium formate ($\geq 99.0\%$), ammonium acetate (99%), and formic acid (99%) were all purchased from Fluka (Buchs, Switzerland).

4.2. Zebrafish Embryos Exposure Experiments

4.2.1. Fish Embryo Test (FET)

The fish embryo test (FET) with zebrafish (*Danio Rerio*) embryos was conducted at the Institute of Evolution and Ecology of the University of Tübingen, Germany, according to the OECD TG 236 guidelines [68]. The zebrafish embryos (ZFE) were exposed to Metoprolol for 96 hours in a range of different concentrations for each pH value which are reported below:

- pH 6: 320.0 – 3000.0 mg L⁻¹
- pH 8: 10.0 - 150.0 mg L⁻¹
- pH 9: 0.10 – 50.00 mg L⁻¹

Additionally, a control exposure experiment (C=0.00 mg L⁻¹) was conducted at each pH value. During the exposure, endpoints, such as hatching success, heart rate, and mortality were evaluated every 12 h. Finally, the LC50 value of Metoprolol for each pH value was determined. The final LC50 values per each pH value are presented below.

- pH 6: 3180 mg L⁻¹
- pH 8: 70 mg L⁻¹
- pH 9: 10 mg L⁻¹

4.2.2. Toxicokinetic Experiment

The ZFE were exposed to Metoprolol at a concentration equivalent to their LC50 of each pH value for 96 h. All ZFE samples were washed, dried, weighed, and transferred to Eppendorf tubes of 1.5 mL, snap-frozen in liquid nitrogen. Samples from the exposure medium were collected both from the start (0 h) and the end (96 h) of the toxicokinetic experiment. The ZFE samples and the water exposure samples were collected and shipped to the Laboratory of Analytical Chemistry, at the Department of Chemistry in Athens, Greece, for analysis.

4.3. Samples

4.3.1. Water exposure samples

The water samples from the toxicokinetic exposure experiment were delivered at the laboratory of Analytical Chemistry, University of Athens in Greece on 16/9/20. For each water sample at each pH value and state (start or end), three separated centrifuge tubes were shipped. The received water exposure samples were stored at -80°C until the analysis. The water exposure samples at the three pH values are presented in the following table (Table 2):

Table 2. Metoprolol water exposure samples

pH	Status	Exposure Concentration of Metoprolol (mg L ⁻¹)
6	start	3180
	end	
8	start	70
	end	
9	start	10
	end	

4.3.2. Zebrafish embryos samples

The ZFE samples from the Metoprolol exposure experiments were shipped into Eppendorf tubes to the Laboratory of Analytical Chemistry in Athens on 16/9/20. Each Eppendorf with ZFE samples was accompanied by information concerning the exposure experiment. More specifically, the number of the embryos, their status at the time of the sample collection (alive or dead), the exact weight per sample, and the labeling of each Eppendorf tube were provided (Table 3). The ZFE samples were stored at -80°C until the analysis. The received ZFE samples are shown in figure 9 below.



Figure 9. The Eppendorf tubes containing the shipped ZFE.

The provided information accompanying the received ZFE samples is presented in the following table (Table 3).

Table 3. Total delivered ZFE samples from Metoprolol exposure experiments

ZFE Metoprolol					
pH	Eppi No.	Status	Embryos No.	Labeling	Fresh weight sample (mg)
6	7	dead	20	pH 6 Metoprolol † 96 hpf no.20	6.30
	14	alive	20	pH 6 Metoprolol * 96 hpf no. 20	6.00
	15	alive	20	pH 6 Metoprolol * 96 hpf no. 20	5.70
	16	alive	17	pH 6 Metoprolol * 96 hpf no. 17	5.50
8	6	dead	14	pH 8 Metoprolol † 96 hpf no.14	3.71
	17	alive	20	pH 8 Metoprolol * 96 hpf no. 20	5.30
	18	alive	8	pH 8 Metoprolol * 96 hpf no. 8	2.60
9	4	alive	15	Met 10mg/L *15 pH9 4	4.80
	11	alive	15	Met 10mg/L pH9 *15 11	4.80
	13	dead	18	Met 10mg/L 18t pH9 13	3.50
	18	alive	7	Met 10mg/L pH9 *7 18	2.30

4.4. Sample Preparation

4.4.1. Water Samples

For each water exposure sample at each pH value and state (start or end), three separated centrifuge tubes were available. So, equal parts of the water exposure samples from each tube were mixed and transferred into a new centrifuge tube. The new mixed samples were diluted properly until the final concentration of Metoprolol reach the linear dynamic range of the instrument ($C_{fin}=100$ ppb). The linear dynamic range for the Metoprolol was already determined with reference standard solutions of Metoprolol. The diluted water samples were filtered with 0.2 RC filter syringes, transferred to glass vials and they were spiked with isotope-labeled internal standard (D7-Metoprolol). The aim of adding internal standards was to account for potential insufficiencies during the sample preparation. The final solutions in the vials should consist of MeOH:H₂O 1:1 v/v. For this reason, the proper amount of MeOH was added to each filtered water sample. The water samples were stored at -80°C until the LC-HRMS analysis. The sample preparation procedure of the exposure water samples is shown in the following figure (figure 10).

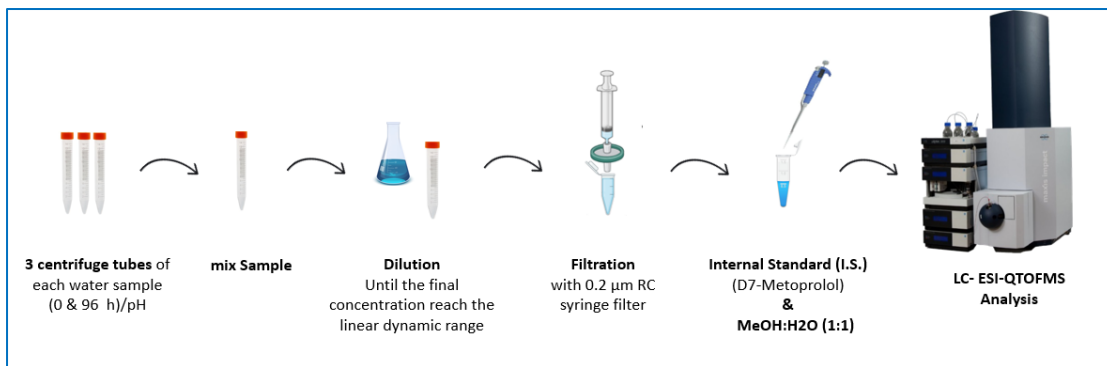


Figure 10. Sample preparation of water samples from exposure experiments to Metoprolol

4.4.2. Zebrafish Embryos (ZFE) Samples

Regarding the sample preparation of the ZFE samples, initially isotope labeled internal standard (D7-Metoprolol) was added, to account for potential insufficiencies during the sample preparation. Subsequently, ice-cold extraction solvents MeOH:H₂O 1:1 v/v were added. The homogenization and the extraction were performed simultaneously on a bead-beating Precellys Evolution 24 homogenizer equipped with a Cryolis Evolution cooler. The homogenizer operated at 8200 rpm at 4°C (three cycles of 15 s with a break of 60 s between each cycle). The homogenized ZFE extracts were centrifuged in a precooled centrifuge NEYA 16R (Remi Neya Centrifuges, Italy) for 10 minutes at 4°C and 11.000 rpm. The supernatants were collected, filtered with 0.2 RC filter syringes, and transferred to glass vials. It should be noticed that the whole sample preparation of the ZFE was conducted at 4°C. For the analysis of the samples with HILIC, the ZFE extracts were evaporated until dryness under N₂ and reconstituted in ACN:H₂O 95:5 v/v. The samples were stored at -80°C until the LC-HRMS analysis. The sample preparation procedure of the ZFE samples is presented in figure 11.



Figure 11. Sample preparation of the ZFE samples from exposure experiments to Metoprolol

4.5. LC-HRMS Analysis

The analysis of the samples was carried out utilizing LC-ESI-QTOF-MS. An ultra-high-performance liquid chromatography (UHPLC) system with an HP-3400 pump (Dionex Ultimate 300 RSLC, Thermo Fischer Scientific, Dreieich, Germany) coupled to a QTOF mass spectrometer (Maxis Impact, Bruker Daltonics, Bremen Germany) was used.

The water samples and ZFE extracts were analyzed using reversed-phase liquid chromatography (RPLC), while the ZFE extracts were analyzed additionally with hydrophilic interaction liquid chromatography (HILIC). The aim of using two different chromatographic techniques was the orthogonal identification of the detected biotransformation products [64]. The ZFE extracts were analyzed in both positive and negative ionization modes.

In the RPLC an Acclaim RSL C18 column (2.1 x 100 mm, 2.2 μ m) purchased from Thermo Fischer Scientific (Dreieich, Germany) was used for the achievement of the chromatographic separation. The column was equipped with a guard pre-column of the same packaging material. The column temperature was thermostated at 30°C. The mobile phase in the positive ionization mode consisted of H₂O:MeOH 90:10 (solvent A) and MeOH (solvent B) both amended with 5mM ammonium formate and 0.01% formic acid. In the negative ionization mode, the mobile phases were H₂O:MeOH 90:10 (solvent A) and MeOH (solvent B), both acidified with 5mM ammonium acetate. A gradient elution program was used in both ionization modes starting with 1% B

with a flow rate of 0.2 mL min⁻¹ for 1 min, and increasing to 39% in 2 min with a flow rate of also 0.2 mL min⁻¹ and then up to 99.9% with a flow rate of 0.4 mL min⁻¹ for the following 11 min. Finally, it keeps constant for 2 min with a flow rate 0.48 mL min⁻¹. Then, initial conditions were restored within 0.1 min, kept for 3 min and then the flow rate decreased to 0.2 mL min⁻¹. The injection volume was set up to 5 µL.

In HILIC, the chromatographic separation was performed on a Waters ACQUITY UPLC BEH Amide column (2.1 x 100 mm, 1.7 µm). A guard pre-column of the same packaging material was used, and the column was thermostated at 40°C. The mobile phase in the positive mode consisted of H₂O (solvent A) and ACN:H₂O 95:5 (solvent B) both amended with 1mM ammonium formate with 0.01% formic acid. In the negative mode, the mobile phase consisted of H₂O (solvent A) and ACN:H₂O 95:5 (solvent B) both amended with 10mM ammonium formate. The adopted gradient elution program, for both ionization modes, started with 100% B for 2 min, decreasing to 5% in 10 min and kept constant for the following 5 min. The initial conditions were restored within 0.1 min and let to re-equilibrate for 8 min. The flow rate was 0.2 mL min⁻¹. The injection volume was set up to 5 µL.

The QTOF system was equipped with an electrospray ionization interface (ESI) operating in positive and negative mode. Nitrogen (N₂) was used both as nebulizer gas (2 bar) and as drying gas (8 L min⁻¹). In the RPLC, the capillary voltage was set at 2500V for the positive mode and 3000V for the negative mode. The end plate offset was at 500V, and the drying temperature was set at 200°C. In HILIC, the capillary voltage was set at 3500V for the positive mode and 2500V for the negative mode. The end plate offset was at 500V, nebulizer pressure 2 bar (N₂), drying gas 10 L min⁻¹ (N₂), and drying temperature was set at 200°C.

The QTOF-MS system operated both in data-independent (broadband collision-induced dissociation, bbCID) acquisition and data-dependent (AutoMS/MS) acquisition modes. Spectra were recorded over the range m/z 30-1000, with a scan rate of 2 Hz. In the case of Bruker bbCID mode, a low energy collision (4 eV) provided the MS spectra whereas MS/MS spectra were acquired at higher collision energies (25 eV). Concerning AutoMS mode, the

collision energy applied was set to predefined values, according to the mass and the charge state of every ion.

The external QTOFMS calibration was performed daily with a sodium formate solution and a segment (0.1-0.25 min) in every chromatogram was used for internal calibration, using a calibrant injection at the beginning of each run. The sodium formate calibration mixture consisted of 10 mM sodium formate in a mixture of H₂O/isopropanol (1:1). The instrument provided a typical resolving power (FWHM) between 36,000-40,000 during calibration (m/z 226.1593, 430.9137 and 702.8636). Acquisition of mass spectra and the subsequent data processing was implemented using Data Analysis 5.1 and TASQ 2.1 (Bruker Daltonics, Bremen, Germany).

4.6. Identification Procedure

For the identification procedure of the parent compound, Metoprolol, target screening approach was followed, while for the identification of the biotransformation products of Metoprolol, suspect and non-target screening approaches were followed. The raw data were processed with the software tools Data Analysis 5.1 and TASQ CLIENT 2.1 (Bruker Daltonics, Germany).

4.6.1. Target Screening

In order to obtain the mandatory analytical evidence for the identification of the substance Metoprolol in the water and ZFE samples, initially reference standard solutions of Metoprolol were analyzed using LC-ESI-QTOF-MS. After the analysis, the following steps were applied to the raw data of the reference standard solutions.

- **Mass calibration** of the raw data with a calibration solution for minimizing potential mass errors (internal calibration)
- **Determination** of the **Retention Time** of Metoprolol by creating its extracted ion chromatogram (EIC). The applied mass window was ± 2 mDa.
- **Evaluation of the isotopic pattern fitting** by determining the mSigma value, which measures the fit between the measured and the theoretical

isotopic pattern. (The lowest the value of mSigma the highest the isotopic fitting).

- **Processing of the MS and MS/MS spectra** for determination of the precursor ion of Metoprolol and its qualifier ions. The determination of the qualifier ions was performed by using data-dependent acquisition mode.

Gathering all the above data, an in-house database was compiled. Subsequently, the samples were screened with the compiled database.

The identification of Metoprolol was based on the following criteria:

- Retention time tolerance (Δ RT: 0.2-0.4 min)
- Mass accuracy: < 2 mDa
- Isotopic pattern fitting – mSigma < 200
- ≥ 2 Qualifier ions

4.6.2. Suspect Screening

The identification of the biotransformation products of Metoprolol relied on the suspect screening approach since no analytical reference standards were available for them. However, information, such as their molecular formula and their structure, was available from the literature and metabolite prediction tools. For the identification of the biotransformation products of Metoprolol, the *in-silico* tool Metabolite Predict (Metabolite Tools 2.0, Bruker Daltonics, Bremen, Germany) was mainly used. This tool predicted potential biotransformation products of Metoprolol based on Phase I and Phase II mammalian reaction rules of the biotransformation procedure. Gathering the information of the tentative biotransformation products, an in-house database was compiled containing their molecular formulas. Subsequently, the samples were screened with this database. Also, the *in-silico* tool Meaboscape and the fragmentation prediction tool MetFrag were used.

4.6.3. Identification Criteria

A series of identification criteria were used for the identification of the suspect biotransformation products. The criteria adapted to the needs of the study. The first criterion that was implemented was the absence of a peak with a similar

retention time R_t (\pm 0.2 min) and intensity (coefficient 0.-10) from control samples. The criterion of the absence of the peak of the biotransformation product from the control samples was implemented because fish tissues are very complex in their nature, and hence the presence of peaks irrelevant to the exposure could occur (e.g., endogenous metabolites). Another criterion was that the peak area and ion intensity threshold were 1000 & 4000 for the ESI (+) and 500 & 2000 for ESI (-), respectively. Additionally, the mass accuracy threshold was \pm 5 ppm and \pm 5 mDa for the monoisotopic peak and the $m/\Delta m$ value < 200 mDa for the isotopic pattern fitting. Also, peak score for considering only peaks exhibiting ratios of Peak Area/Peak Intensity greater than 4 was assessed.

For the structural proposal of the tentative biotransformation products, further confirmatory criteria were taken into account. More specifically, the MS/MS spectra of the tentative biotransformation products were compared with that of the parent compound. A common fragmentation pattern and/or the characteristic neutral loss were evaluated. Additionally, the MS/MS spectra fragmentation ions of each biotransformation product were compared with the available fragments from online databases (e.g. MassBank and Metlin).

The enhancement of the identification confidence of the detected biotransformation products relied on the simultaneous detection of the biotransformation products in both polarities, as well as on the detection of adduct ions, such as $[M+Na]^+$, $[M+NH_4]^+$, $[M+K]^+$, $[M-H_2O-H]^-$ in positive ionization mode, and $[M+HCOOH-H]^-$ in negative ionization mode. Finally, orthogonal analytical approaches are crucial for the identification of the biotransformation products. For this reason, HILIC was used as a complementary technique to RPLC for achieving orthogonal identification of the detected biotransformation products.

Regarding the metabolites detected through the non-target approach, an additional criterion needs to be implemented in the identification workflow. This is the “xenobiotic metabolism relevance of the tentative bio-TP”. The detected biotransformation products via this approach need to be explained by the xenobiotic metabolism rules to accept them as tentative metabolites. A sum-up

of the criteria used for the identification of the biotransformation products is presented in figure 12 below:

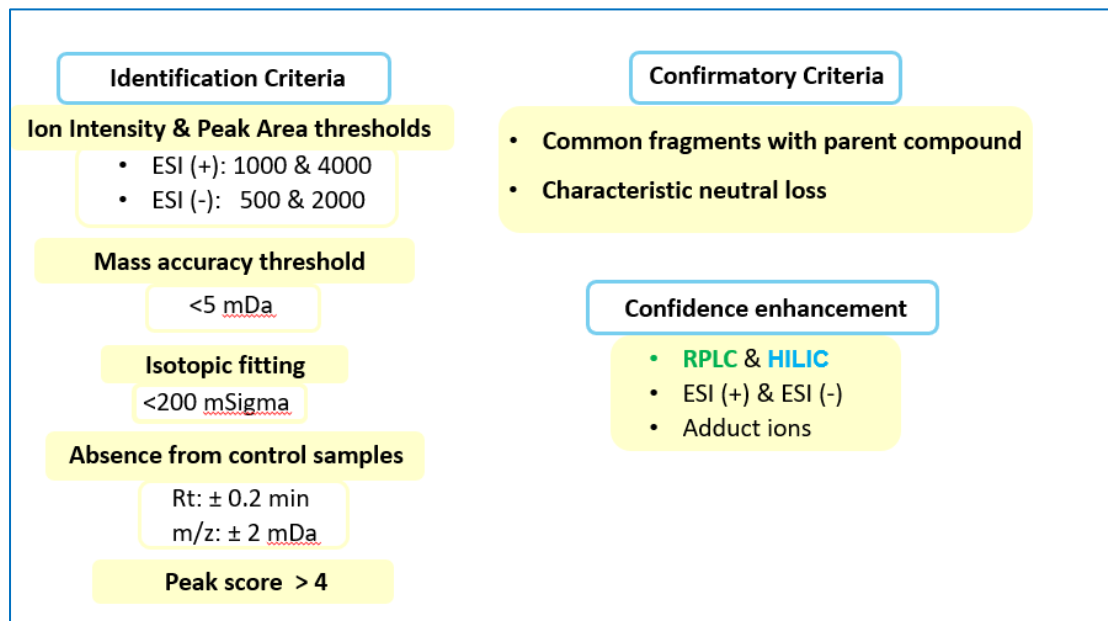


Figure 12. Identification and confirmation criteria for the identification of the bio-TPs.

4.6.4. Identification Confidence levels

Depending the experimental evidence, each one detected biotransformation product was assigned to a specific level of confidence of identification using the scheme proposed by Schymanski et al., as mentioned in Chapter 2. Briefly, **Level 1** corresponds to the confirmed structure using a reference standard, **level 2a** to a probable structure based on spectra match with available libraries, **level 2b** to a probable structure via MS and MS/MS diagnostic evidence, **level 3** to tentative candidate(s), with possible proposed structures, **level 4** to an unequivocal molecular formula and **level 5** to exact mass of interest [67].

4.7. Quantification procedure of Metoprolol

4.7.1. Calibration curve of Metoprolol

The quantification of Metoprolol in water and ZFE samples was performed using reference standard calibration curve. The calibration curve of Metoprolol was constructed using reference standard solutions at seven different concentration levels: 2, 5, 10, 25, 50, 100 and 200 ng mL⁻¹. The standard

solutions of Metoprolol were spiked with D7-Metoprolol (C: 100 ng mL⁻¹). The I.S. was used to achieve reliable and accurate quantitative results. More specifically, the aim of using I.S. was to account for potential insufficiencies during the sample preparation and/or signal suppression during the instrumental analysis. For this reason, relative areas, namely the absolute areas of Metoprolol divided with the area of the I.S. (D7-Metoprolol) (equation 1) were used in the calibration curve of Metoprolol.

$$\text{Relative Area} = \frac{\text{Absolute Area of Metoprolol}}{\text{Area of I.S. (D7-Metoprolol)}} \quad (1)$$

The calibration curve of Metoprolol was constructed using the linear regression model. The regression line (equation 2) was determined by the least-squares method, and was of the form:

$$\text{Rel. Area} = (a \pm Sa) * C + (b \pm Sb) \quad (2)$$

where,

Rel. Area: the relative area of the Metoprolol

C: the concentration of Metoprolol in the standard solution

a: the slope of the curve

Sa: the standard deviation of the slope

b: the intercept, and

Sb: the standard deviation of the intercept

The concentration of metoprolol in the water and ZFE samples was determined by using equation 2.

4.7.2. LOD and LOQ

The Limit of Detection (LOD) and Quantification (LOQ) were calculated using the calibration curve. For the determination of the aforementioned analytical characteristics, the following equations were used:

$$\text{LOD } (\mu\text{g L}^{-1}) = \frac{3.3 sb}{a} \quad (3)$$

$$\text{LOQ } (\mu\text{g L}^{-1}) = \frac{10 sb}{a} \quad (4)$$

where,

sb: the standard deviation of the intercept of the standard calibration curve

a: the slope of the curve

4.7.2. Quantification of Metoprolol in the samples

Initially, for the quantification of metoprolol in the water and ZFE samples the relative areas were determined (equation 1). Afterwards, the concentrations of Metoprolol in the samples were estimated by using equation 2.

Concerning the ZFE extracts, the concentration of Metoprolol corresponding to the 0.5 mL of MeOH: H₂O (1:1 v/v) mixture that was used for the extraction was calculated. For the estimation of the respective mass contained in the 0.5 mL of the extract the following equation (5) was used:

$$M (\text{ng}) = C (\text{ng mL}^{-1}) * 0.5 \text{ mL} \quad (5)$$

For the calculation of the internal concentration of Metoprolol, the exact weight of the ZFE contained in each delivered Eppendorf was used (equation 6).

$$C_{int} (mg\ kg^{-1}) = C_{int} (ng\ mg^{-1}) = \frac{M (ng)}{weight\ of\ the\ sample} \quad (6)$$

4.7.3. Bioconcentration Factors (BCFs)

The bioconcentration factors were determined to estimate the extent of the bioaccumulation of Metoprolol in the ZFE at the three different pH values. For the calculation of the BCF values, the equation 7 was used.

$$BCF = \frac{C_{internal}}{C_{external}} \quad (7)$$

where,

$C_{internal}$: the measured internal concentration of Metoprolol in the ZFE and

$C_{external}$: the theoretical exposure concentration of Metoprolol (LC50 values)

Chapter 5

Results and Discussion

5.1. Results from the Metoprolol exposure experiments

5.1.1. Acute toxicity (LC50 values) results from FET with ZFE

The LC50 values of Metoprolol in the exposure experiments at the different pH values (pH: 6, 8, and 9) were determined. The LC50 value of Metoprolol from the exposure experiments at pH 6 was 3180 mg L^{-1} , 70 mg L^{-1} at pH 8, and 10 mg L^{-1} at pH 9. Therefore, the LC50 value of Metoprolol at pH 9 was approximately 300 times lower than the LC50 value at pH 6. The LC50 values from the exposure experiment of Metoprolol at each pH value are presented in the figure below (figure 13). The LC50 values that correspond to different pH values are indicated with a different color.

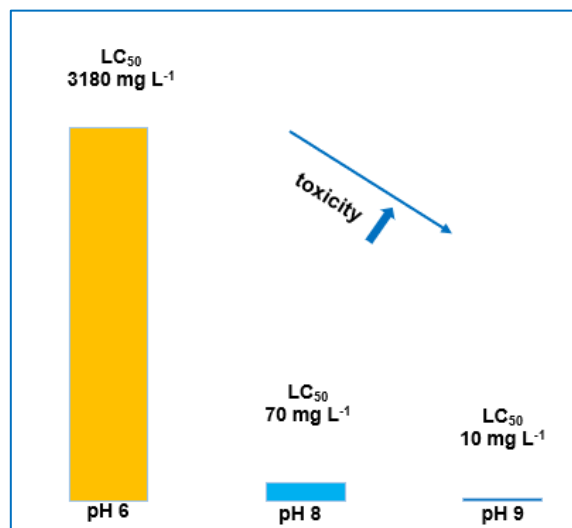


Figure 13. The LC50 values from the exposure experiment of Metoprolol at each pH value

The differences in the LC50 values of Metoprolol, and as a result in the toxicity, at the different pH values could be explained by the differences in the % percentage of the neutral species of Metoprolol at the different pH values. As mentioned in chapter 1, Metoprolol is a base with $\text{pK}_a = 9.68$. As a result, the % percentage of the neutral species of Metoprolol is increasing at alkaline pH values. More specifically, as it is shown in figure 14, the % percentage of the

neutral species of Metoprolol at pH 9 is approximately 800 times higher than the % percentage of the neutral species at pH 6.

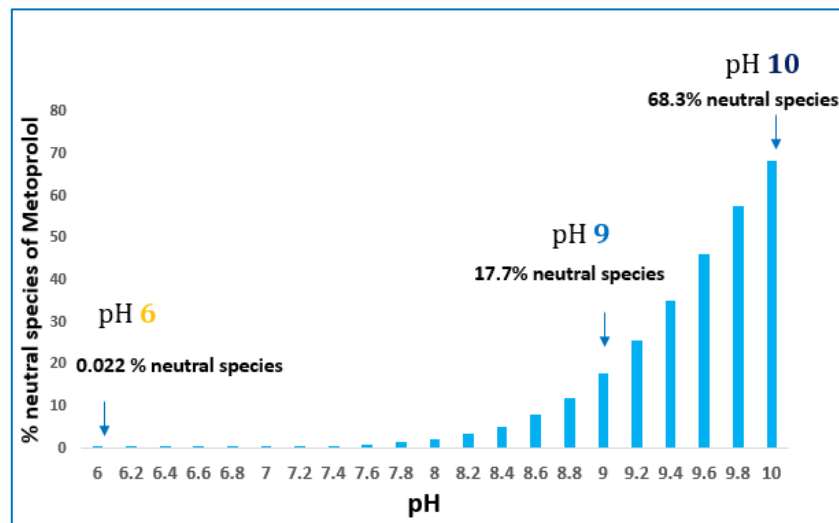


Figure 14. The % percentage of neutral species of Metoprolol at each pH value.

The permeability of the neutral species through the membranes of the organisms is higher. Therefore, the fact that the LC50 value of Metoprolol at pH 9 is significantly lower than the LC50 value at pH6, and the toxicity higher, is a result of the higher uptake of the increased % percentage of the neutral species of Metoprolol.

In figure 15 below, the plot diagram of logD versus pLC50 values of Metoprolol at the different pH values is presented. A satisfactory correlation between logD and LC50 values at the different pH values is observed. The good correlation confirms that the higher toxicity (lower LC50 values) at alkaline pH values is the result of a higher % percentage of the neutral form of Metoprolol.

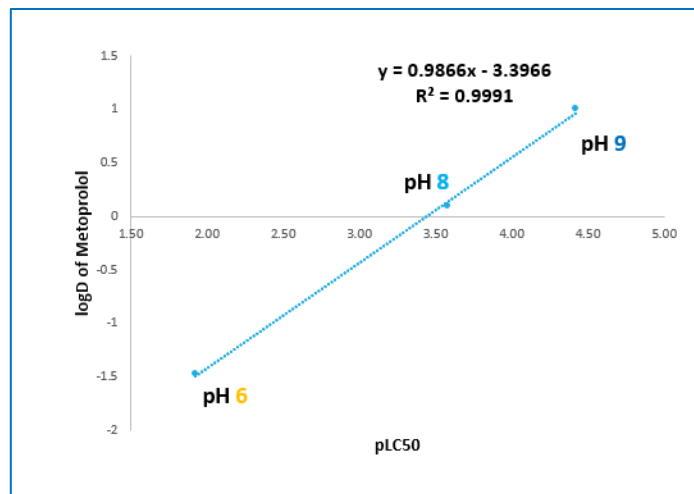


Figure 15. Diagram of logD versus the pLC50 of Metoprolol at each pH values.

5.1.2. Determination of the concentration of Metoprolol in water samples from the exposure experiment

The measured concentrations of Metoprolol accompanied by the standard deviation ($C_{\text{measured}} \pm \text{SD}$) in the water samples from the exposure experiment at the three different pH values 6, 8 and 9 are presented in Table 4.

Table 4. The measured concentrations of Metoprolol in the water samples from the exposure experiment.

pH	status	C_{measured} of Metoprolol \pm SD (ng mL $^{-1}$)
6	start	2997 \pm 210
	end	3350 \pm 235
8	start	77.1 \pm 5.4
	end	74.0 \pm 5.2
9	start	11.60 \pm 0.81
	end	10.39 \pm 0.73

The measured concentrations ($C_{\text{measured}} \pm \text{SD}$) in the water samples are illustrated in the following figures (figures 16-18). The measured concentrations that correspond to different pH values are indicated with different color. It can be noticed that the measured concentrations of Metoprolol are at the same level as the theoretical corresponding concentrations of the exposure experiment.

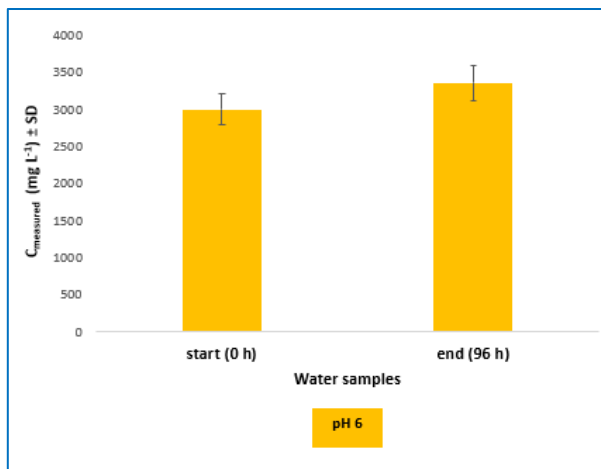


Figure 16. The measured concentrations of Metoprolol in the water samples at pH 6 from the start and the end of the exposure experiment.

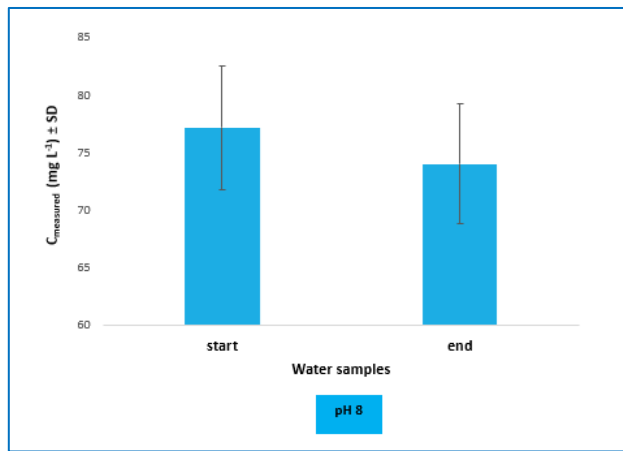


Figure 17. The measured concentrations of Metoprolol in the water samples at pH 8 from the start and the end of the exposure experiment.

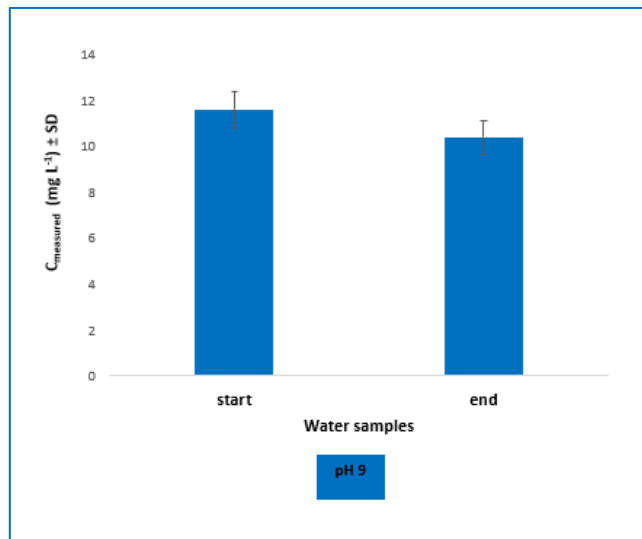


Figure 18. The measured concentrations of Metoprolol in the water samples at pH 9 from the start and the end of the exposure experiment.

5.1.3. Determination of the internal concentrations of Metoprolol in the zebrafish embryos samples from the exposure experiments

The measured internal concentrations of Metoprolol ($C_{internal} \pm SD$) in the ZFE samples from the exposure experiments at the three different pH values, are presented in the below table (Table 5). The table also includes information for the ZFE samples, such as the number of the embryos containing in each Eppendorf, their status (alive or dead), and the exact weight of each sample.

Table 5. The measured internal concentrations of Metoprolol in the ZFE samples.

ZFE Metoprolol						
pH	Eppi No.	Status	Embryos No.	Labeling	Fresh weight sample (mg)	$C_{int} (\text{mg kg}^{-1}) \pm SD$
6	7	dead	20	pH 6 Metoprolol † 96 hpf no.20	6.30	1627 ± 16
	14	alive	20	pH 6 Metoprolol * 96 hpf no. 20	6.00	1527 ± 15
	15	alive	20	pH 6 Metoprolol * 96 hpf no. 20	5.70	1394 ± 15
	16	alive	17	pH 6 Metoprolol * 96 hpf no. 17	5.50	1097 ± 12
8	6	dead	14	pH 8 Metoprolol † 96 hpf no.14	3.71	66.78 ± 0.09
	17	alive	20	pH 8 Metoprolol * 96 hpf no. 20	5.30	1020 ± 12
	18	alive	8	pH 8 Metoprolol * 96 hpf no. 8	2.60	1218 ± 28
9	4	alive	15	Met 10mg/L *15 pH9 4	4.80	747.9 ± 9.4
	11	alive	15	Met 10mg/L pH9 *15 11	4.80	597.6 ± 7.5
	13	dead	18	Met 10mg/L 18t pH9 13	3.50	894 ± 15
	18	alive	7	Met 10mg/L pH9 *7 18	2.30	514 ± 13

The measured internal concentrations of Metoprolol in the ZFE accompanied by the SD at the three different pH values are also illustrated in figure 19. The measured internal concentrations that correspond to different pH values are presented with different color.

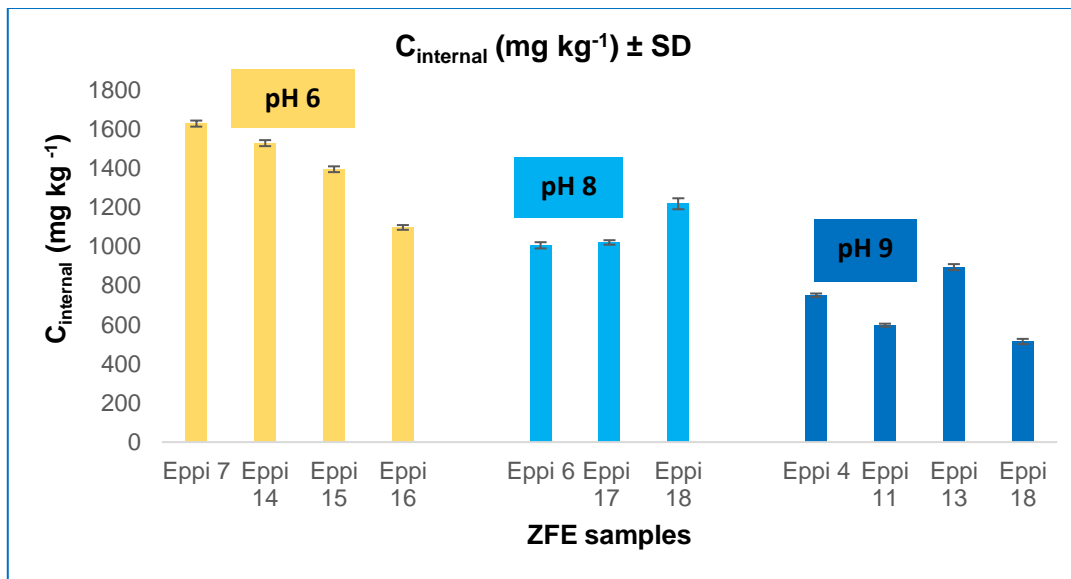


Figure 19. The measured internal concentrations of Metoprolol in the ZFE samples.

As it can be observed from the above figure, the measured internal concentrations in the ZFE samples have slight variations at the different pH values, even though the external exposure concentrations (LC50 values) have significant variations among the three pH values.

5.1.4. Determination of Bioconcentration Factors (BCFs) of Metoprolol in the zebrafish embryos samples

The Bioconcentration Factors (BCFs) of Metoprolol were determined to access the extent of the bioaccumulation of Metoprolol in the ZFE and to evaluate if the extent of the bioaccumulation is affected by the different pH values of the exposure medium. For the calculation of the BCF (L kg⁻¹) of Metoprolol in ZFE, internal concentration (mg kg⁻¹) and exposure concentration (mg L⁻¹) were used. BCF values of Metoprolol were determined separately for all ZFE samples and subsequently, an average value of BCF was calculated for each pH value. The average BCF values of Metoprolol at the different pH values accompanied by the SD are presented in the following table (Table 6).

Table 6. The average BCF values of Metoprolol ± SD at the different pH values

pH	BCF _{average} of Metoprolol ± SD (L kg ⁻¹)
pH 6	0.444 ± 0.072
pH 8	15.4 ± 1.7
pH 9	69 ± 17

The BCF values are presented using Boxplots for each pH value in figure 20 below.

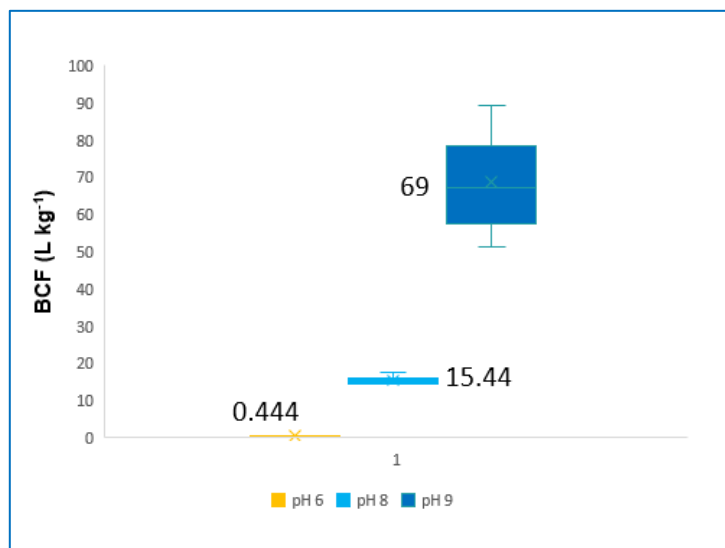


Figure 20. Boxplots with BCF data of ZFE samples per pH value from Metoprolol exposure experiments.

As it can be observed from the bar charts in figure 20, the $BCF_{average}$ value of Metoprolol at pH 9 (69 L kg^{-1}) is approximately 155 times higher than the $BCF_{average}$ value at pH 6. At alkaline pH values, such as pH 9, the % percentage of neutral species of Metoprolol is increasing and as a result its permeation through membranes as well as the bioaccumulation are higher too. Therefore, the increased BCF values of Metoprolol at alkaline pH values can be explained by the enhanced uptake due to the increased % percentage neutral species.

5.2. Metoprolol biotransformation results

A total of ten (10) biotransformation products (bio-TPs) of Metoprolol were detected in the ZFE extracts through suspect screening (4.6.3.). The majority of the detected bio-TPs were the result of the phase I reactions of the biotransformation procedure, while the only phase II reaction that was observed was the glucuronidation (glucuronide of metoprolol and glucuronide of hydroxy metoprolol). The majority of the bio-TPs were detected by both chromatographic techniques, RPLC and HILIC, in positive ionization mode as

$[M+H]^+$ and/or as adduct ions. In negative ionization mode, only the M241 was detected as $[M-H]^-$ by RPLC. From all the detected bio-TPs, the hydroxy metoprolol and Metoprolol acid were the main bio-TPs. For this reason, new bio-TPs could be formed through the biotransformation of these two bio-TPs, as is suggested in the metabolic pathway of Metoprolol below (5.3).

Finally, for the tentative bio-TPs for which MS/MS spectrum in data-dependent mode was available, and thus, (a) possible structure(s) could be proposed, identification confidence level 2 or 3 was achieved, while for the bio-TPs for which MS/MS spectrum did not exist, we end up in lower identification level 4.

The table 7 below includes identity evidence for the ten detected bio-TPs, such as their exact molecular mass and their molecular formula. Also, information, regarding the chromatographic technique, polarity, and the form that the bio-TPs were detected, was included in the table. For the bio-TPs for which MS/MS spectrum in data-dependent ionization mode existed, the fragment ions which were crucial for their structural proposal were listed in the table. Finally, their proposed identification levels were involved.

Table 7. A summary of the detected and identified bio-TPs of Metoprolol in the ZFE.

Candidate bio-TP	Theoretical molecular mass (m/z)	Proposed Name	Molecular Formula	RP (+) R.T. (min)	RP (+) detected forms	HILIC (+) R.T. (min)	HILIC (+) detected forms	Fragment ions (m/z)	Identification Level
M284	284.1856	Hydroxy metoprolol	C ₁₅ H ₂₅ NO ₄	3.6	[M+H] ⁺ / [M+K] ⁺	6.6	[M+H] ⁺	56.0494, 74.0600, 98.0964, 116.1070, 133.0648, 151.0754, 207.1016, 224.1287	3
M254	254.1751	Demethyl-metoprolol	C ₁₄ H ₂₄ NO ₃	3.8 4.3	[M+H] ⁺	6.6	[M+H] ⁺	117.0910, 212.1281, 236.1645	2b
M268	268.1543	Metoprolol acid	C ₁₄ H ₂₁ NO ₄	3.7	[M+H] ⁺ / [M+K] ⁺	7.0	[M+H] ⁺ / [M+K] ⁺	56.0495, 116.1070, 145.0648, 165.546, 191.0703, 226.1074, 250.1438	2b
M226	226.1438	N-deisopropyl-metoprolol	C ₁₂ H ₁₉ NO ₃	4.3	[M+H] ⁺ / [M+K] ⁺	6.7	[M+H] ⁺	56.0495, 74.0600, 121.0642, 159.0804, 165.0930, 191.1067	2b
M241	241.1071	Deaminated metoprolol	C ₁₂ H ₁₆ O ₅	5.0	[M+NH ₄] ⁺	-	-	-	4
M254	254.1387		C ₁₃ H ₁₉ NO ₄	3.4	[M+H] ⁺	6.5	[M+Na] ⁺	-	4
M270	270.1700	Hydroxy-demethyl metoprolol	C ₁₄ H ₂₃ NO ₄	2.6	[M+H] ⁺	-	-	-	4
M282	282.1700		C ₁₅ H ₂₃ NO ₄	3.7	[M+H] ⁺	6.6	[M+H] ⁺	-	4
M460	460.2177	Glucuronide of hydroxy metoprolol	C ₂₁ H ₃₃ NO ₁₀	3.3	[M+H] ⁺	7.4	[M+H] ⁺ / [M+Na] ⁺	116.1070, 284.1856	3
M444	444.2228	Glucuronide of metoprolol	C ₂₁ H ₃₃ NO ₉	4.9	[M+H] ⁺	6.5	[M+H] ⁺	-	4

In the following paragraphs, a detailed discussion concerning the identification process of each plausible bio-TP will be provided, and according to the analytical evidence of each of the afore-mentioned bio-TP, an identification confidence level was proposed.

5.2.1. Identification of M284

The M284 was detected in the ZFE extracts and it could be a result of the xenobiotic biotransformation of Metoprolol (MET) in the ZFE, since it did not exist in the control samples. The M284 was detected by both chromatographic techniques, RPLC and HILIC, in positive ionization mode, with similar sensitivity. Neither the precursor ion $[M-H]^-$ nor any adduct ion of M284 were detected in negative ionization mode, neither in RPLC nor HILIC.

In positive ionization mode, the EIC of M284 was obtained by extracting the exact molecular mass (284.1856 m/z) of its precursor ion $[M+H]^+$. The mass of the protonated molecule M284 was 16 Da higher than that of MET (268.1907 m/z), which corresponds to the mass of an oxygen atom indicating the addition of a hydroxyl group in the parent compound MET. Hydroxylation is a phase I reaction of the biotransformation procedure. The hydroxylation of MET resulting in the formation of hydroxy metoprolol is presented in figure 21 below.

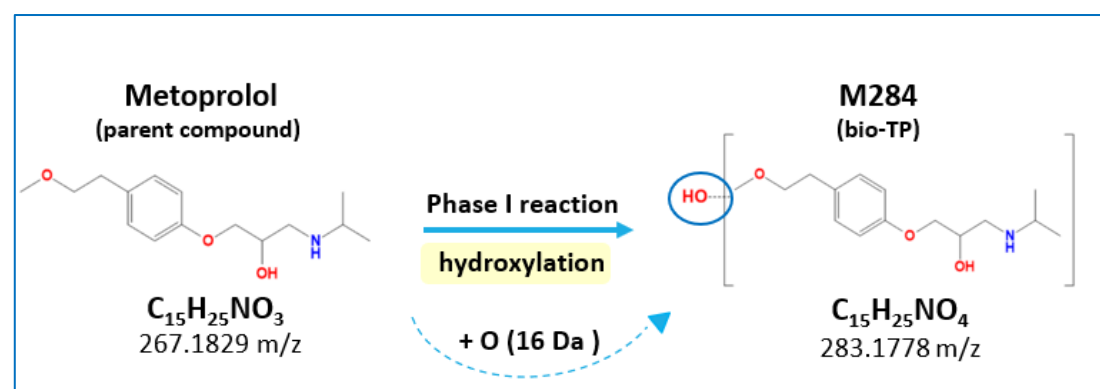


Figure 21. Hydroxylation of Metoprolol

So, it is suggested that the M284 is the hydroxy metoprolol with the structure presented in the figure below:

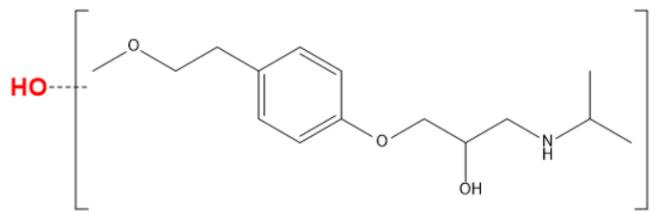


Figure 22. Structure of hydroxy metoprolol

The retention time of M284 was 3.6 min in RPLC and 6.6 min in HILIC in positive ionization mode (figure 23).

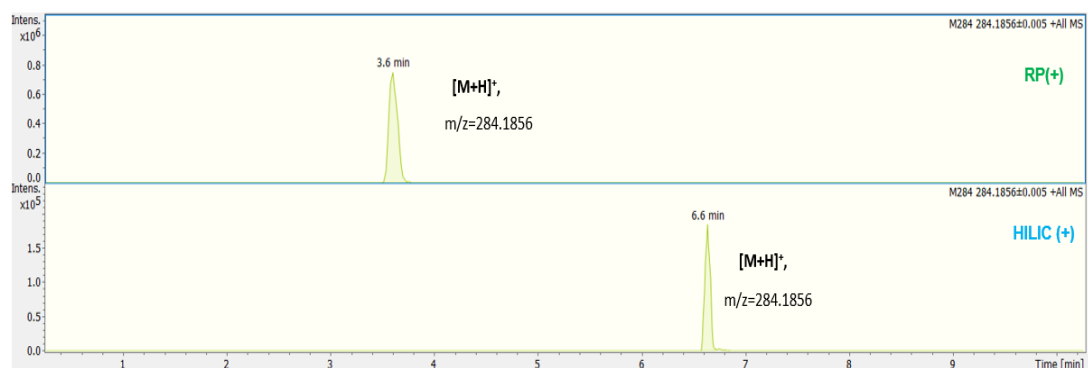


Figure 23. EIC of M284 in RPLC (above) and HILIC (below) in positive ionization mode

In the MS spectrum obtained by RPLC in positive ionization mode, the potassium adduct ion of M284 $[M+K]^+$, 332.145 m/z, was also detected. Its intensity was lower in comparison with the precursor ion $[M+H]^+$. However, no adduct ion of M284 was detected in HILIC in positive ionization mode. The MS spectra of M284 in RPLC and HILIC in positive ionization mode are obtained with data-independent acquisition (DIA) mode are shown in figure 24 below.

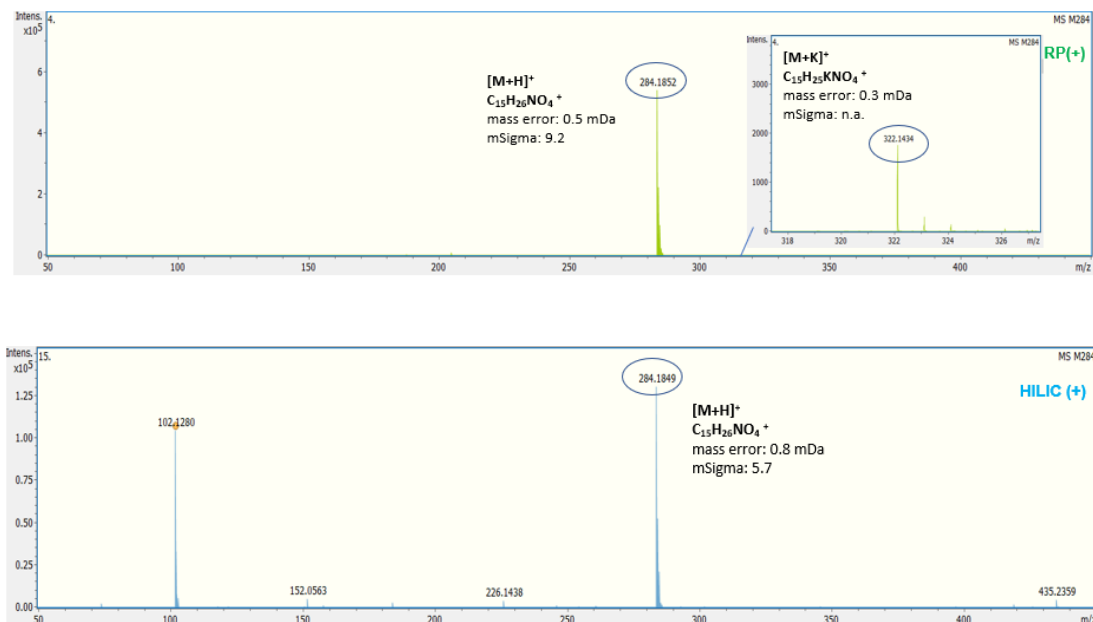


Figure 24. MS spectra of M284 in RPLC (above) and HILIC (below) in positive ionization mode.

The structural proposal of M284 relied on the interpretation of MS/MS spectra. Firstly, the fragment ions from data-dependent acquisition mode (auto-MS) were studied in both RPLC and HILIC in positive ionization mode, and subsequently, they were investigated in the MS/MS obtained by data independent acquisition mode (bbCID).

Firstly, the fragment ion 207.1016 m/z ($\text{C}_{12}\text{H}_{15}\text{O}_3^+$) was detected in the MS/MS spectra of M284 obtained by both chromatographic techniques in positive ionization mode. It is important to mention the fragment ion 207.1016 m/z ($\text{C}_{12}\text{H}_{15}\text{O}_3^+$) is 16 Da higher than the characteristic fragment 191.1067 m/z ($\text{C}_{12}\text{H}_{15}\text{O}_2^+$) of the parent compound MET. The difference of 16 Da corresponds to the mass of an oxygen atom, indicating that M284 and MET have the same fragmentation pattern. More specifically, the fragments 207.1016 m/z ($\text{C}_{12}\text{H}_{15}\text{O}_3^+$) of M284 and 191.1067 m/z ($\text{C}_{12}\text{H}_{15}\text{O}_2^+$) of MET have been formed both by the same neutral loss of 77.0835 m/z ($\text{C}_3\text{H}_{11}\text{NO}$).

Therefore, the fragment ion 207.1016 m/z ($\text{C}_{12}\text{H}_{15}\text{O}_3^+$) seems to be a diagnostic fragment for the M284.

Additionally, more fragments were detected in the MS/MS spectra of the M284. These fragments were the below: 133.0648 m/z ($\text{C}_9\text{H}_9\text{O}^+$), 74.0600 ($\text{C}_3\text{H}_8\text{NO}^+$)

and 56.0494 m/z ($\text{C}_3\text{H}_8\text{N}^+$). The above fragments were also detected in the MS/MS spectra of the parent compound MET. Also, the fragments of the M284 116.1070 m/z ($\text{C}_6\text{H}_{14}\text{NO}^+$) and the 98.0964 m/z ($\text{C}_6\text{H}_{12}\text{N}^+$), which was formed through the loss of H_2O of 116.1070 m/z ($\text{C}_6\text{H}_{14}\text{NO}^+$), were common fragments with that of Metoprolol. Therefore, it was concluded that M284 presented the same fragmentation pattern as that of its parent compound (MET). This evidence was a confirmatory criterion for its identification. The MS/MS spectra of M284 and MET and their common fragments are shown in figure 25 below.

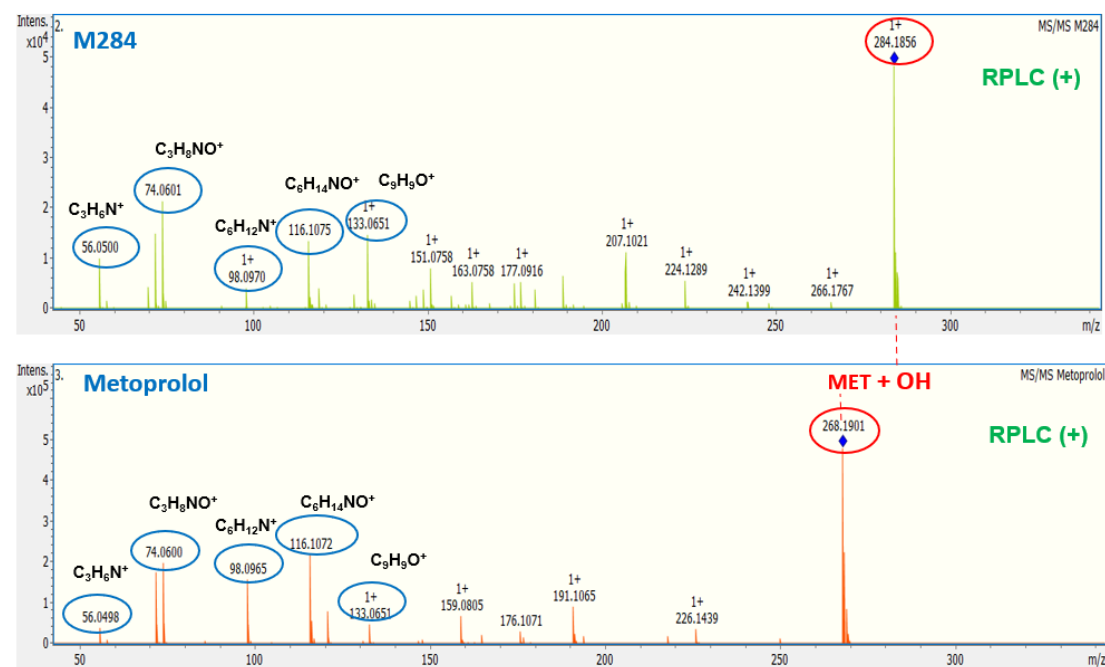


Figure 25. Common fragment ions in the MS/MS spectra of M284 (above) and Metoprolol (below)

Additionally, the MS/MS spectrum of the hydroxy Metoprolol in different online libraries (such as Metlin) was investigated, and this spectrum was compared with the MS/MS data of the M284 in the current study. Many common fragments were observed among the MS/MS spectra of the tentative biotransformation product M284 with that of the hydroxy Metoprolol in the online library Metlin. More specifically, the common fragments were the below: 56.0494 m/z ($\text{C}_3\text{H}_8\text{N}^+$), 74.0600 ($\text{C}_3\text{H}_8\text{NO}^+$), 98.0964 m/z ($\text{C}_6\text{H}_{12}\text{N}^+$), 116.1070 m/z ($\text{C}_6\text{H}_{14}\text{NO}^+$), 133.0648 m/z ($\text{C}_9\text{H}_9\text{O}^+$), and 207.1016 m/z ($\text{C}_{12}\text{H}_{15}\text{O}_3^+$). This fact enhanced the identification confidence of M284. Also, it could be noticed that the fragments 207.1016 m/z, 116.1070 m/z ($\text{C}_6\text{H}_{14}\text{NO}^+$), 133.0648 m/z ($\text{C}_9\text{H}_9\text{O}^+$), and 224.1287 m/z ($\text{C}_{12}\text{H}_{18}\text{NO}_3^+$) were in accordance with those that

were reported in the literature as fragment ions of the hydroxy Metoprolol [26,41].

Furthermore, the MS/MS spectra of M284 in RPLC and HILIC in positive ionization mode were investigated. Many common fragments were observed among the two chromatographic techniques, achieving the orthogonal identification of M284. This fact is an additional confirmatory element for the identification of M284 and pointing the importance of using two different chromatographic techniques. The MS/MS spectra of M284 obtained by RPLC and HILIC are shown in figure 26 below.

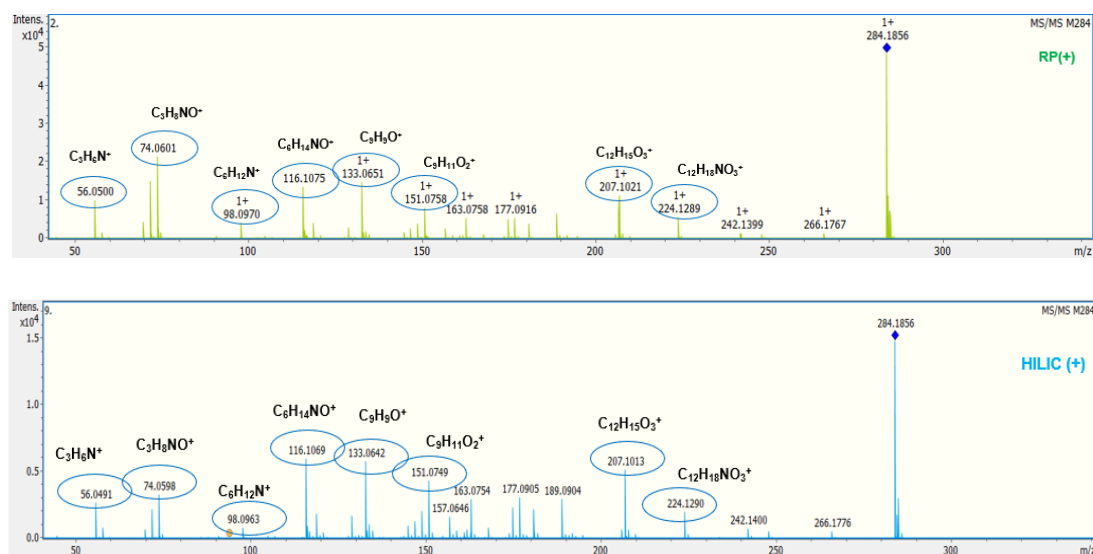
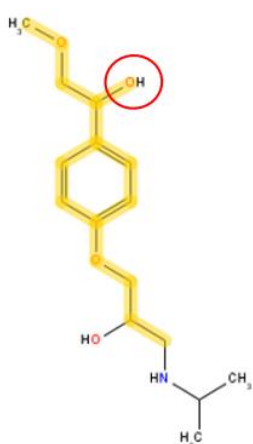


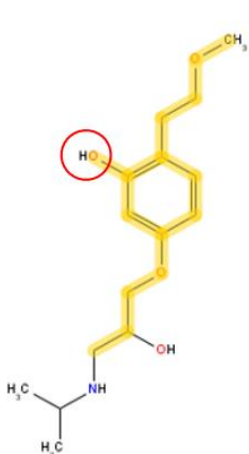
Figure 26. MS/MS spectra of M284 in RPLC (above) and HILIC (below) in positive ionization mode.

According to all the above information, it is recommended that the M284 is the hydroxy metoprolol. However, there are more than one potential hydroxylation sites where the hydroxyl group can be sited. Utilizing the *in-silico* fragmentation prediction tool MetFrag (through Metaboscape), three different sites of hydroxylation of MET were suggested, as shown in figures 27-29. However, in the MS/MS spectra of each structural isomer, it could be observed that the diagnostic fragment 207.1016 m/z was detected in the cases of a-hydroxylation and benzylic hydroxylation of Metoprolol (as presented in figures 27-28).



Ion Formula	m/z meas.	$\Delta m/z$ [mDa]	Int.	IntCov. [%]
$[\text{C3H7N-H}]^+$	56.050	[1H] 0.0	12024.893	6.1
$[\text{C3H8N}]^+$	58.064	1.3	2143.701	1.1
$[\text{C4H10N}]^+$	72.081	0.3	19037.023	9.6
$[\text{C3H7NO}]^+ \cdot \text{H}^+$	74.060	[-1H] 0.4	27144.748	13.7
$[\text{C3H7O2}]^+$	75.044	0.2	2217.554	1.1
$[\text{C6H13N-H}]^+$	98.096	[1H] 1.2	5109.330	2.6
$[\text{C6H14NO}]^+$	116.106	1.9	14746.230	7.4
$[\text{C8H8O-H}]^+$	119.048	[1H] 1.8	4661.925	2.4
$[\text{C6H11NO2}]^+$	129.069	10.0	3197.783	1.6
$[\text{C9H10O-H}]^+$	133.064	[1H] 1.4	16156.190	8.1
$[\text{C9H10O}]^+ \cdot \text{H}^+$	135.080	[-1H] 1.5	1398.852	0.7
$[\text{C9H8O2}]^+ \cdot \text{H}^+$	149.060	[-1H] 0.6	4328.852	2.2
$[\text{C9H11O2}]^+$	151.075	0.6	8932.924	4.5
$[\text{C10H10O2}]^+ \cdot \text{H}^+$	163.076	[-1H] 0.1	6171.284	3.1
$[\text{C9H11NO2+2H}]^+ \cdot \text{H}^+$	168.103	[-3H] -0.6	1497.139	0.8
$[\text{C10H13O3}]^+$	181.087	-0.4	4308.878	2.2
$[\text{C12H15O3}]^+$	207.102	-0.4	12339.545	6.2
$[\text{C12H17NO3}]^+ \cdot \text{H}^+$	224.129	[-1H] -0.4	5873.694	3.0
$[\text{C12H18NO4+H}]^+ \cdot \text{H}^+$	242.140	[-2H] -0.3	1447.742	0.7
$[\text{C15H23NO3}]^+ \cdot \text{H}^+$	266.176	[-1H] -0.5	1477.561	0.7

Figure 27. Structure and detected fragment ions of α -hydroxy metoprolol obtained by MetFrag.



Ion Formula	m/z meas.	$\Delta m/z$ [mDa]	Int.	IntCov. [%]
$[\text{C3H7N-H}]^+$	56.050	[1H] 0.0	12024.893	6.1
$[\text{C3H8N}]^+$	58.064	1.3	2143.701	1.1
$[\text{C4H10N}]^+$	72.081	0.3	19037.023	9.6
$[\text{C3H7NO}]^+ \cdot \text{H}^+$	74.060	[-1H] 0.4	27144.748	13.7
$[\text{C3H6O2}]^+ \cdot \text{H}^+$	75.044	[-1H] 0.2	2217.554	1.1
$[\text{C6H13N-H}]^+$	98.096	[1H] 1.2	5109.330	2.6
$[\text{C6H14NO}]^+$	116.106	1.9	14746.230	7.4
$[\text{C8H8O-H}]^+$	119.048	[1H] 1.8	4661.925	2.4
$[\text{C6H11NO2}]^+$	129.069	10.0	3197.783	1.6
$[\text{C9H10O-H}]^+$	133.064	[1H] 1.4	16156.190	8.1
$[\text{C9H10O}]^+ \cdot \text{H}^+$	135.080	[-1H] 1.5	1398.852	0.7
$[\text{C6H9NO3+H}]^+ \cdot \text{H}^+$	145.065	[-2H] 9.2	1747.599	0.9
$[\text{C9H8O2}]^+ \cdot \text{H}^+$	149.060	[-1H] 0.6	4328.852	2.2
$[\text{C9H11O2}]^+$	151.075	0.6	8932.924	4.5
$[\text{C7H10NO3}]^+ \cdot \text{H}^+$	157.065	[-1H] 8.6	2748.194	1.4
$[\text{C10H10O2}]^+ \cdot \text{H}^+$	163.076	[-1H] 0.1	6171.284	3.1
$[\text{C9H14NO2}]^+$	168.103	-0.6	1497.139	0.8
$[\text{C10H13O3}]^+$	181.087	-0.4	4308.878	2.2
$[\text{C12H16NO2}]^+$	206.119	-0.9	1359.856	0.7
$[\text{C12H15O3}]^+$	207.102	-0.4	12339.545	6.2
$[\text{C12H18NO3}]^+$	224.129	-0.4	5873.694	3.0
$[\text{C12H18NO4+H}]^+ \cdot \text{H}^+$	242.140	[-2H] -0.3	1447.742	0.7
$[\text{C15H23NO3}]^+ \cdot \text{H}^+$	266.176	[-1H] -0.5	1477.561	0.7

Figure 28. Structure and detected fragment ions of bio-TP formed through benzylic hydroxylation of Metoprolol obtained by MetFrag.

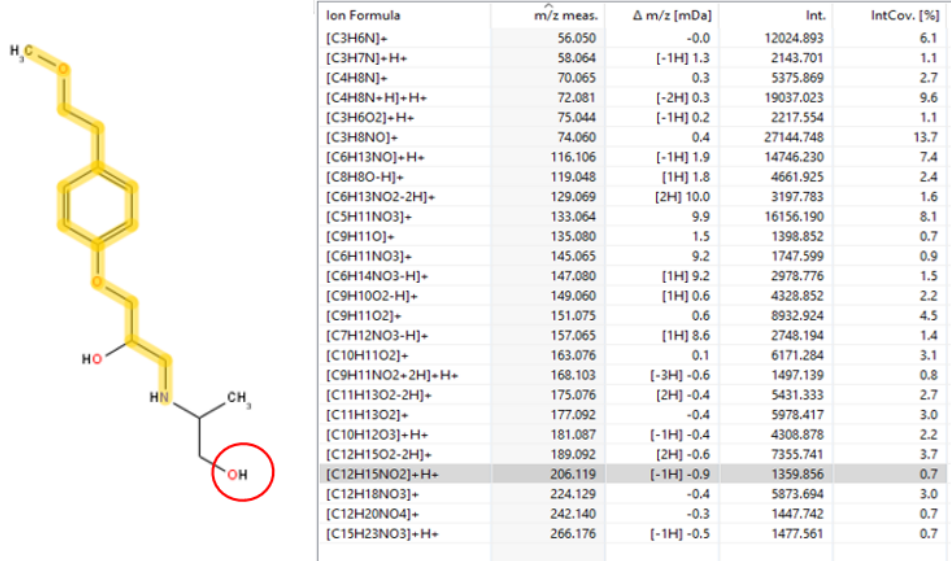


Figure 29 . Structure and detected fragment ions of bio-TP formed through hydroxylation of the isopropyl group of Metoprolol obtained by MetFrag.

The fact that the diagnostic fragment 207.1016 m/z was not detected in the case of the hydroxylation of the isopropyl group of Metoprolol excluded the case of hydroxyl entering this site. Therefore, it is concluded that the M284 is the hydroxy metoprolol formed through α -hydroxylation or benzylic hydroxylation of Metoprolol. The structures of the two tentative structural isomers are presented in figures 30-31.

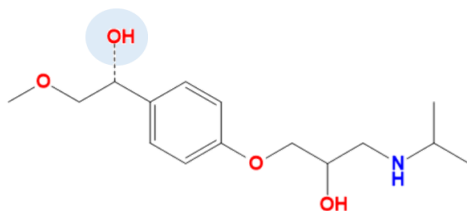


Figure 30. Structure of α -hydroxy metoprolol

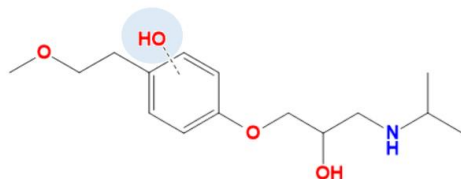


Figure 31. Structure of hydroxybenzyl metoprolol

However, the exact position of hydroxylation could not be determined, since no available reference standards were available. Therefore, M284 is the **hydroxy metoprolol** with **identification level 3**. Finally, it can be highlighted that the hydroxy metoprolol is one of the main biotransformation products of MET detected in the ZFE.

5.2.2. Identification of M254

The M254 could be a biotransformation product of MET, because it was absent in the control samples, but it was detected in the ZFE extracts by both chromatographic techniques, RPLC and HILIC, in positive ionization mode. Neither the precursor ion $[M-H]^-$ nor any adduct ion of M254 were detected in negative ionization mode, neither by RPLC nor HILIC.

In positive ionization mode, the EIC of M254 was obtained by extracting the exact molecular mass (254.1751 m/z) of the precursor ion $[M+H]^+$. The molecular mass of M254 is 14 Da lower than the mass of the parent compound MET (268.1907 m/z) which corresponds to the cleavage of a CH_2 group from MET. Therefore, the M254 could be formed through demethylation (phase I reaction of the biotransformation procedure) of the MET. Thus, it is proposed that the M254 is the O-demethyl metoprolol with the below structure (figure 32):

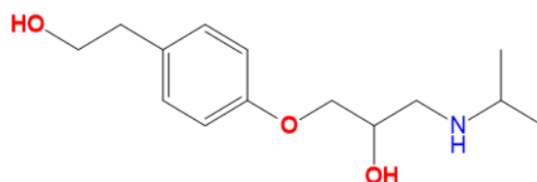


Figure 32. Structure of O-demethyl metoprolol

By extracting the exact mass (254.1751 m/z) in RPLC in positive ionization mode, two peaks were eluted. The first peak has a retention time 3.8 min, whereas the second one 4.3 min. In HILIC, the M254 was eluted in 6.6 min. The EICs of M254 in RPLC and HILIC in positive ionization mode are presented in figure 33 below.

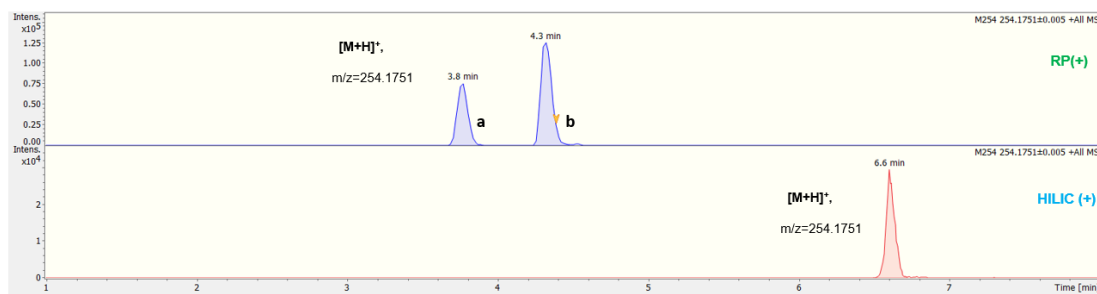


Figure 33. EIC of M254 in RPLC (above) and HILIC (below) in positive ionization mode.

In the MS spectra of M254 obtained by both chromatographic techniques, no adduct ion was found (figure 34). In the MS spectra corresponding to both chromatographic peaks in RPLC, the mass error of the precursor ion $[M+H]^+$ as well as the isotopic fitting (mSigma value) were acceptable. The above criteria were also met in the MS Spectrum obtained by HILIC. Additionally, in the MS spectrum of M254 obtained by HILIC, the detected ion 102.1277 m/z ($C_6H_{16}N^+$) corresponds to an in-source fragment of the M254.

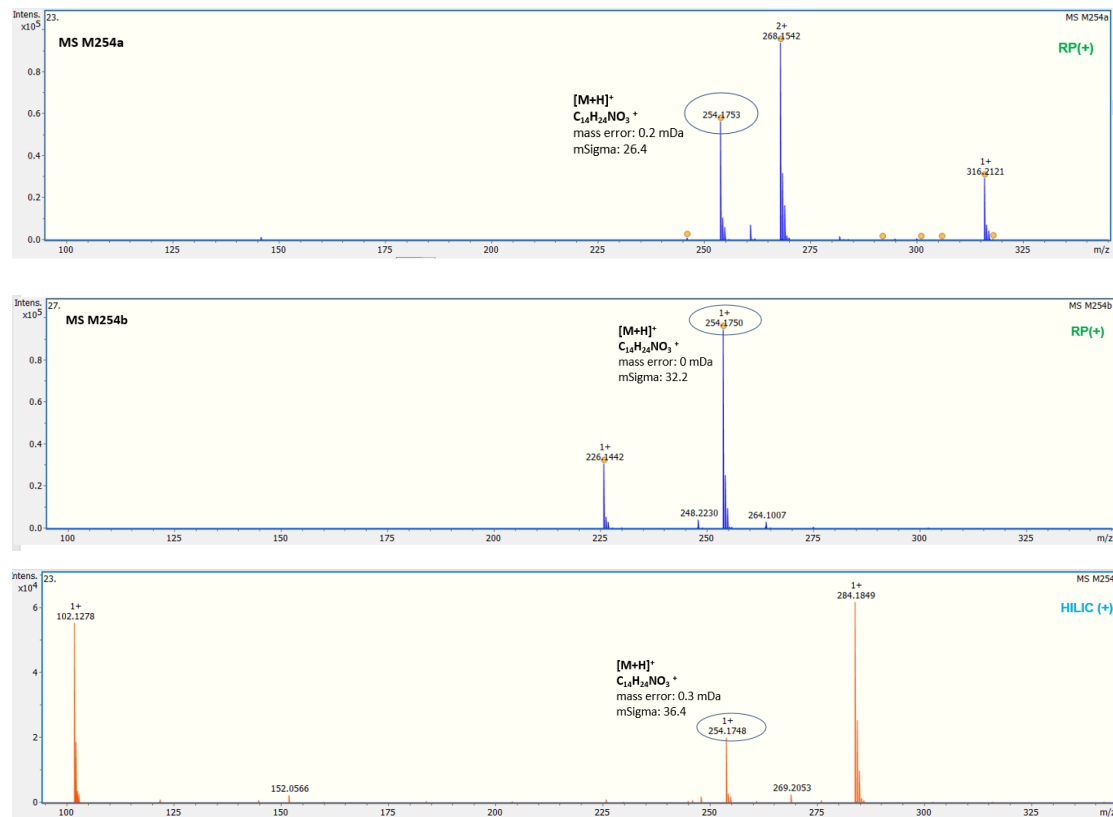


Figure 34: MS spectra of M254 in RPLC and HILIC in positive ionization mode.

Information for the structure of M254 could be obtained from the interpretation of the MS/MS spectra of M254 obtained by both chromatographic techniques (figure 35).

M254a (RPLC): In the MS/MS spectrum of M254a obtained by RPLC in positive ionization mode the below fragments were observed: 116.1070 m/z ($C_6H_{14}N^+$), 133.0648 m/z ($C_9H_9O^+$), 159.0804 m/z ($C_{11}H_{11}O^+$), 177.0910 m/z ($C_{11}H_{13}O_2^+$), 212.1281 m/z ($C_{11}H_{18}NO_3^+$) and 236.1645 ($C_{14}H_{22}NO_2^+$).

From the above fragments, the following were in accordance with the literature as fragments of the O-demethyl metoprolol: 116.1070 m/z ($C_6H_{14}N^+$), 177.0910 m/z ($C_{11}H_{13}O_2^+$), 212.1281 m/z ($C_{11}H_{18}NO_3^+$) and 236.1645 ($C_{14}H_{22}NO_2^+$).

Also, it can be noticed that the fragment ion 177.0910 m/z ($C_{11}H_{13}O_2^+$) is a diagnostic fragment for the O-demethyl metoprolol, because it is 14 Da lower than the characteristic fragment ion 191.1067 m/z ($C_{12}H_{15}O_2^+$) of the parent compound MET. This mass corresponds to a loss of - CH_2 group, indicating that the M254a and MET have the same fragmentation pattern. Additionally, comparing the MS/MS spectra of M254a and the parent compound MET the fragments 116.1070 m/z ($C_6H_{14}N^+$) and 133.0648 m/z ($C_9H_9O^+$) were common.

M254b (RPLC): In the MS/MS spectrum of M254b obtained by RPLC in positive ionization mode the below fragments were observed: 58.0651 m/z ($C_3H_8N^+$), 133.0648 m/z ($C_9H_9O^+$), 159.0804 m/z ($C_{11}H_{11}O^+$), 165.0910 m/z ($C_{10}H_{13}O_2^+$), 177.0910 m/z ($C_{11}H_{13}O_2^+$), 191.1067 m/z ($C_{12}H_{15}O_2^+$), 204.1388 m/z ($C_{13}H_{18}NO^+$), and the 236.1645 m/z ($C_{14}H_{22}NO_2^+$).

It was observed that the characteristic fragment ion of O-demethyl metoprolol 177.0910 m/z ($C_{11}H_{13}O_2^+$), was also found in the MS/MS spectrum of M254b. Furthermore, the MS/MS spectrum of M254b had the following common fragments with the parent compound MET: 133.0648 m/z ($C_9H_9O^+$) and 191.1067 m/z ($C_{12}H_{15}O_2^+$). Additionally, the fragments: 177.0910 m/z ($C_{11}H_{13}O_2^+$) and 236.1645 m/z ($C_{14}H_{22}NO_2^+$) were in accordance with the literature.

M254 (HILIC): In the MS/MS spectrum of M254b obtained by RPLC in positive ionization mode were detected the following fragments: 58.0651 m/z ($C_3H_8N^+$), 133.0648 m/z ($C_9H_9O^+$), 159.0804 m/z ($C_{11}H_{11}O^+$), 165.0910 m/z ($C_{10}H_{13}O_2^+$), 177.0910 m/z ($C_{11}H_{13}O_2^+$), 191.1067 m/z ($C_{12}H_{15}O_2^+$), 204.1388 m/z ($C_{13}H_{18}NO^+$), 212.1281 m/z ($C_{11}H_{18}NO_3^+$) and the 236.1645 m/z ($C_{14}H_{22}NO_2^+$).

Also, it was observed that all of the above fragments except the 212.1281 m/z ($C_{11}H_{18}NO_3^+$) were common with that of the MS/MS of M254b in RPLC. Furthermore, comparing the MS/MS of M254 obtained by HILIC with the literature, the following fragment ions were found as common: 177.0910 m/z ($C_{11}H_{13}O_2^+$), 212.1281 m/z ($C_{11}H_{18}NO_3^+$) and 236.1645 m/z ($C_{14}H_{22}NO_2^+$) [26,41]. Additionally, it could be noticed that the fragments 133.0648 m/z ($C_9H_9O^+$) and 191.1067 m/z ($C_{12}H_{15}O_2^+$) were also detected in the MS/MS spectrum of the parent compound MET. Finally, it was observed that the diagnostic fragment 177.0910 m/z ($C_{11}H_{13}O_2^+$) of the O-demethyl metoprolol also existed in the MS/MS spectrum obtained by HILIC. These facts could confirm that the M254 is a bio-TP of MET.

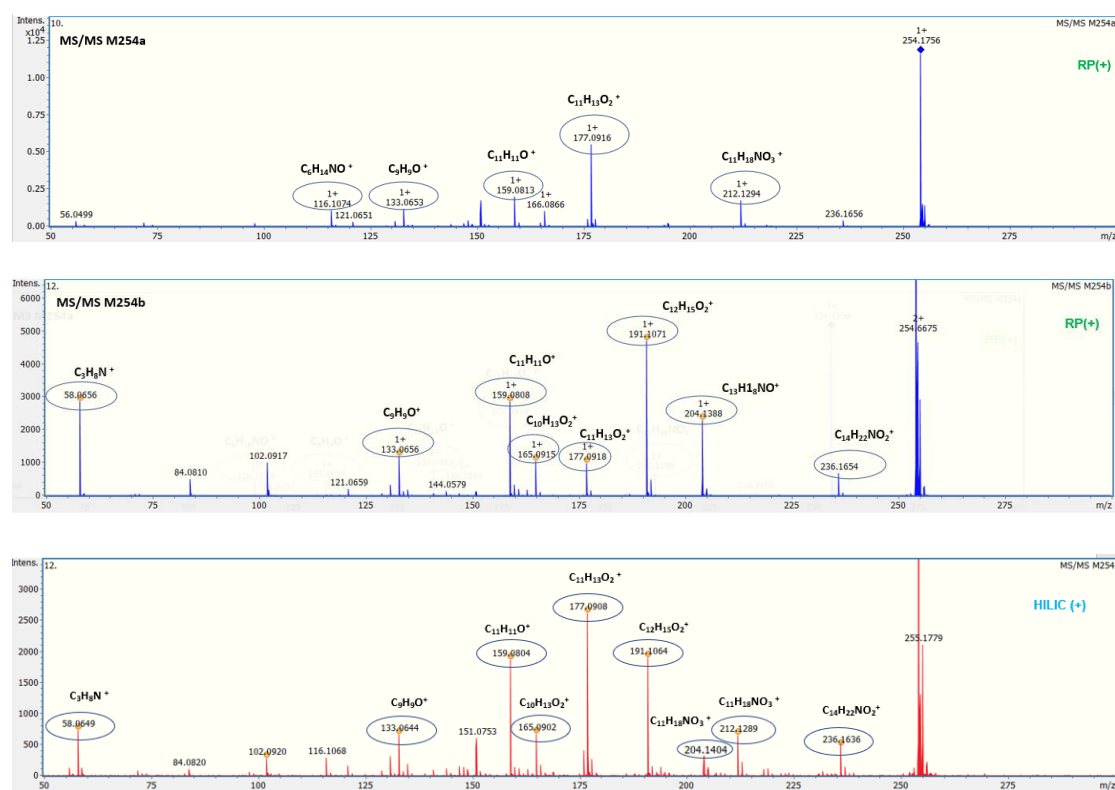


Figure 35. MS/MS spectra of M254 in RPLC and HILIC in positive ionization mode.

By extracting the exact mass of M254 in RPLC two chromatographic peaks were eluted. However, no reference standard for the demethyl metoprolol was available to determine its retention time, and therefore it was not possible to further investigate and identify the M254 in RPLC. Based on the evidence obtained in HILIC, which was in accordance with the literature, it is concluded that M254 is the **demethyl metoprolol with identification level 2b**.

5.2.3. Identification of M268

M268 was considered to be a product of the biotransformation procedure of MET in the ZFE, since it was detected in the ZFE extracts, but it was absent from the control samples. The M268 was detected by both chromatographic techniques, RPLC and HILIC, in positive ionization mode. Neither the precursor ion $[M-H]^-$ nor any adduct ions of M268 were detected by RPLC and HILIC in negative ionization mode.

In positive ionization mode, the EIC of M268 was obtained by extracting the exact molecular mass (268.1543 m/z) of the precursor ion $[M+H]^+$. The sensitivity of the M268 in RPLC was higher compared to that of HILIC. The M268 was suggested to be the biotransformation product metoprolol acid. Metoprolol acid could be formed through oxidation (phase I biotransformation reaction) of the O-demethyl metoprolol (M254). The structure of metoprolol acid is presented in the following figure.

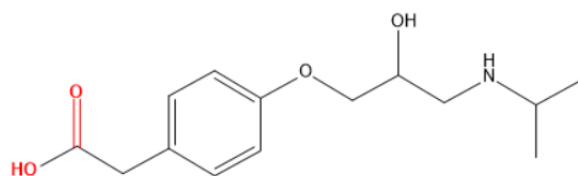


Figure 36. Structure of Metoprolol acid.

The retention time of M268 was 3.7 min in RPLC and 7.0 min in HILIC, in positive ionization mode, as it is shown in figure 37.

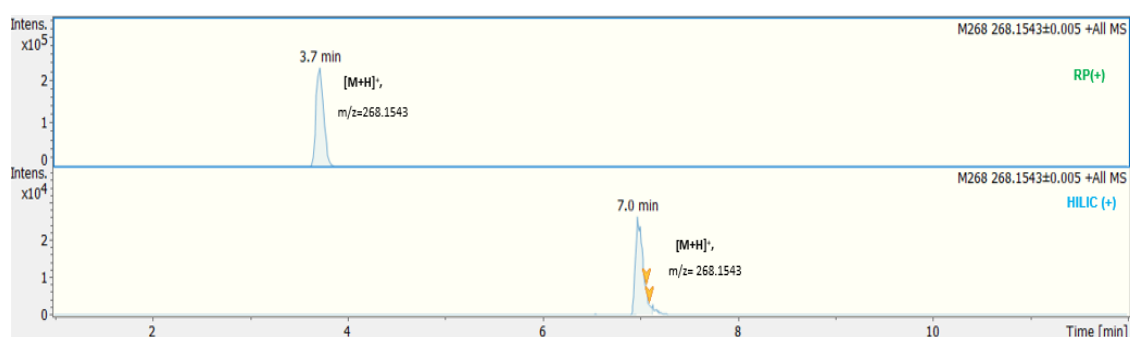


Figure 37. EIC of M268 in RPLC (above) and HILIC (below) in positive ionization mode.

The potassium adduct ion of the M268 $[M+K]^+$, 306.1102 m/z, was also detected in lower intensity in comparison with the $[M+H]^+$ in the MS spectra

obtained by both chromatographic techniques, in positive ionization mode. However, the evaluation of the isotopic fitting of $[M+K]^+$ was not feasible utilizing the mSigma value due to the low intensity of the $[M+K]^+$.

The MS spectra obtained by RPLC and HILIC in positive ionization mode are presented in figure 38 below.

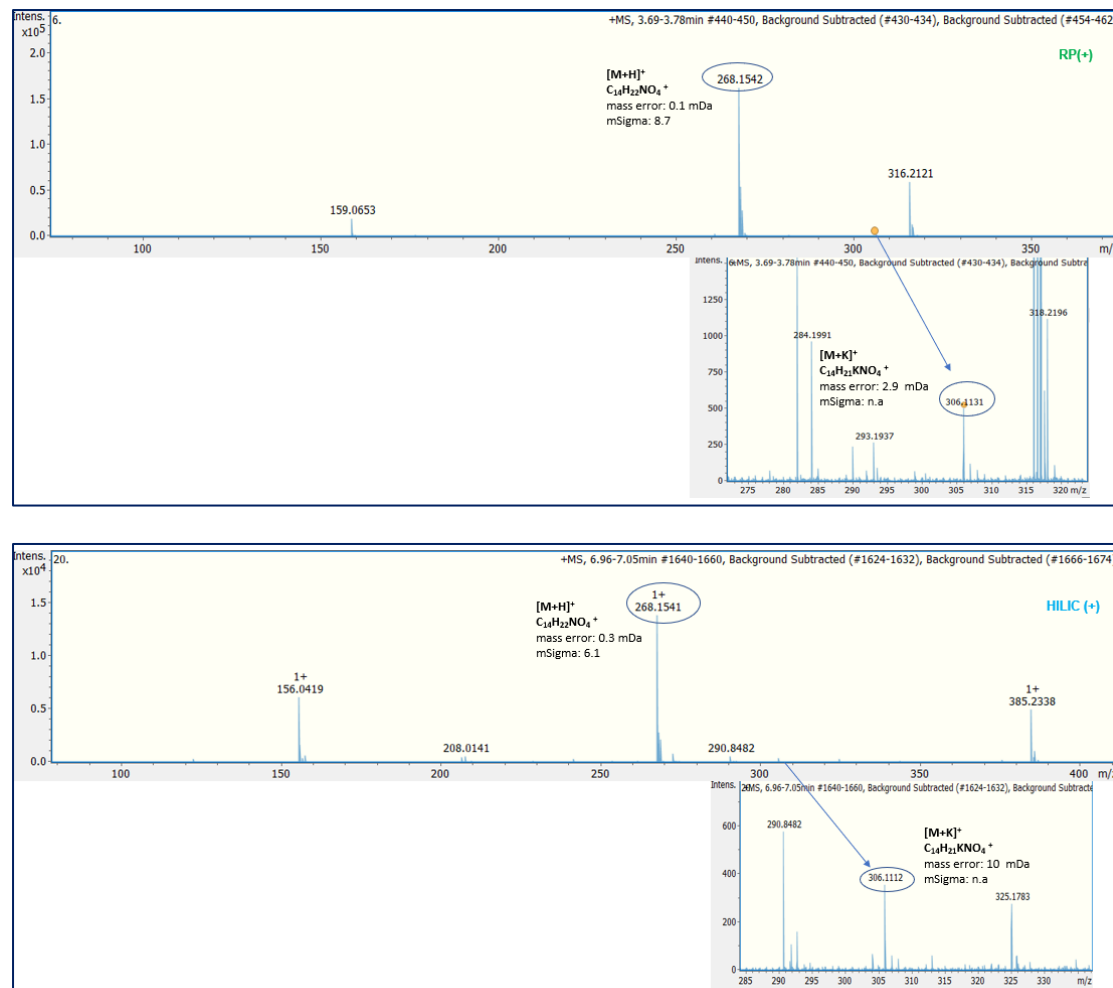


Figure 38. MS spectra of M268 in RPLC (above) and HILIC (below) in positive ionization mode.

Information for the structure of M268 was obtained through the investigation of its MS/MS spectra in both chromatographic techniques. The fragments of M268 that they were detected in the MS/MS spectra obtained by both RPLC and HILIC in positive ionization mode are the following: 56.0495 m/z ($C_3H_6N^+$), 116.1070 m/z ($C_6H_{14}NO^+$), 145.0648 m/z ($C_{10}H_9O^+$), 165.0546 m/z ($C_9H_9O_3^+$), 191.0703 m/z ($C_{11}H_{11}O_3^+$), 226.1074 m/z ($C_{11}H_{16}NO_4^+$) and 250.1438 m/z ($C_{14}H_{20}NO_3^+$). The reversed elution order of M268 in RPLC and HILIC and the common fragmentation pattern of M268 in both chromatographic indicated the

orthogonal identification of M268. This evidence is an important confirmatory element in its identification.

Moreover, some of the detected fragments, such as 116.1070 ($C_6H_{14}NO^+$), 191.0703 m/z ($C_{11}H_{11}O_3^+$), 226.1074 m/z ($C_{11}H_{16}NO_4^+$) m/z, 145.0648 m/z ($C_{10}H_9O^+$), and 250.1438 m/z ($C_{14}H_{20}NO_3^+$) are in accordance with the literature [26,41]. Additionally, the fragments 56.0495 m/z ($C_3H_6N^+$) and 116.1070 ($C_6H_{14}NO^+$) were common with the fragments of the parent compound MET. This fact is an additional confirmatory element that M268 is a biotransformation product of MET. The MS/MS spectra obtained by RPLC and HILIC in positive ionization mode are presented in figure 39 below.

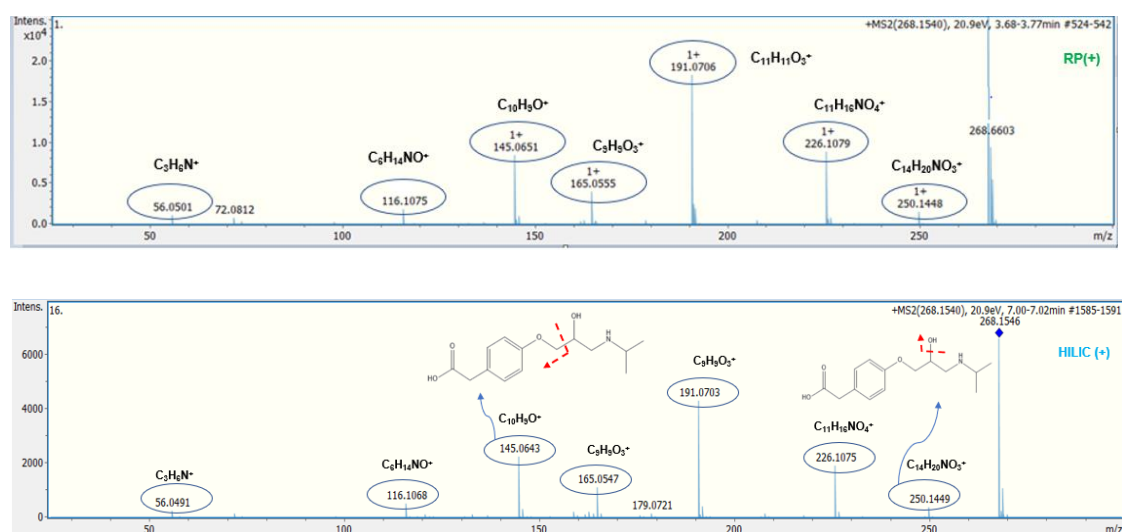


Figure 39. MS/MS spectra of M268 in RPLC (above) and HILIC (below) in positive ionization mode.

Overall, a probable structure for M268 could be proposed relied on the existence and interpretation of the MS/MS spectra of M268. Hence, M268 is the metoprolol acid with identification confidence level 2b. Finally, it can be highlighted that the metoprolol acid is one of the main bio-TPs detected in the ZFE.

5.2.4. Identification of M226

The biotransformation product M226 was suspected to be a metabolite of the parent compound MET, since it was existed only in the ZFE extracts and not in the control samples. The M226 was detected by both RPLC and HILIC only in positive ionization mode. The RPLC was more sensitive chromatographic

technique in detecting M226 compared to HILIC, whereas higher intensity in the EIC of M226 in RPLC was observed. Its EIC was obtained by extracting the exact molecular mass (226.1438 m/z) of the precursor ion $[M+H]^+$. The protonated molecular mass of M226 was 42 Da lower compared to the protonated molecular mass of MET, indicating the loss of the N-isopropyl group of the parent compound. Thus, M226 was recommended to be the N-deisopropyl metoprolol. N-deisopropyl metoprolol has been occurred through N-deacetylation of Metoprolol, a phase I reaction of the biotransformation procedure. The structure of the N-deisopropyl metoprolol is presented in the following figure.

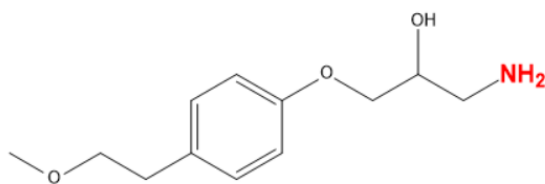


Figure 40. Structure of N-deisopropyl metoprolol

The retention time of M284 was 4.3 min in RPLC and 6.7 min in HILIC in positive ionization mode. The differences in the elution time as well as in the peak intensity of $[M+H]^+$ in both chromatographic techniques (RPLC and HILIC) are presented in the figure below (figure 41).

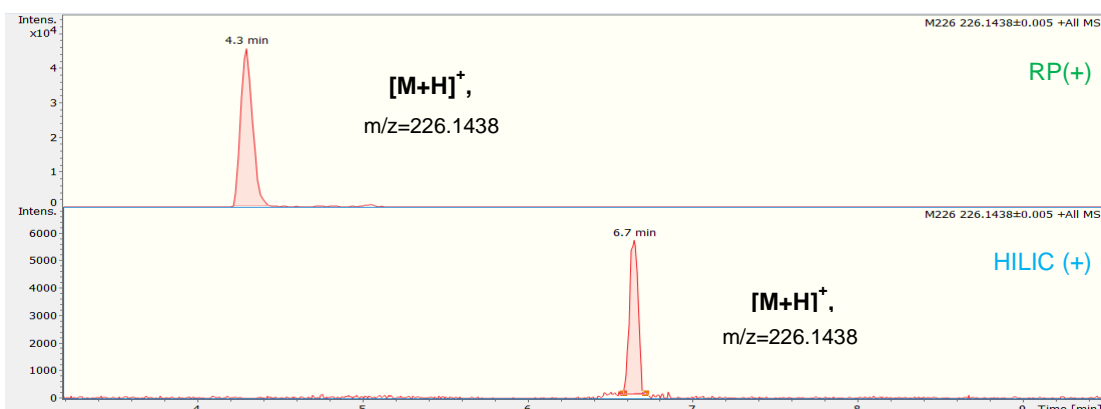


Figure 41. EIC of M226 in RPLC (above) and HILIC (below) in positive ionization mode

The potassium adduct ion of the M226 $[M+K]^+$, 264.0997 m/z, was also observed in lower intensity in the MS spectrum obtained by RPLC in positive ionization mode. No adduct ion of M226 has been detected by HILIC. The MS

spectra obtained by RPLC and HILIC in positive ionization mode are presented in figure 42 below.

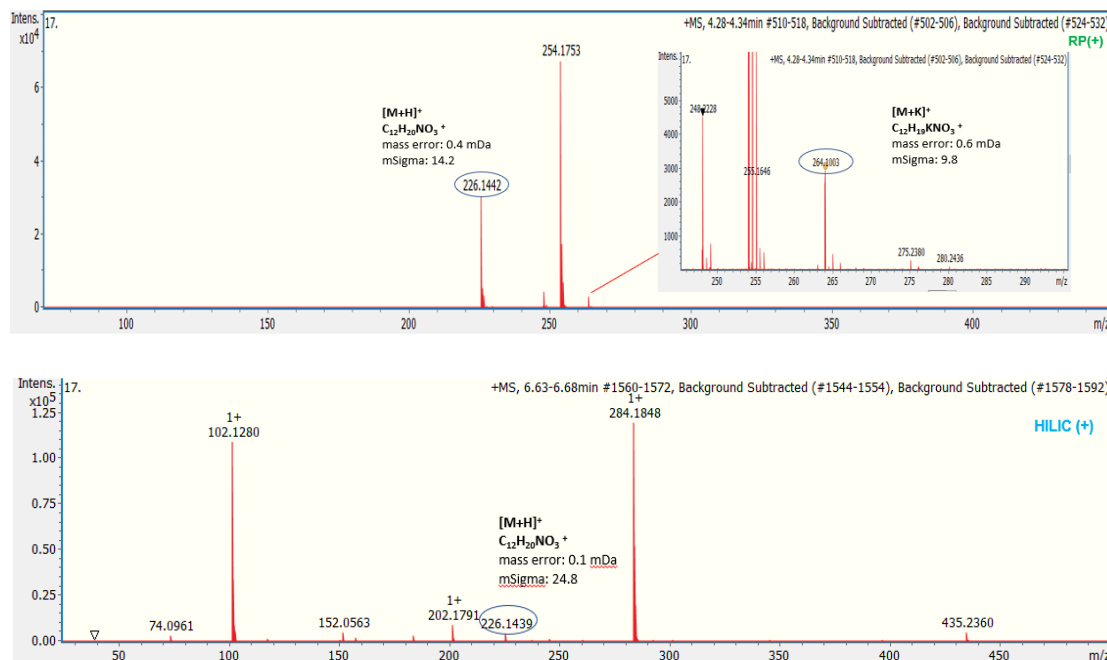


Figure 42. MS spectra of M226 in RPLC (above) and HILIC (below) in positive ionization mode.

Since for this metabolite an analytical standard was unavailable, investigation of MS and MS/MS spectra in data-dependent and data-independent modes in both chromatographic techniques was carried out, so that evidence for structural proposal would be obtained.

It was observed that many fragments that were detected in the MS/MS spectra of M226 in both RPLC and HILIC in positive ionization mode, were also found in the MS/MS spectra of MET. More specifically, the common fragments of M226 and its parent compound were the below: 56.0495 m/z (C₃H₆N⁺), 74.0600 m/z (C₃H₈NO⁺), 133.0648 m/z (C₉H₉O⁺), 159.0804 m/z (C₁₁H₁₁O⁺), and 191.1067 m/z (C₁₂H₁₅O₂⁺). Thus, it was concluded that the M226 presented the same fragmentation pattern as that of MET, which could confirm that the M226 is a biotransformation product of MET.

Moreover, many common fragments were detected in the MS/MS spectra of M226 by the two different chromatographic techniques (RPLC & HILIC) in positive ionization mode. More specifically, the common fragments were the below: 56.0495 m/z (C₃H₆N⁺), 74.0600 m/z (C₃H₈NO⁺), 121.0642 m/z (C₈H₉O⁺),

133.0648 m/z ($\text{C}_9\text{H}_9\text{O}^+$), 159.0804 m/z ($\text{C}_{11}\text{H}_{11}\text{O}^+$), 165.0930 m/z ($\text{C}_{10}\text{H}_{13}\text{O}_2^+$) and 191.1067 m/z ($\text{C}_{12}\text{H}_{15}\text{O}_2^+$). The common fragmentation of the M226 in the MS/MS spectra obtained by RPLC and HILIC indicated the orthogonal identification of M226 and enhanced its identification confidence. The MS/MS spectra of M226 obtained by RPLC and HILIC are presented in figure 43 below.

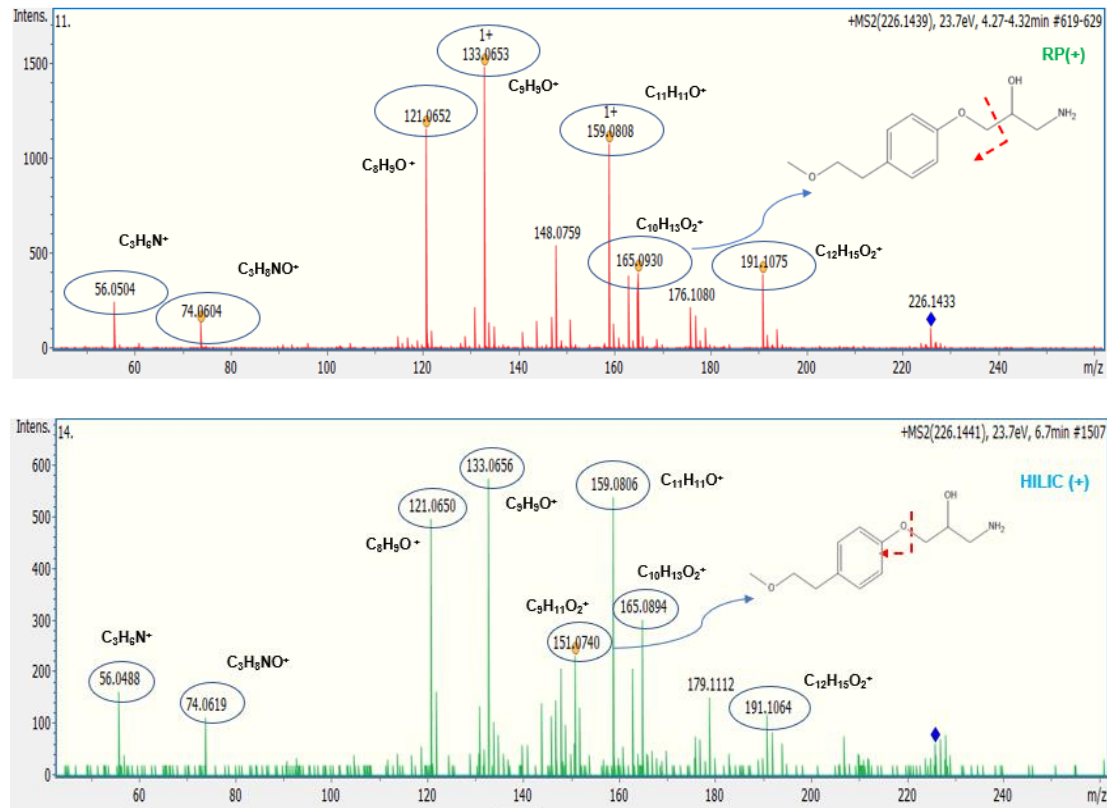


Figure 43. MS/MS spectra of M226 in RPLC (above) and HILIC (below) in positive ionization mode.

Additionally, it should be noticed that the fragments 74.0600 m/z ($\text{C}_3\text{H}_8\text{NO}^+$), 121.0642 m/z ($\text{C}_8\text{H}_9\text{O}^+$), and 191.1067 m/z ($\text{C}_{12}\text{H}_{15}\text{O}_2^+$) were reported in the literature as fragments of the N-deisopropyl metoprolol [26,41].

From all the above information, and since a possible structure could be suggested through the investigation of the MS/MS spectra of M226, it is proposed that the metabolite M226 is the compound **N-deisopropyl metoprolol** with **identification confidence level 2b**.

5.2.5. Identification of M241

The bio-TP M241 was detected through suspect screening in both polarities in the ZFE extracts. However, it was absent from the control samples and therefore the M241 was supposed to be a biotransformation product of MET.

In RPLC in positive ionization mode, only the ammonium adduct ion of M241 was detected. Its EIC was obtained by extracting the exact molecular mass (258.1336 m/z) of the ammonium adduct ion $[M+NH_4]^+$. The retention time of M241 was 5.0 min in RPLC in positive ionization mode (figure 44). Additionally, M241 was detected by RPLC in negative ionization mode with low intensity peak. Its EIC was obtained by extracting the exact molecular mass (239.0925 m/z) of the precursor ion $[M-H]^-$. The retention time of M241 was 4.3 min in RPLC in negative ionization mode (figure 44). Neither the precursor ions $[M+H]^+$ and $[M-H]^-$ nor any adduct ion of M241 were detected by HILIC in positive and negative ionization mode, respectively. The fact that M241 was detected in both polarities enhanced its identification confidence.

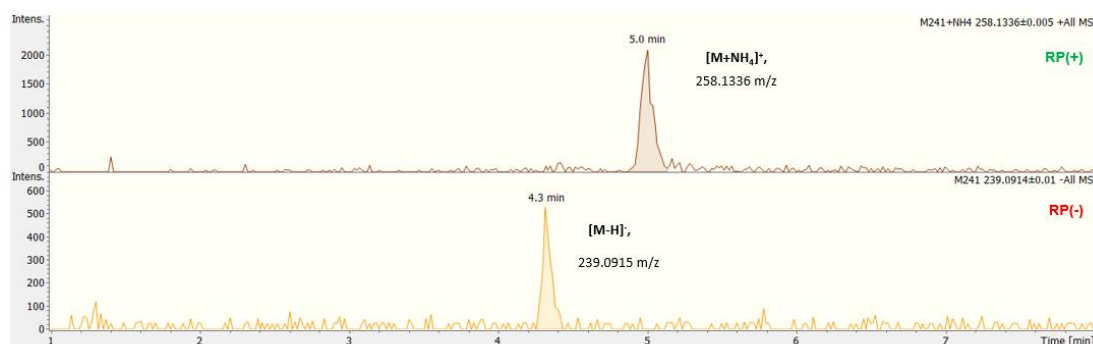


Figure 44. EIC of M241 in RPLC in positive (above) and negative (below) ionization modes

The MS spectrum of $[M+NH_4]^+$ obtained by RPLC in positive ionization mode and the MS spectrum of $[M-H]^-$ obtained by RPLC in negative ionization mode are presented in figure 45 below. However, due to the low ion intensity peaks in both positive and negative ionization modes, no MS/MS spectra in the data-dependent mode were acquired and therefore no additional evidence for a potential structure of M241 was available.

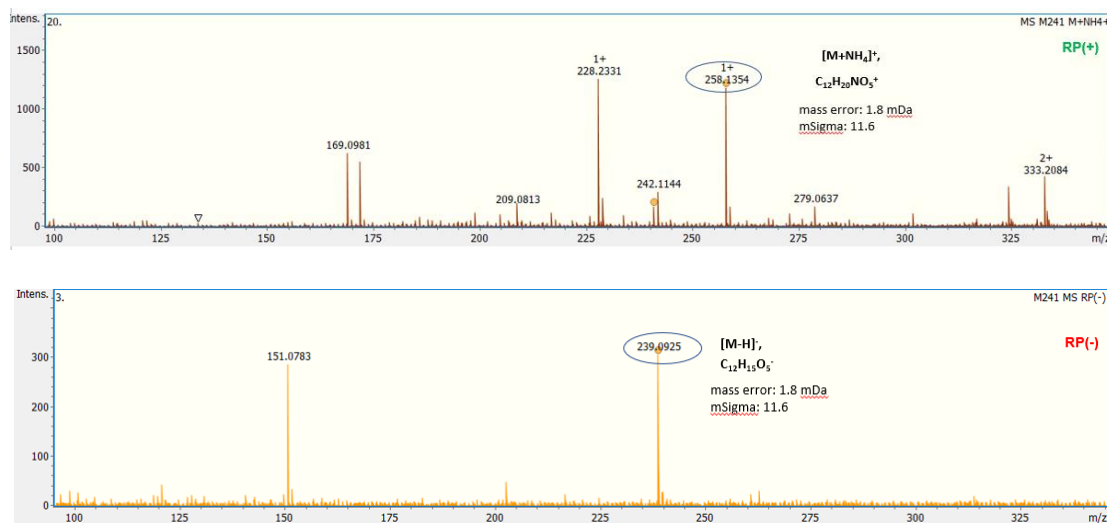


Figure 45. MS spectra of M241 in RPLC in positive (above) and negative (below) ionization modes

According to the literature, M241 was suggested to be the deaminated metoprolol. Deaminated metoprolol was recommended to be formed through oxidative deamination of the parent compound MET, a phase I reaction of the biotransformation procedure. The proposed from literature structure of the deaminated metoprolol is shown in the figure below [41,69,70].

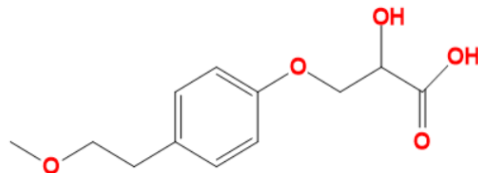


Figure 46. Structure of deaminated metoprolol

Therefore, due to the unequivocal molecular formula (C₁₂H₁₉NO₅), but because of the absence of the MS/MS spectra to propose a structure, it is concluded that the **identification confidence level** of the **M241** is **4**.

5.2.6. Identification of M254

The M254 did not exist in the control samples, but it was detected in the ZFE extracts. Therefore, it could be a biotransformation product of MET in the ZFE. M254 was detected as [M+H]⁺ in RPLC in positive ionization mode, while only the sodium adduct ion of M254 [M+Na]⁺ was detected in HILIC in positive ionization mode. The EICs of M254 were obtained by extracting the exact

molecular mass (254.2387 m/z) of the precursor ion $[M+H]^+$ in RPLC and (276.1206 m/z) of the sodium adduct ion $[M+Na]^+$ in HILIC. M284 was eluted in 3.4 min RPLC and $[M+Na]^+$ in 6.5 min in HILIC in positive ionization mode (figure 47).

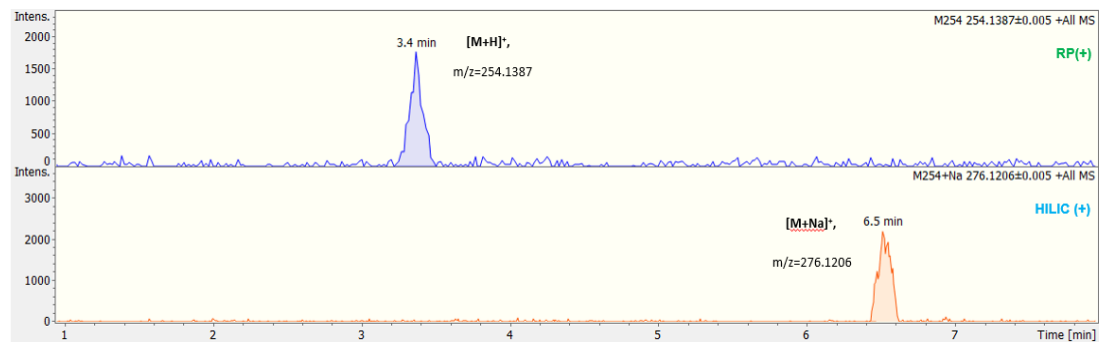


Figure 47. EIC of M254 in RPLC (above) and HILIC (below) in positive ionization mode

From the MS spectra of M254 obtained by both chromatographic techniques, it could be noticed that the sensitivity of HILIC in detecting the sodium adduct ion $[M+Na]^+$ was equal to that of RPLC in detecting the $[M+H]^+$. The MS spectra obtained by RPLC and HILIC in positive ionization mode are presented in figure 48 below.

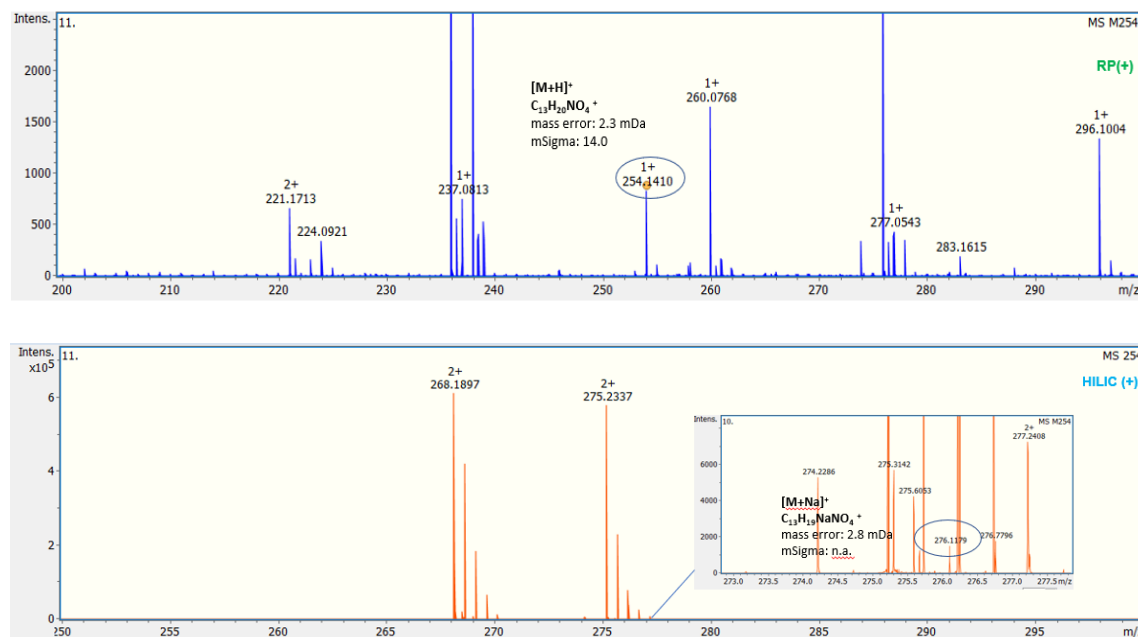


Figure 48. MS spectra of M254 in RPLC (above) and HILIC (below) in positive ionization mode

However, no MS/MS spectra obtained by data-dependent acquisition mode were available neither in HILIC nor in RPLC in positive ionization mode, and therefore a structure for M254 could not be proposed.

Although, according to the literature, the biotransformation product M254 was formed through two successive reactions, benzylic hydroxylation, and oxidation, of the M254 (O-demethyl metoprolol) with the below-proposed structure [26]:

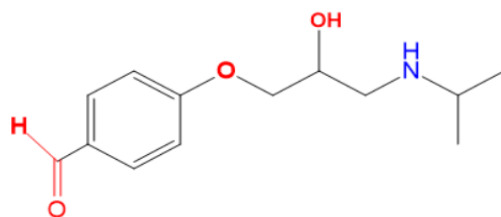


Figure 49. Structure of M254

From all the above analytical data, it is concluded that the molecular formula ($C_{13}H_{19}NO_4$) of **M254** is unequivocal. Therefore, due to the inefficient experimental evidence to propose a possible structure, the **identification level** of M254 is **4**.

5.2.7. Identification of M270

The M270 could be a product of the xenobiotic biotransformation of MET, because it was absent from the control samples, but it existed in the ZFE extracts. M270 was detected only by RPLC in positive ionization mode. In negative ionization mode (by RPLC and HILIC), neither the precursor ion $[M-H]^-$ nor any adduct of M270 were detected.

Its EIC was obtained by extracting the exact molecular mass (270.1700 m/z) of the precursor ion $[M+H]^+$ with low intensity. The exact molecular mass of M270 is 16 Da higher than the mass of M254 (O-demethyl metoprolol) which corresponds to the mass of an oxygen atom indicating that M270 could be formed through hydroxylation (phase I reaction of the biotransformation procedure) of M254. Also, the mass of M270 is 14 Da lower than the mass of M284 (hydroxy metoprolol) corresponds to the mass of a loss of $-CH_2$ group. Thus, M270 could be formed through demethylation (phase I reaction of

biotransformation procedure) of M284. To sum up, the M270 could be formed from two different metabolic pathways according to the literature and the biotransformation rules. Thus, M270 was recommended to be the hydroxy-demethyl metoprolol with the below structure [26,41,69]:

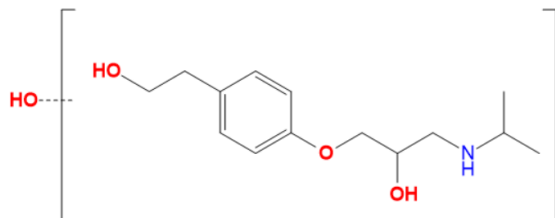


Figure 50. Structure of hydroxy-demethyl metoprolol

The retention time of M270 was 2.6 min in RPLC in positive ionization mode (figure 51).

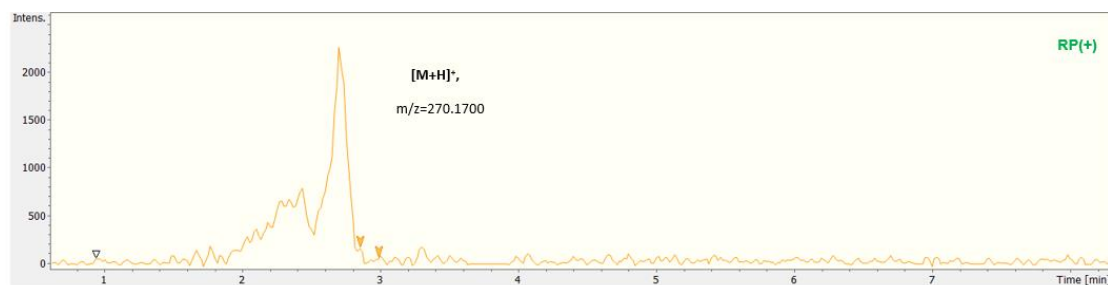


Figure 51. EIC of M270 in RPLC in positive ionization mode

In the MS spectrum obtained by RPLC, no adduct ion of M270 was found. Additionally, due to the low ion intensity of $[M+H]^+$, MS/MS spectrum of M270 in data-dependent mode was not acquired (figure 52).

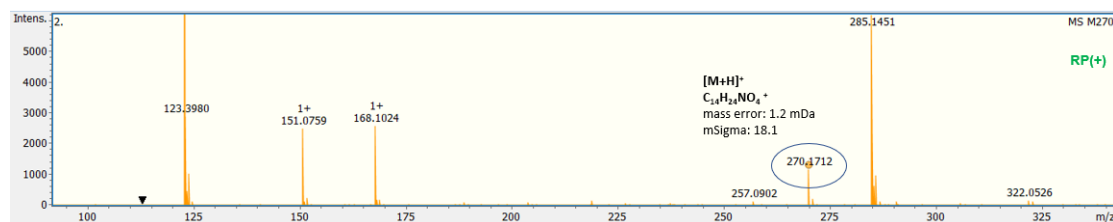


Figure 52. MS spectrum of M270 in RPLC in positive ionization mode

Since the analytical evidence for **M270** was limited, a probable structure could not be proposed and only **level 4** for its **identification** (unequivocal formula) could be achieved.

5.2.8. Identification of M282

Since M282 was absent from the control samples, but it was detected in the ZFE extracts by both chromatographic techniques, RPLC and HILIC, in positive ionization mode, it could be a biotransformation product of MET. The EIC of M282 was obtained by extracting its exact molecular mass (282.1700 m/z). RPLC was a more sensitive technique in detecting the $[M+H]^+$ in comparison with HILIC. The retention time of M282 in RPLC was 3.7 min and 6.6 min in HILIC in positive ionization mode (figure 53).

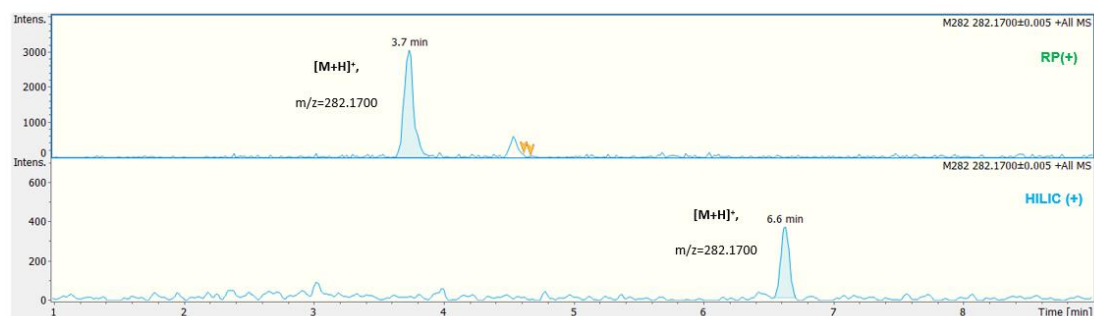


Figure 53. EIC of M282 in RPLC (above) and HILIC (below) in positive ionization mode

Since the signal intensity of M282 in HILIC was very low, it was not possible to be investigated further. In the MS spectrum obtained by RPLC (figure 54) in positive ionization mode only the precursor ion $[M+H]^+$ of M282 was detected.

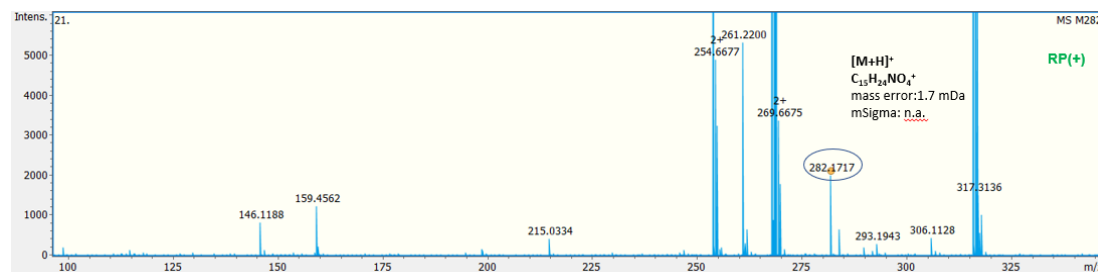


Figure 54. MS spectrum of M282 in RPLC in positive ionization mode

MS/MS spectrum in data-dependent mode in RPLC in positive ionization mode was not acquired, and therefore further information for a possible structure of M282 did not exist.

However, according to the literature and the *in-silico* tool Metabolite Predict, M282 could be formed through the alcohol oxidation (phase I reaction) of the biotransformation product M284 (hydroxy metoprolol) [26]. Gathering all the

above data, the molecular formula ($C_{15}H_{23}NO_4$) of M282 is unambiguous, but since MS/MS spectra were not available, the **identification level of M282 is 4**.

5.2.9. Identification of M460

The M460 was suggested to be a biotransformation product of MET, since it was absent from control samples, but it was detected in the ZFE extracts. M460 was detected by RPLC and HILIC only in positive ionization mode. Neither its precursor ion $[M-H]^-$ nor any adduct ion of M460 was detected in negative ionization mode by none of the two chromatographic techniques. In positive ionization mode, the EIC of M460 was obtained by extracting the exact molecular mass (460.2177 m/z) of the precursor ion $[M+H]^+$. The protonated molecular formula of M460 was 177 Da higher than that of M284. The mass 177 Da corresponds to the mass of glucuronic acid. The glucuronic acid can link to other compounds through a reaction called glucuronidation. Glucuronidation is a reaction of phase II of the biotransformation procedure. The substances resulting from glucuronidation are known as glucuronides. M284 was recommended to be the hydroxy metoprolol. Thus, the M460 was supposed to be the glucuronide of hydroxy metoprolol. The M460 could be formed through the glucuronidation of the metabolite M284. The suggested structure of M460 is presented in the figure below.

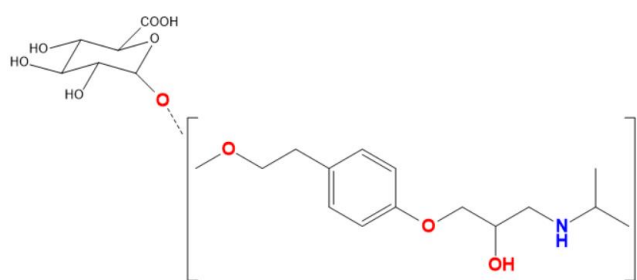


Figure 55. Structure of glucuronide of hydroxy metoprolol

The RPLC was a more sensitive chromatographic technique in detecting the M460 in positive ionization mode compared to HILIC. The retention time of M460 was 3.3 min in RPLC and 7.4 min in HILIC in positive ionization mode, as is shown in figure 56 below.

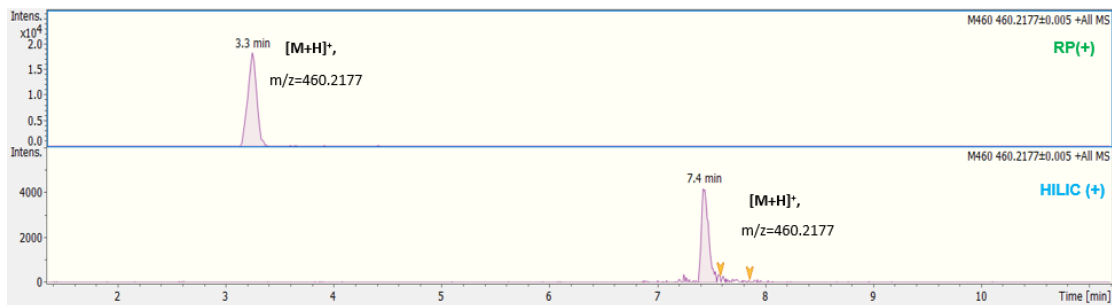


Figure 56. EIC of M460 in RPLC (above) and HILIC (below) in positive ionization mode

Except for the precursor ion of M460 $[M+H]^+$, its potassium adduct ion $[M+Na]^+$ was detected in the MS spectrum of M460 obtained by HILIC in positive ionization mode. The intensity of the ion peak $[M+Na]^+$ was lower than that of the $[M+H]^+$ in the MS spectrum. Additionally, no adduct ion of M460 was detected by RPLC in positive ionization mode. The MS spectra obtained by RPLC and HILIC in positive ionization mode are presented in the figure below.

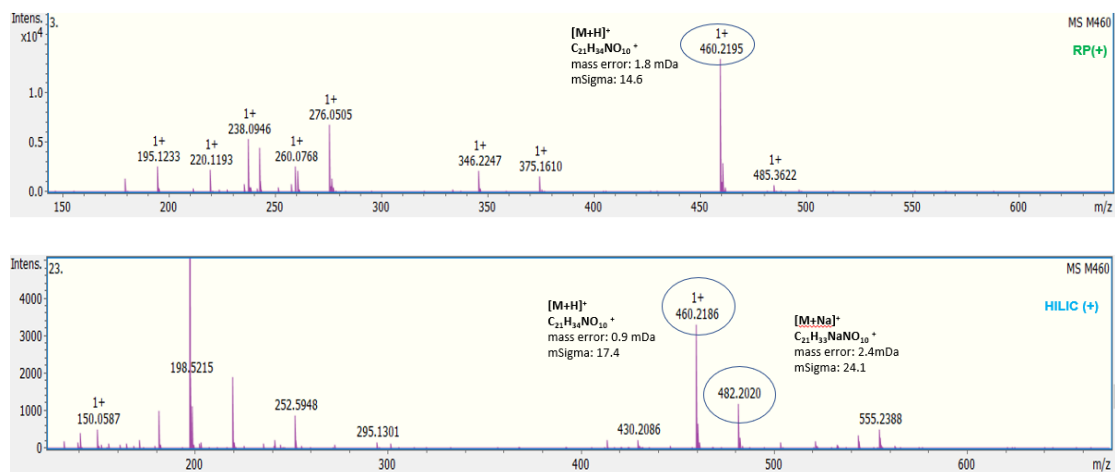


Figure 57. MS spectra of M460 in RPLC (above) and HILIC (below) in positive ionization mode.

From the interpretation of the MS/MS spectra of M460 obtained by both chromatographic techniques in positive ionization mode, information for its structure could be obtained. In both MS/MS spectra, the detected fragments were the following: 116.1070 ($C_6H_{14}NO^+$) and 284.1856 m/z ($C_{15}H_{26}NO_4^+$) which corresponds to the hydroxy metoprolol (M284). The common fragments of M460 in the MS/MS obtained by RPLC and HILIC enhanced the confidence level of its identification. Moreover, fragment 116.1070 ($C_6H_{14}NO^+$) was also found in the MS/MS spectra of MET. This fact is a confirmatory evidence that

M460 is a biotransformation product of MET. The MS/MS spectra obtained by RPLC and HILIC in positive ionization mode are presented in figure 58 below.

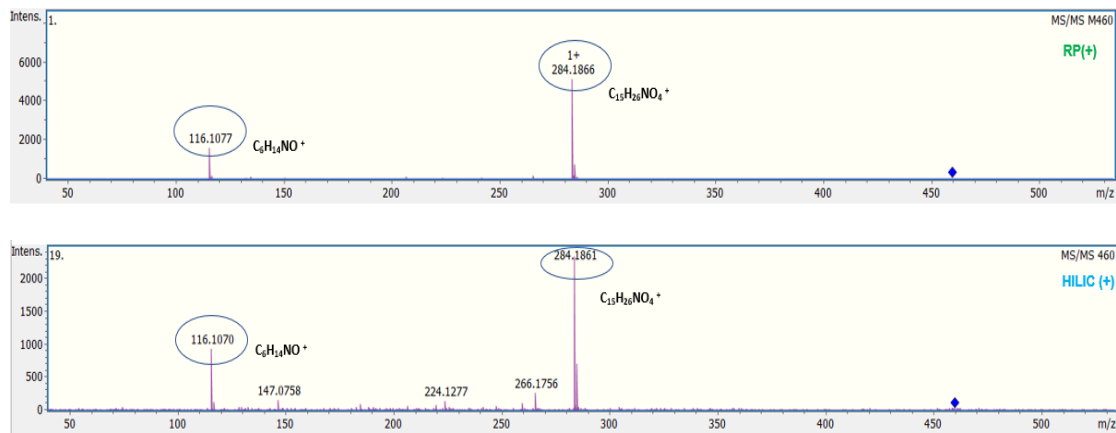


Figure 58. MS/MS spectra of M460 in RPLC (above) and HILIC (below) in positive ionization mode.

Regarding all the above information, the M460 is the **glucuronide of hydroxy metoprolol** with **identification confidence level 3**. To the best of our knowledge, this is the first time that the glucuronide of hydroxy metoprolol is reported as a biotransformation product of Metoprolol.

5.2.10. Identification of M444

The M444 could be a result of the xenobiotic biotransformation of MET in the ZFE because it was absent from the control samples, but it was detected in the ZFE extracts by both RPLC and HILIC in positive ionization mode. Neither its precursor ion $[M-H]^-$ nor any adduct ion of M444 was detected in negative ionization mode. The EIC of M444 was obtained by extracting the exact molecular mass (444.2228 m/z) of the precursor ion $[M+H]^+$. The exact molecular mass of M444 is 177 Da higher than that of the parent compound MET (268.1907 m/z), which corresponds to the mass of glucuronic acid. Therefore, it was suggested that the M444 is the glucuronide of metoprolol and it was formed through glucuronidation, a phase II reaction of the biotransformation procedure. The recommended structure is presented in the figure below:

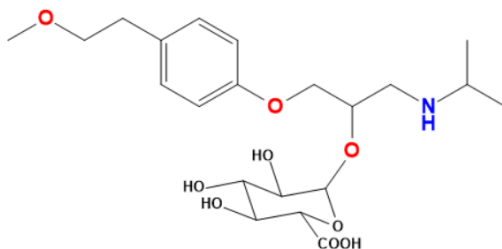


Figure 59. Structure of glucuronide of metoprolol

The retention time of M444 was 4.9 min in RPLC and 6.6 min in HILIC in positive ionization mode (figure 60).

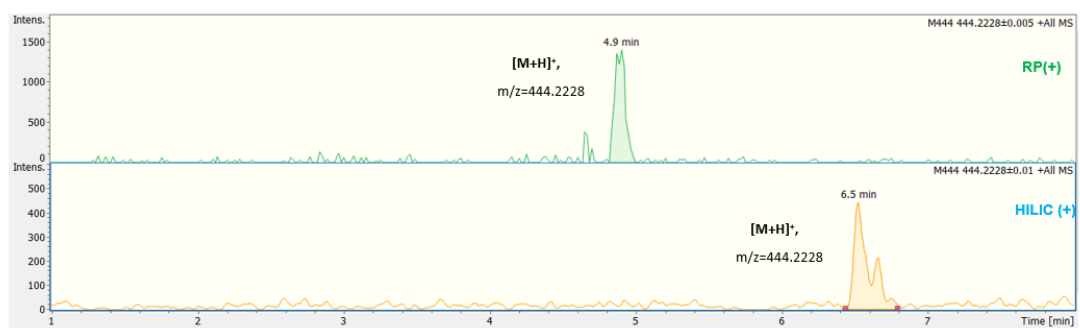


Figure 60. EIC of M444 in RPLC (above) and HILIC (below) in positive ionization mode.

However, the signals (intensity) of M444 were very low, and for this reason, they were not further investigated. In the MS spectrum obtained by RPLC in positive ionization mode, only the precursor ion $[M+H]^+$ of M444 was detected (figure 61).

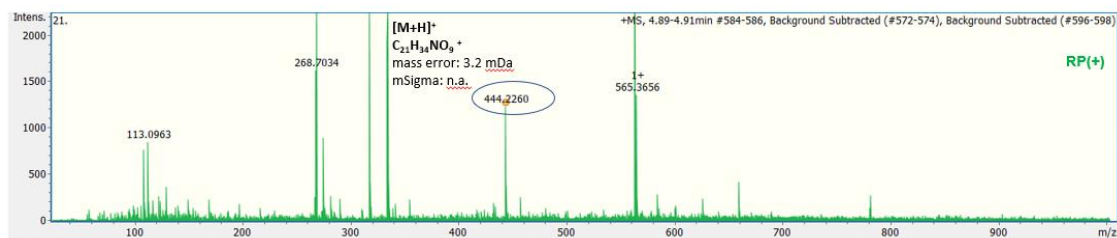


Figure 61. MS spectrum of M444 in RPLC in positive ionization mode.

Furthermore, the MS/MS spectrum of M444 in data-dependent mode was not available, and therefore its proposed structure could not be confirmed.

Consequently, since the molecular formula ($C_{21}H_{33}NO_9$) of M444 was unambiguous, but MS/MS spectra did not exist, M444 is the glucuronide of metoprolol with **identification confidence level 4**.

5.3. Proposed biotransformation pathway of Metoprolol

Gathering all the above bio-TPs, a possible biotransformation pathway of Metoprolol in the ZFE was proposed. For the proposed metabolic pathway, which is illustrated in the figure below (figure 62), the biotransformation rules were taken into account. The functional groups corresponding to phase I reactions are presenting with light blue color, while for the functional groups corresponding to phase II reactions, turquoise color was used. In the frames, the main bio-TPs of Metoprolol are shown (hydroxy-metoprolol and metoprolol acid).

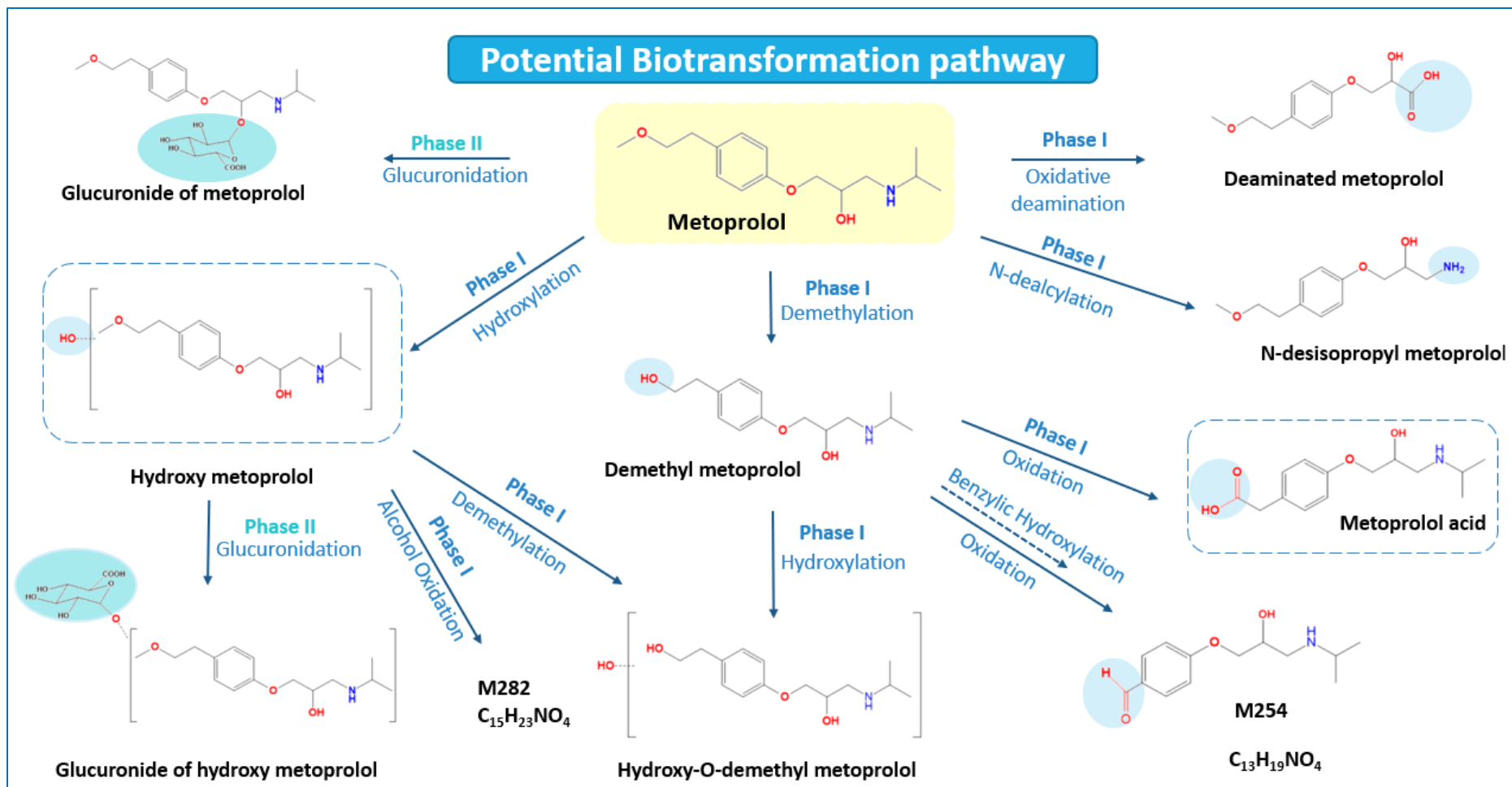


Figure 62. Proposed Biotransformation pathway of Metoprolol in ZFE.

Chapter 6

Conclusions

The different pH values of the environment influence the speciation (neutral or ionic form) of the IOCs. The neutral form of an IOC can permeate more easily through membranes than the corresponding ionic one resulting in higher uptake. Consequently, in the pH values where the neutral form of an IOC is the predominant one, the uptake, and as a result, the toxicity is higher.

Regarding the IOC Metoprolol, it is a base with $pK_a = 9.68$. Thus, at alkaline pH values, the neutral species of Metoprolol is increasing resulting in higher uptake and toxicity. More specifically, it was concluded from the results of this study that Metoprolol at pH 9 is more toxic and the LC50 value was significantly lower than the LC50 value at pH 6. Therefore, the toxicity of Metoprolol is pH-dependent. On the other hand, low variations were observed in the measured internal concentrations of Metoprolol in the ZFE at the different pH values. Thus, it can be concluded that the internal concentrations are pH-independent. For this reason, it is strongly recommended to use the internal concentration as a more accurate measurement of the toxicity of the IOCs in the toxicity tests.

Additionally, the bioaccumulation of Metoprolol was higher at alkaline pH values, due to the increased % percentage of its neutral form. More specifically, it was found that the average BCF value of Metoprolol was approximately 155 times higher than the BCF value at pH 6. So, it can be concluded that the BCF values, and so the bioaccumulation, of Metoprolol are strongly affected by the different pH values. These findings indicate the importance of investigating the pH factor in the environmental toxicity tests of the IOCs. Otherwise, the toxicity of the IOCs may be under- or over-estimated.

As regards the biotransformation results, they indicated that the ZFE have a great capacity to metabolize the compound Metoprolol, with phase I biotransformation reactions being favoured. More specifically, the main metabolite path seems to be the hydroxylation and therefore, the hydroxy metoprolol was the main biotransformation product. To the best of our knowledge, this is the first time that the biotransformation of Metoprolol in the

ZFE is investigated. In our study, a total of ten (10) bio-TPs were detected and the glucuronide of hydroxy metoprolol was detected for the first time as bio-TP of Metoprolol. Additionally, most of the bio-TPs were detected by both RPLC and HILIC. The combinational usage of both RPLC and HILIC in both ionization polarities provided extra analytical evidence (e.g. more or different fragment ions and/or adduct ions). Also, by using two different chromatographic techniques could be achieved orthogonal identification of the detected bio-TPs.

Therefore, the fact that the compound Metoprolol is highly biotransformed in the ZFE highlights the importance to study thoroughly its biotransformation in toxicokinetic studies.

Chapter 7

Future Perspectives

First of all, the potential effects of pH on the uptake, bioaccumulation, and toxicity of more weak bases and acids are going to be investigated in the following months. Additionally, *Daphnia magna* and *Lemna minor* from exposure experiments to weak bases and acids are going to be analyzed to evaluate the potential pH-dependent toxicity effects of weak acids and bases in other aquatic organisms, except ZFE. The final goal of the PHION project is the creation of a novel model approach that can assess the toxicity of IOCs at different pH values, even if toxicity data are only available for one pH value.

So far, different studies focus on the potential effects of pH in high exposure concentrations in ZFE have been studied. However, the environmental concentrations of the emerging contaminants are significantly lower. Therefore, future studies could focus on pH-dependent effects on toxicity at environmentally relevant concentrations.

In addition, as mentioned in Chapter 1, there is a literature gap in studying the chronic effects of IOCs. However, since aquatic organisms are exposed to such chemicals for long periods, investigations focused on the chronic effects of weak bases and acids is an important step forward. Moreover, pharmaceuticals exist in the aquatic environment in mixtures, and not as single compounds. The effects of mixtures of different substances may be different. However, the knowledge about the mixture's effects is still sparse. So, there is a need for further investigation. For instance, the effects of a mixture of b-blockers, such as Metoprolol and Propranolol, could be assessed in the future.

Regarding the biotransformation, in this study, a suspect screening approach was implemented. However, for a thorough investigation of the biotransformation of Metoprolol in ZFE, non-target approach will also be followed in the future. Additionally, the biotransformation of more weak acids and bases will be studied in ZFE, *Daphnia magna* and *Lemna minor*.

ACRONYMS –ABBREVIATIONS

LC	Liquid Chromatography
MS	Mass Spectrometry
HRMS	High Resolution Mass Spectrometry
RPLC	Reversed phase liquid chromatography
HILIC	Hydrophilic interaction liquid chromatography
bbCID	Broadband collision-induced dissociation
WWTPs	Wastewater treatment plants
ZFE	Zebrafish embryos
FET	Fish embryo test
OECD	Organization for Economic-Co-operation and Development
hpf	Hours post fertilization
dpf	Days post fertilization
IOCs	Ionizable Organic Compounds
MET	Metoprolol
I.S.	Internal standard
EC50	Effective concentration, 50%
LC50	Lethal concentration, 50%
C_{int}	Internal concentration
NOEC	No observed effect concentration
BCF	Bioconcentration factor
bio-TP	Biotransformation product
LOD	Limit of Detection
LOQ	Limit of Quantification
SD	Standard deviation

Appendix

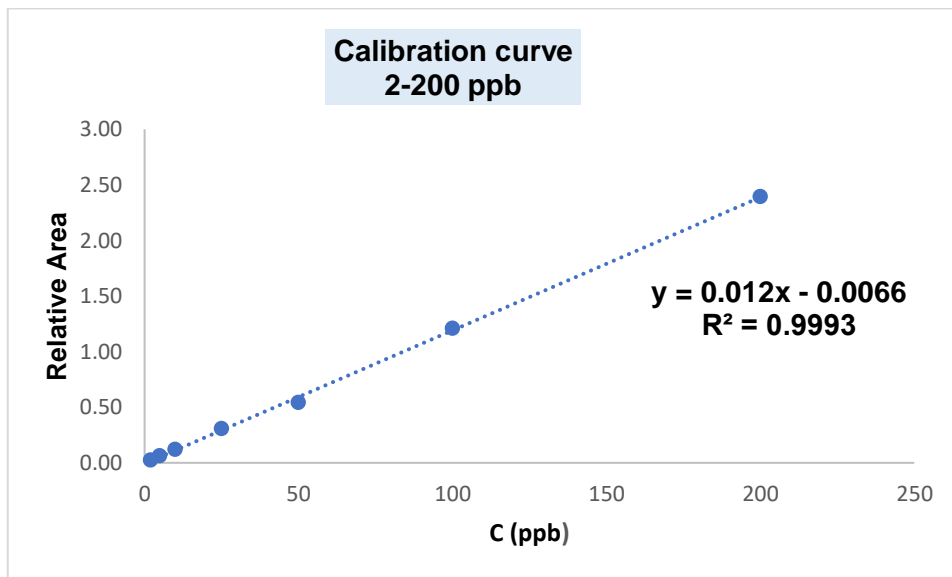


Figure 63. Calibration curve of Metoprolol

Table 8. LOD and LOQ derived from the calibration curve of Metoprolol

Metoprolol	
LOD (ppb)	3.3
LOQ (ppb)	10

References

- [1] V. Geissen, H. Mol, E. Klumpp, G. Umlauf, M. Nadal, M. van der Ploeg, S.E.A.T.M. van de Zee, C.J. Ritsema, Emerging pollutants in the environment: A challenge for water resource management, International Soil and Water Conservation Research, vol. 3, 2015, pp. 57–65.
- [2] M. la Farré, S. Pérez, L. Kantiani, D. Barceló, Fate and toxicity of emerging pollutants, their metabolites and transformation products in the aquatic environment, *TrAC - Trends in Analytical Chemistry*, vol. 27, 2008, pp. 991–1007.
- [3] S. Sauvé, M. Desrosiers, A review of what is an emerging contaminant, *Chemistry Central Journal*, vol. 8, 2014, pp. 1–7.
- [4] <https://www.norman-network.net>, (Last visit: 19/10/2021).
- [5] M. Petrović, S. Gonzalez, D. Barceló, Analysis and removal of emerging contaminants in wastewater and drinking water, *TrAC - Trends in Analytical Chemistry*, vol. 22, 2003, pp. 685–696.
- [6] A. Gogoi, P. Mazumder, V.K. Tyagi, G.G. Tushara Chaminda, A.K. An, M. Kumar, Occurrence and fate of emerging contaminants in water environment: A review, *Groundwater for Sustainable Development*, vol. 6, 2018, pp. 169–180.
- [7] M. Mezzelani, S. Gorbi, F. Regoli, Pharmaceuticals in the aquatic environments: Evidence of emerged threat and future challenges for marine organisms, *Marine Environmental Research*, vol. 140, 2018, pp. 41–60.
- [8] K. Fent, A.A. Weston, D. Caminada, Ecotoxicology of human pharmaceuticals, *Aquatic Toxicology*, vol. 76, 2006, pp. 122–159.
- [9] A. Jelic, M. Gros, A. Ginebreda, R. Cespedes-Sánchez, F. Ventura, M. Petrovic, D. Barcelo, Occurrence, partition and removal of pharmaceuticals in sewage water and sludge during wastewater treatment, *Water Research*, vol. 45, 2011, pp. 1165–1176.
- [10] A.J. Ebele, M. Abou-Elwafa Abdallah, S. Harrad, Pharmaceuticals and

personal care products (PPCPs) in the freshwater aquatic environment, Emerging Contaminants, vol. 3, 2017, pp. 1–16.

- [11] A.B.A. Boxall, M.A. Rudd, B.W. Brooks, D.J. Caldwell, K. Choi, S. Hickmann, E. Innes, K. Ostapyk, J.P. Staveley, T. Verslycke, G.T. Ankley, K.F. Beazley, S.E. Belanger, J.P. Berninger, P. Carriquiriborde, A. Coors, P.C. DeLeo, S.D. Dyer, J.F. Ericson, F. Gagné, J.P. Giesy, T. Gouin, L. Hallstrom, M. V. Karlsson, D.G. Joakim Larsson, J.M. Lazorchak, F. Mastrocco, A. McLaughlin, M.E. McMaster, R.D. Meyerhoff, R. Moore, J.L. Parrott, J.R. Snape, R. Murray-Smith, M.R. Servos, P.K. Sibley, J.O. Straub, N.D. Szabo, E. Topp, G.R. Tetreault, V.L. Trudeau, G. Van Der Kraak, Pharmaceuticals and personal care products in the environment: What are the big questions?, Environmental Health Perspectives, vol. 120, 2012, pp. 1221–1229.
- [12] Y. Luo, W. Guo, H.H. Ngo, L.D. Nghiem, F.I. Hai, J. Zhang, S. Liang, X.C. Wang, A review on the occurrence of micropollutants in the aquatic environment and their fate and removal during wastewater treatment, Science of the Total Environment, vol. 473–474, 2014, pp. 619–641.
- [13] L.H.M.L.M. Santos, A.N. Araújo, A. Fachini, A. Pena, C. Delerue-Matos, M.C.B.S.M. Montenegro, Ecotoxicological aspects related to the presence of pharmaceuticals in the aquatic environment, Journal of Hazardous Materials, vol. 175, 2010, pp. 45–95.
- [14] A. Kühnert, C. Vogs, R. Altenburger, E. Küster, The internal concentration of organic substances in fish embryos-A toxicokinetic approach, Environmental Toxicology and Chemistry, vol. 32, 2013, pp. 1819–1827.
- [15] B. Escher, J.L.M. Hermens, Internal Exposure: LINKING Bioavailability to Effects, Environmental Science and Technology, 2004, pp. 455–462.
- [16] S. Brox, A.P. Ritter, E. Küster, T. Reemtsma, A quantitative HPLC-MS/MS method for studying internal concentrations and toxicokinetics of 34 polar analytes in zebrafish (*Danio rerio*) embryos, Analytical and Bioanalytical Chemistry, vol. 406, 2014, pp. 4831–4840.
- [17] A. Kretschmann, R. Ashauer, T.G. Preuss, P. Spaak, B.I. Escher, J. Hollender, Toxicokinetic model describing bioconcentration and

biotransformation of diazinon in daphnia magna, Environmental Science and Technology, vol. 45, 2011, pp. 4995–5002.

[18] R. Ashauer, A. Hintermeister, I. O'Connor, M. Elumelu, J. Hollender, B.I. Escher, Significance of xenobiotic metabolism for bioaccumulation kinetics of organic chemicals in gammarus pulex, Environmental Science and Technology, vol. 46, 2012, pp. 3498–3508.

[19] B.I. Escher, R. Ashauer, S. Dyer, J.L.M. Hermens, J.H. Lee, H.A. Leslie, P. Mayer, J.P. Meador, M.S.J. Warnekk, Crucial role of mechanisms and modes of toxic action for understanding tissue residue toxicity and internal effect concentrations of organic chemicals, Integrated Environmental Assessment and Management, vol. 7, 2011, pp. 28–49.

[20] B.I. Escher, K. Fenner, Recent advances in environmental risk assessment of transformation products, Environmental Science and Technology, vol. 45, 2011, pp. 3835–3847.

[21] D.T.H.M. Sijm, J.L.M. Hermens, Internal Effect Concentration: Link Between Bioaccumulation and Ecotoxicity for Organic Chemicals, Bioaccumulation – New Aspects and Developments, vol. 2, 2005, pp. 167–199.

[22] S. Brox, B. Seiwert, E. Küster, T. Reemtsma, Toxicokinetics of Polar Chemicals in Zebrafish Embryo (*Danio rerio*): Influence of Physicochemical Properties and of Biological Processes, Environmental Science and Technology, vol. 50, 2016, pp. 10264–10272.

[23] Q. Fu, D. Fedrizzi, V. Kosfeld, C. Schlechtriem, V. Ganz, S. Derrer, D. Rentsch, J. Hollender, Biotransformation Changes Bioaccumulation and Toxicity of Diclofenac in Aquatic Organisms, Environmental Science and Technology, vol. 54, 2020, pp. 4400–4408.

[24] L.A. Stanley, Drug Metabolism, Elsevier Inc., 2017.

[25] C. Nebbia, Biotransformation enzymes as determinants of xenobiotic toxicity in domestic animals, Veterinary Journal, vol. 161, 2001, pp. 238–252.

[26] A. Jaén-Gil, F. Castellet-Rovira, M. Llorca, M. Villagrasa, M. Sarrà, S.

Rodríguez-Mozaz, D. Barceló, Fungal treatment of metoprolol and its recalcitrant metabolite metoprolol acid in hospital wastewater: Biotransformation, sorption and ecotoxicological impact, *Water Research*, vol. 152, 2019, pp. 171–180.

[27] C. Ioannides, Xenobiotic Metabolism: An Overview, 2002.

[28] L. Bittner, N. Klüver, L. Henneberger, M. Mühlenbrink, C. Zarfl, B.I. Escher, Combined Ion-Trapping and Mass Balance Models to Describe the pH-Dependent Uptake and Toxicity of Acidic and Basic Pharmaceuticals in Zebrafish Embryos (*Danio rerio*), *Environmental Science and Technology*, vol. 53, 2019, pp. 7877–7886.

[29] L. Bittner, E. Teixido, B. Seiwert, B.I. Escher, N. Klüver, Influence of pH on the uptake and toxicity of B-blockers in embryos of zebrafish, *Danio rerio*, *Aquatic Toxicology*, vol. 201, 2018, pp. 129–137.

[30] M. V. Karlsson, L.J. Carter, A. Agatz, A.B.A. Boxall, Novel Approach for Characterizing pH-Dependent Uptake of Ionizable Chemicals in Aquatic Organisms, *Environmental Science and Technology*, vol. 51, 2017, pp. 6965–6971.

[31] L. Bittner, E. Teixidó, I. Keddi, B.I. Escher, N. Klüver, pH-Dependent Uptake and Sublethal Effects of Antihistamines in Zebrafish (*Danio rerio*) Embryos, *Environmental Toxicology and Chemistry*, vol. 38, 2019, pp. 1012–1022.

[32] C. Rendal, K.O. Kusk, S. Trapp, Optimal choice of pH for toxicity and bioaccumulation studies of ionizing organic chemicals, *Environmental Toxicology and Chemistry*, vol. 30, 2011, pp. 2395–2406.

[33] G.G. Anskjær, C. Rendal, K.O. Kusk, Effect of pH on the toxicity and bioconcentration of sulfadiazine on *Daphnia magna*, *Chemosphere*, vol. 91, 2013, pp. 1183–1188.

[34] C. Rendal, K.O. Kusk, S. Trapp, The effect of pH on the uptake and toxicity of the bivalent weak base chloroquine tested on *Salix viminalis* and *Daphnia magna*, *Environmental Toxicology and Chemistry*, vol. 30, 2011, pp. 354–359.

[35] J.M. Armitage, R.J. Erickson, T. Luckenbach, C.A. Ng, R.S. Prosser, J.A. Arnot, K. Schirmer, J.W. Nichols, Assessing the bioaccumulation potential of ionizable organic compounds: Current knowledge and research priorities, *Environmental Toxicology and Chemistry*, vol. 36, 2017, pp. 882–897.

[36] M. Yi, Q. Sheng, Q. Sui, H. Lu, β -blockers in the environment: Distribution, transformation, and ecotoxicity, *Environmental Pollution*, vol. 266, 2020.,

[37] B. Berger, F. Bachmann, U. Duthaler, S. Krähenbühl, M. Haschke, Cytochrome P450 enzymes involved in metoprolol metabolism and use of metoprolol as a CYP2D6 phenotyping probe drug, *Frontiers in Pharmacology*, vol. 9, 2018, pp. 1–11.

[38] S.H. Bae, J.K. Lee, D.Y. Cho, S.K. Bae, Simultaneous determination of metoprolol and its metabolites, α -hydroxymetoprolol and O-desmethylmetoprolol, in human plasma by liquid chromatography with tandem mass spectrometry: Application to the pharmacokinetics of metoprolol associated with CYP2D6 g, *Journal of Separation Science*, vol. 37, 2014, pp. 1256–1264.

[39] J. Maszkowska, S. Stolte, J. Kumirska, P. Łukaszewicz, K. Mioduszewska, A. Puckowski, M. Caban, M. Wagil, P. Stepnowski, A. Białk-Bielńska, Beta-blockers in the environment: Part II. Ecotoxicity study, *Science of the Total Environment*, vol. 493, 2014, pp. 1122–1126.

[40] C.N. Brocker, T. Velenosi, H.K. Flaten, G. McWilliams, K. McDaniel, S.K. Shelton, J. Saben, K.W. Krausz, F.J. Gonzalez, A.A. Monte, Metabolomic profiling of metoprolol hypertension treatment reveals altered gut microbiota-derived urinary metabolites, *Human Genomics*, vol. 14, 2020, pp. 1–9.

[41] B. Ma, H.H. Huang, X.Y. Chen, Y.M. Sun, L.H. Lin, D.F. Zhong, Biotransformation of metoprolol by the fungus Cunninghamella blakesleeana, *Acta Pharmacologica Sinica*, vol. 28, 2007, pp. 1067–1074.

[42] A.A. Godoy, F. Kummrow, P.A.Z. Pamplin, Occurrence, ecotoxicological

effects and risk assessment of antihypertensive pharmaceutical residues in the aquatic environment - A review, *Chemosphere*, vol. 138, 2015, pp. 281–291.

[43] J. Maszkowska, S. Stolte, J. Kumirska, P. Łukaszewicz, K. Mioduszewska, A. Puckowski, M. Caban, M. Wagil, P. Stepnowski, A. Białk-Bielinska, Beta-blockers in the environment: Part I. Mobility and hydrolysis study, *Science of the Total Environment*, vol. 493, 2014, pp. 1112–1121.

[44] R. Triebeskorn, H. Casper, V. Scheil, J. Schwaiger, Ultrastructural effects of pharmaceuticals (carbamazepine, clofibrate acid, metoprolol, diclofenac) in rainbow trout (*Oncorhynchus mykiss*) and common carp (*Cyprinus carpio*), *Analytical and Bioanalytical Chemistry*, vol. 387, 2007, pp. 1405–1416.

[45] E. Praskova, E. Voslarova, Z. Siroka, L. Plhalova, S. Macova, P. Marsalek, V. Pistekova, Z. Svobodova, Assessment of diclofenac LC50 reference values in juvenile and embryonic stages of the zebrafish (*Danio rerio*), *Polish Journal of Veterinary Sciences*, vol. 14, 2011, pp. 545–549.

[46] A.J. Hill, H. Teraoka, W. Heideman, R.E. Peterson, Zebrafish as a model vertebrate for investigating chemical toxicity, *Toxicological Sciences*, vol. 86, 2005, pp. 6–19.

[47] H.S. Jones, Xenobiotic metabolism and zebrafish (*Danio Rerio*) Larvae, PhD thesis, 2010.

[48] A.L. Rubinstein, Zebrafish assays for drug toxicity screening, *Expert Opinion on Drug Metabolism and Toxicology*, vol. 2, 2006, pp. 231–240.

[49] J.A.R. Jonathan Posner and Bradley S. Peterson, The State of the Art of the Zebrafish Model for Toxicology and Toxicologic Pathology Research—Advantages and Current Limitations, *Toxicol Pathol*, vol. 23, 2003, pp. 1–7.

[50] S. Ali, D.L. Champagne, H.P. Spaink, M.K. Richardson, Zebrafish embryos and larvae: A new generation of disease models and drug screens, *Birth Defects Research Part C - Embryo Today: Reviews*, vol.

93, 2011, pp. 115–133.

- [51] S. RBenjamin, The State of the Art of the Zebrafish Model for Toxicology and Toxicologic Pathology Research—Advantages and Current Limitations, *Bone*, vol. 23, 2008, pp. 1–7.
- [52] R. Gonzalo-Lumbreras, J. Sanz-Landaluze, J. Guinea, C. Cámara, Miniaturized extraction methods of triclosan from aqueous and fish roe samples. Bioconcentration studies in zebrafish larvae (*Danio rerio*), *Analytical and Bioanalytical Chemistry*, vol. 403, 2012, pp. 927–937.
- [53] S. Berghmans, P. Butler, P. Goldsmith, G. Waldron, I. Gardner, Z. Golder, F.M. Richards, G. Kimber, A. Roach, W. Alderton, A. Fleming, Zebrafish based assays for the assessment of cardiac, visual and gut function - potential safety screens for early drug discovery, *Journal of Pharmacological and Toxicological Methods*, vol. 58, 2008, pp. 59–68.
- [54] H.S. Jones, H.T. Trollope, T.H. Hutchinson, G.H. Panter, J.K. Chipman, Metabolism of ibuprofen in zebrafish larvae, *Xenobiotica*, vol. 42, 2012, pp. 1069–1075.
- [55] S. Yu, T. Lin, W. Chen, H. Tao, The toxicity of a new disinfection by-product, 2,2-dichloroacetamide (DCAcAm), on adult zebrafish (*Danio rerio*) and its occurrence in the chlorinated drinking water, *Chemosphere*, vol. 139, 2015, pp. 40–46.
- [56] M. Cleuvers, Initial risk assessment for three β -blockers found in the aquatic environment, *Chemosphere*, vol. 59, 2005, pp. 199–205.
- [57] D.B. Huggett, B.W. Brooks, B. Peterson, C.M. Foran, D. Schlenk, Toxicity of select beta adrenergic receptor-blocking pharmaceuticals (B-blockers) on aquatic organisms, *Archives of Environmental Contamination and Toxicology*, vol. 43, 2002, pp. 229–235.
- [58] E.J. van den Brandhof, M. Montforts, Fish embryo toxicity of carbamazepine, diclofenac and metoprolol, *Ecotoxicology and Environmental Safety*, vol. 73, 2010, pp. 1862–1866.
- [59] T.H. Miller, N.R. Bury, S.F. Owen, L.P. Barron, Uptake, biotransformation and elimination of selected pharmaceuticals in a freshwater invertebrate

measured using liquid chromatography tandem mass spectrometry, *Chemosphere*, vol. 183, 2017, pp. 389–400.

- [60] A. Ribbenstedt, J.P. Benskin, Rapid in-plate screening of biotransformation products in single zebrafish embryos, *RSC Advances*, vol. 11, 2021, pp. 27812–27819.
- [61] A. Rubirola, M. Llorca, S. Rodriguez-Mozaz, N. Casas, I. Rodriguez-Roda, D. Barceló, G. Buttiglieri, Characterization of metoprolol biodegradation and its transformation products generated in activated sludge batch experiments and in full scale WWTPs, *Water Research*, vol. 63, 2014, pp. 21–32.
- [62] D.E. Damalas, A.A. Bletsou, A. Agalou, D. Beis, N.S. Thomaidis, Assessment of the Acute Toxicity, Uptake and Biotransformation Potential of Benzotriazoles in Zebrafish (*Danio rerio*) Larvae Combining HILIC- with RPLC-HRMS for High-Throughput Identification, *Environmental Science and Technology*, vol. 52, 2018, pp. 6023–6031.
- [63] S. Brox, B. Seiwert, N. Haase, E. Küster, T. Reemtsma, Metabolism of clofibric acid in zebrafish embryos (*Danio rerio*) as determined by liquid chromatography-high resolution-mass spectrometry, *Comparative Biochemistry and Physiology Part - C: Toxicology and Pharmacology*, vol. 185–186, 2016, pp. 20–28.
- [64] D.E. Damalas, A.A. Bletsou, A. Agalou, D. Beis, N.S. Thomaidis, Assessment of the Acute Toxicity, Uptake and Biotransformation Potential of Benzotriazoles in Zebrafish (*Danio rerio*) Larvae Combining HILIC- with RPLC-HRMS for High-Throughput Identification, *Environmental Science and Technology*, vol. 52, 2018, pp. 6023–6031.
- [65] A.A. Bletsou, J. Jeon, J. Hollender, E. Archontaki, N.S. Thomaidis, Targeted and non-targeted liquid chromatography-mass spectrometric workflows for identification of transformation products of emerging pollutants in the aquatic environment, *TrAC - Trends in Analytical Chemistry*, vol. 66, 2015, pp. 32–44.
- [66] V.G. Beretsou, A.K. Psoma, P. Gago-Ferrero, R. Aalizadeh, K. Fenner, N.S. Thomaidis, Identification of biotransformation products of citalopram

formed in activated sludge, *Water Research*, vol. 103, 2016, pp. 205–214.

- [67] E.L. Schymanski, J. Jeon, R. Gulde, K. Fenner, M. Ruff, H.P. Singer, J. Hollender, Identifying small molecules via high resolution mass spectrometry: Communicating confidence, *Environmental Science and Technology*, vol. 48, 2014, pp. 2097–2098.
- [68] O. Guidelines, F.O.R. The, T. Of, *OECD guidelines for testing of chemicals*, *Dermatotoxicology*, 2013, pp. 509–511.
- [69] A. Svan, M. Hedeland, T. Arvidsson, J.T. Jasper, D.L. Sedlak, C.E. Pettersson, Identification of transformation products from β -blocking agents formed in wetland microcosms using LC-Q-ToF, *Journal of Mass Spectrometry*, vol. 51, 2016, pp. 207–218.
- [70] B.I. Escher, N. Bramaz, M. Richter, J. Lienert, Comparative ecotoxicological hazard assessment of beta-blockers and their human metabolites using a mode-of-action-based test battery and a QSAR approach, *Environmental Science and Technology*, vol. 40, 2006, pp. 7402–7408.